

การปรับปรุงความต้านทานการเกิดฟาวลิงของเชื้อเลือกผ่านแบบฟิล์มบางคอมพอสิต โดยการเติม
ไทเทเนียม ไดออกไซด์



นายพลัช เกศชัยกุลรัตน์

จุฬาลงกรณ์มหาวิทยาลัย

บทคัดย่อและแฟ้มข้อมูลฉบับเต็มของวิทยานิพนธ์ตั้งแต่ปีการศึกษา 2554 ที่ให้บริการในคลังปัญญาจุฬาฯ (CUIR)
เป็นแฟ้มข้อมูลของนิสิตเจ้าของวิทยานิพนธ์ ที่ส่งผ่านทางบัณฑิตวิทยาลัย

The abstract and full text of theses from the academic year 2011 in Chulalongkorn University Intellectual Repository (CUIR)
are the thesis authors' files submitted through the University Graduate School.

วิทยานิพนธ์นี้เป็นส่วนหนึ่งของการศึกษาตามหลักสูตรปริญญาวิศวกรรมศาสตรมหาบัณฑิต

สาขาวิชาวิศวกรรมเคมี ภาควิชาวิศวกรรมเคมี

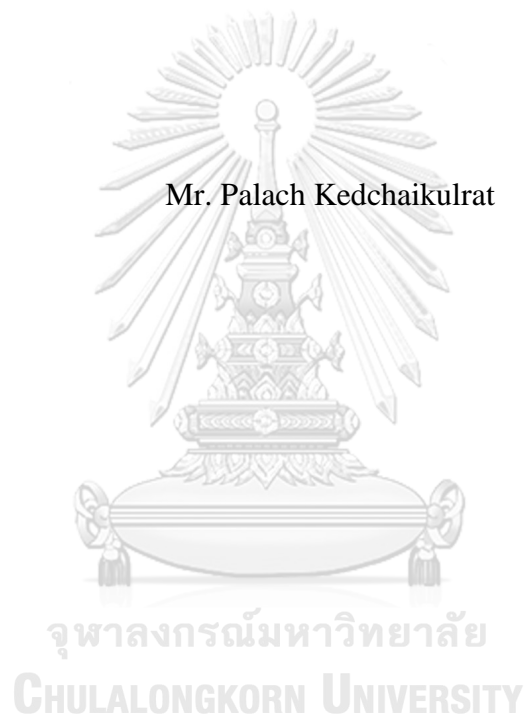
คณะวิศวกรรมศาสตร์ จุฬาลงกรณ์มหาวิทยาลัย

ปีการศึกษา 2560

ลิขสิทธิ์ของจุฬาลงกรณ์มหาวิทยาลัย

IMPROVING FOULING RESISTANCE OF THIN FILM COMPOSITE
MEMBRANES BY ADDITION OF TiO₂

Mr. Palach Kedchaikulrat



A Thesis Submitted in Partial Fulfillment of the Requirements
for the Degree of Master of Engineering Program in Chemical Engineering
Department of Chemical Engineering
Faculty of Engineering
Chulalongkorn University
Academic Year 2017
Copyright of Chulalongkorn University

Thesis Title	IMPROVING FOULING RESISTANCE OF THIN FILM COMPOSITE MEMBRANES BY ADDITION OF TiO ₂
By	Mr. Palach Kedchaikulrat
Field of Study	Chemical Engineering
Thesis Advisor	Chalida Klaysom, Ph.D.

Accepted by the Faculty of Engineering, Chulalongkorn University in
Partial Fulfillment of the Requirements for the Master's Degree

..... Dean of the Faculty of Engineering
(Associate Professor Supot Teachavorasinskun, D.Eng.)

THESIS COMMITTEE

..... Chairman
(Professor Suttichai Assabumrungrat, Ph.D.)

..... Thesis Advisor
(Chalida Klaysom, Ph.D.)

..... Examiner
(Paravee Vas-Umuay, Ph.D.)

..... External Examiner
(Kajornsak Faungnawakij, D.Eng.)

จุฬาลงกรณ์มหาวิทยาลัย
CHULALONGKORN UNIVERSITY

พลัซ เกศชัยกุลรัตน์ : การปรับปรุงความต้านทานการเกิดฟาวลิงของเยื่อเลือกผ่านแบบฟิล์มบางคอมพอสิตโดยการเติมไทเทเนียมไดออกไซด์ (IMPROVING FOULING RESISTANCE OF THIN FILM COMPOSITE MEMBRANES BY ADDITION OF TiO₂) อ.ที่ปรึกษาวิทยานิพนธ์หลัก: ดร. ชลิดา คล้ายโสม, 93 หน้า.

เยื่อเลือกผ่านฟิล์มบางพอลิเอไมด์นาโนคอมพอสิตที่มีการเติมแต่งของอนุภาคไทเทเนียมไดออกไซด์ขนาดนาโนถูกสังเคราะห์ด้วยวิธีการพอลิเมอไรเซชันแบบระหว่างวัฏภาคบนชั้นรองรับพอลิอะคริโลไนไตร เช่นเดียวกับกับเยื่อเลือกผ่านฟิล์มบางคอมพอสิตที่มีการเติมแต่งด้วยแต่ละส่วนประกอบในสารละลายคอลลอยด์ไทเทเนียมไดออกไซด์ ประกอบไปด้วย เอทานอล อนุภาคไทเทเนียมไดออกไซด์ขนาดนาโน และกรดไนตริก ถูกศึกษาประสิทธิภาพในด้านของ การกักกันเกลือโซเดียมคลอไรด์ ค่าการยอมให้น้ำผ่าน และ ความสามารถในการต่อต้านการเกิดฟาวลิง การวิเคราะห์คุณลักษณะของเยื่อเลือกผ่านถูกดำเนินการเพื่อสังเกตคุณสมบัติที่หลากหลาย เช่น ลักษณะทางพื้นฐานวิทยา ความขรุขระของพื้นผิว เคมีพื้นผิว และ ความชอบน้ำ ผลการศึกษาแสดงให้เห็นว่าการเติมสารละลายคอลลอยด์ไทเทเนียมไดออกไซด์ในสารละลายเอมีนที่มีน้ำมีอิทธิพลที่สำคัญต่อรูปแบบและประสิทธิภาพของฟิล์มบาง เยื่อเลือกผ่านฟิล์มบางนาโนคอมพอสิตที่มีการเติมสารละลายคอลลอยด์ไทเทเนียมไดออกไซด์ในสารละลายเอมีนที่มีน้ำแสดงค่าการกักกันเกลือ ค่าการยอมให้น้ำผ่าน และความสามารถต่อต้านการเกิดฟาวลิงที่โดดเด่นเมื่อถูกเปรียบเทียบกับเยื่อเลือกผ่านฟิล์มบางคอมพอสิตที่ไม่มีการเติม ด้วยสถานะที่เหมาะสมที่การเติมร้อยละ 20 ของอัตราส่วนโดยปริมาตรของสารละลายคอลลอยด์ไทเทเนียมไดออกไซด์ค่าการกักกันเกลือเพิ่มขึ้นอย่างมากจากร้อยละ 79.22 ถึงร้อยละ 94.20 โดยปราศจากการลดลงของค่าการยอมให้น้ำผ่าน ยิ่งไปกว่านั้นยังแสดงให้เห็นถึงประสิทธิภาพการต่อต้านการเกิดฟาวลิงที่ดีมากกว่าเยื่อเลือกผ่านฟิล์มบางคอมพอสิตที่ไม่มีการเติมและเยื่อเลือกผ่านเชิงพาณิชย์ NF270 เป็นผลมาจากค่าความชอบน้ำที่ถูกทำให้เพิ่มขึ้น ความขรุขระของพื้นผิวที่ลดลง และประจุลบที่เพิ่มขึ้นจากอนุภาคไทเทเนียมไดออกไซด์ขนาดนาโน

ภาควิชา วิศวกรรมเคมี

ลายมือชื่อนิสิต

สาขาวิชา วิศวกรรมเคมี

ลายมือชื่อ อ.ที่ปรึกษาหลัก

ปีการศึกษา 2560

5970394021 : MAJOR CHEMICAL ENGINEERING

KEYWORDS: THIN FILM NANOCOMPOSITE / TITANIUM DIOXIDE
NANOPARTICLES / FOULING RESISTANCE / INTERFACIAL
POLYMERIZATION / ANTIFOULING

PALACH KEDCHAIKULRAT: IMPROVING FOULING RESISTANCE
OF THIN FILM COMPOSITE MEMBRANES BY ADDITION OF TiO₂.
ADVISOR: CHALIDA KLAYSOM, Ph.D., 93 pp.

Polyamide thin film nanocomposite (TFN) membranes with the addition of titanium dioxide (TiO₂) nanoparticles (NPs) were synthesized via an interfacial polymerization (IP) on polyacrylonitrile (PAN) support. Also, the TFC membranes with addition of individual components in the TiO₂ colloidal solution, ethanol, TiO₂ NPs and nitric acid, were individually studied. The performances of the fabricated membranes were evaluated in terms of NaCl salt rejection, water permeability and anti-fouling capability. Membranes characterizations were conducted to observe various characteristics of membranes such as morphology, surface roughness, surface chemistry and hydrophilicity. The results revealed that the addition of TiO₂ colloidal solution in aqueous amine solution has a crucial influence on thin film formation and performance. The TFN prepared from the addition of TiO₂ colloidal solution in aqueous monomer performed outstanding salt retention, permeability and fouling resistance compared to the bare TFC membrane. With the optimum condition at 20 vol% loading of TiO₂ colloidal solution, the salt rejection elevated from 79.22% to 94.20% without sacrifice of water permeability. Moreover, the optimum TFN membrane exhibited superior anti-fouling performance compared to the bare TFC membrane and the NF270 commercial membrane. This was resulted from the enhanced hydrophilicity, lower surface roughness and increased negative charge from TiO₂ NPs.

Department: Chemical Engineering Student's Signature

Field of Study: Chemical Engineering Advisor's Signature

Academic Year: 2017

ACKNOWLEDGEMENTS

I would like to show gratitude and appreciation to my adviser Dr. Chalida Klaysome for giving knowledge, suggestion, support and opportunities through the years as a master student. Furthermore, i also would like to express my thankfulness and appreciation to Prof. Dr. Suttichai Assabumrungrat as the chairman, Dr.Paravee Vas-Umnuay as the examiner and Dr. Kajornsak Faungnawakij as the external examiner for advantageous recommendations, comments and being thesis committee.

This research was supported by the financial support Chulalongkorn University via the Grants for Development of New Faculty Staff (Ratchadaphiseksomphot Endowment Fund).

Finally, my thankful goes to my family, friends, Center of Excellence in Particle Technology (CEPT) and my colleagues for all of their support and willingness bringing me through this work.

CONTENTS

	Page
THAI ABSTRACT	iv
ENGLISH ABSTRACT.....	v
ACKNOWLEDGEMENTS	vi
CONTENTS.....	vii
CHAPTER 1	9
INTRODUCTION	9
1.1 Introduction	9
CHAPTER 2	11
BACKGROUND AND LITERATURE.....	11
2.1 Background.....	11
2.1.1 Membrane and its technology for water purification	11
2.1.2 NF and RO membranes	14
2.1.3 Fabrication of TFC membrane	15
2.1.4 Membrane Fouling	22
2.2 Literature review	28
Recent development of fouling resistance membranes	28
CHAPTER 3	37
SCOPE OF WORK.....	37
3.1 Objectives	37
3.2 Scope of work	37
3.2.1 Membrane preparation and characterization	37
CHAPTER 4	39
RESEARCH METHODOLOGY.....	39
4.1 Materials	39
4.2 Synthesis of TiO ₂ colloidal solution	39
4.3 Fabrication of membranes	39
4.4 Membrane characterizations	40

	Page
4.5 Membrane performance test	41
CHAPTER 5	43
RESULTS AND DISCUSSION	43
5.1 The influence of TiO ₂ colloidal solution on the formation and performance of TFN membrane	43
5.2 Effects of the individual component in TiO ₂ colloidal solution	51
5.2.1 Effect of ethanol	51
5.2.2 Effect of Nitric acid (pH)	57
5.2.3 Effect of Titanium dioxide (TiO ₂)	62
5.3 Fouling evaluation	75
5.4 TiO ₂ embedded TFN membranes performance comparison	77
CHAPTER 6	79
CONCLUSIONS AND RECOMMENDATIONS	79
6.1 Conclusions	79
6.2 Recommendations	80
REFERENCES	81
APPENDIX	86
Appendix A: Sample calculation of membrane performances	86
Salt rejection	86
Water permeability and water flux	88
Appendix B: characterization of TiO ₂ colloidal solution	91
Size distribution of synthesized TiO ₂ NPs in solution form	91
Appendix C: Surface roughness of fabricated membranes	92
VITA	93

CHAPTER 1

INTRODUCTION

1.1 Introduction

Purifying and reusing of wastewater is one of considerate topics in many industries. Resupplying of purified water back to the process can minimize a wastewater discharge and increase a sustainable capacity of clean water utility. Recently, membrane technology is considered as an alternative separation process using a semi-permeable membrane to purify wastewater in various industries such as petrochemical, pharmaceutical, food and beverage, and steel and power generation. Membrane in wastewater treatment accounts for 36% of Southeast Asian Membrane Technologies market value in 2017 with 398 million US dollars revenue [1].

Membrane as the widely used technology in waste water treatment owns various benefits such as efficient separation capability for ion filtration, relatively low energy consumption, compact size, and simple operation. In the other hand, the most problems always occurring to membranes are concentration polarization and fouling. Concentration polarization can be easily minimized by adjusting operating conditions of the system, while fouling is more complicated and requires more systematic solutions. To prevent or reduce the acceleration of fouling, intensive pre-treatment of feed water is required. However, the pre-treatment can only partially solve the problem and temporary extend the duration of fouling mechanism but does not directly overcome this crucial obstacle.

Hence, one of the most limitations of membrane technology for wastewater treatment is an accumulation of foulants depositing on membrane surface after a period of operation [2]. In addition, an irreversible fouling, which is hard to be removed by physical surface cleaning, can also be formed and hence results in a decline in membrane performance and frequent membrane replacements. So the modification of membranes to repel fouling and improve irreversible fouling resistance is of necessary to minimize the limitations and expand the membrane lifetime.

To improve the anti-fouling property, various hydrophilic nanoparticles (NPs) were cooperated into the membrane selective film to improve the membranes properties [3] Among many NPs, titanium dioxide (TiO_2) nanoparticles (NPs) owns many good profits such as ultra-hydrophilic, antibacterial, antiseptic, commercialize and easy for synthesis. Therefore, TiO_2 NPs have gained the attention to be incorporated with the thin film composite (TFC) membranes to enhance the fouling resistance properties.

The aims of this work is to enhance the anti-fouling properties of the membrane via the embedding of TiO_2 NPs into the thin film layer forming thin film nanocomposite (TFN) membrane.



CHAPTER 2

BACKGROUND AND LITERATURE

2.1 Background

2.1.1 Membrane and its technology for water purification

Membrane technology is a separation technique using a semi-permeable membrane as a selective barrier to allow and restrict the transport of specific species. Membranes are normally classified by their symmetrical structure into isotropic and anisotropic membranes. Symmetrical membranes or isotropic type can be further divided to a porous membrane, a nonporous dense membrane and an electrically charged membrane, while anisotropic membrane type is sub-classified to a Loeb-Sourirajan membrane, a thin-film composite membrane, and a supported liquid membrane as shown in Figure 1.

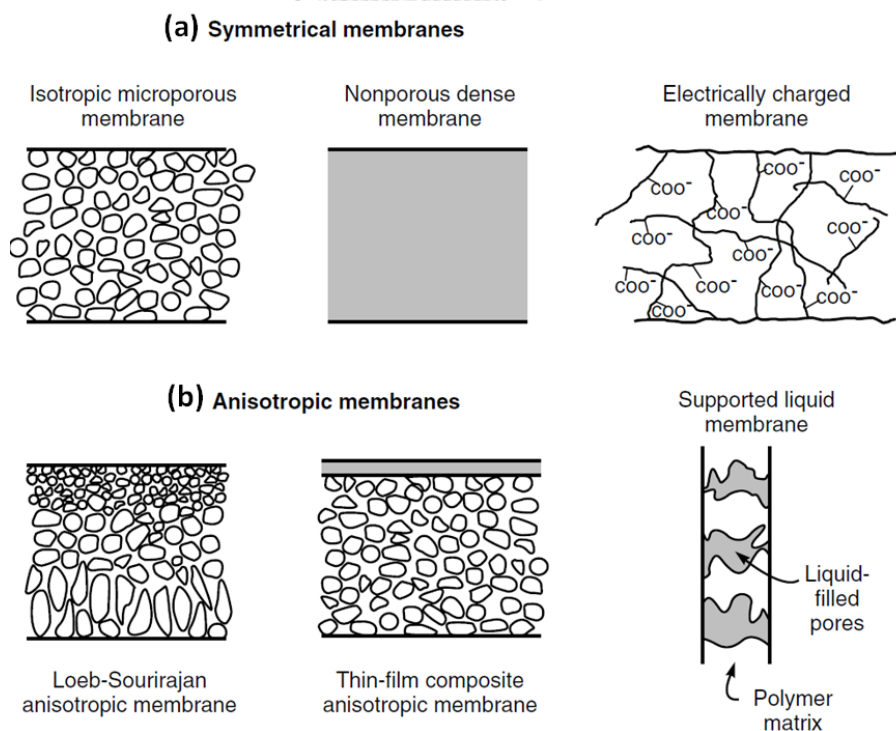


Figure 1 Schematic diagram of the principal types of membranes

(a) symmetrical membranes and (b) anisotropic membranes.

Membrane system is typically used for wastewater treatment including reverse osmosis (RO), nanofiltration (NF), ultrafiltration (UF), and membrane bioreactor (MBR). These processes are pressure driven processes that have the ability to separate substances in different molecular sizes (see Figure 2).

Microfiltration (MF) and UF can retain microbials, colloids, proteins, polymers, cells and suspended particles, while NF and RO can filter pesticides, glucose, salts and low molecular weight ions. In waste water treatment, MF and UF are normally used as the pretreatment steps to screen out big or suspended particles prior to RO and NF. This research focuses on the membrane material used in final purification step as in NF or RO.

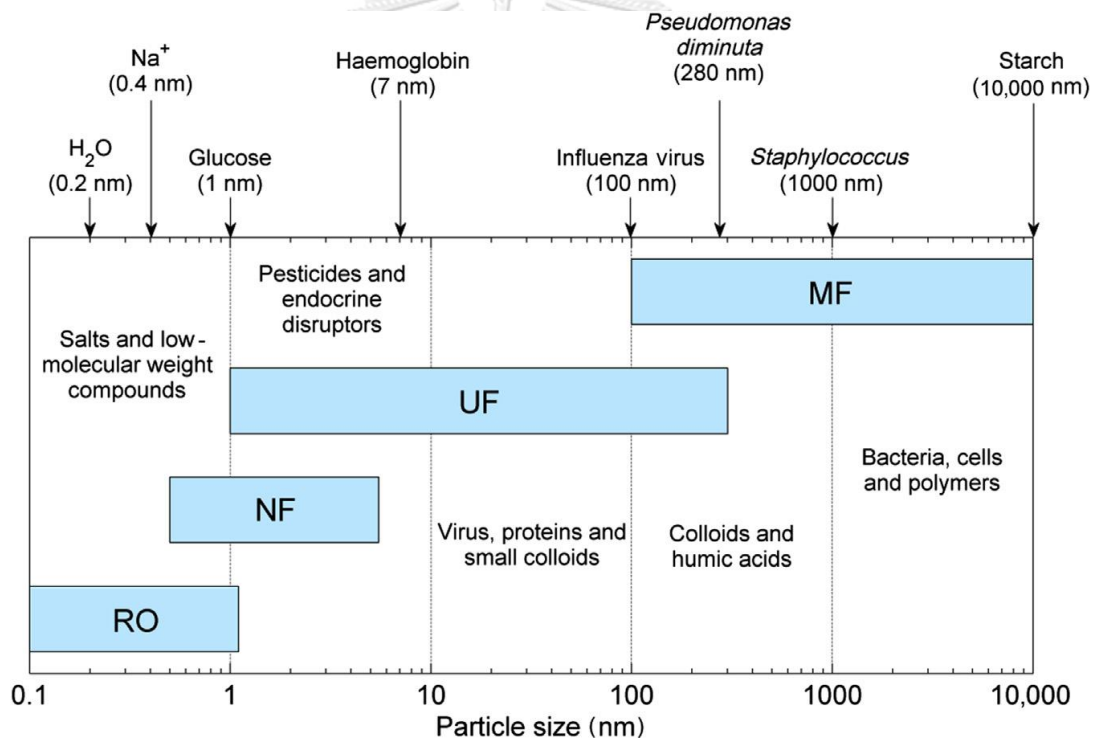


Figure 2 Selective size of particle for pressure driven membrane process [4].

For water purification by a dense membrane like in RO and NF, water molecules are permeated through a membrane, meanwhile other molecules are rejected because of the differences in their solubility and mobility to diffuse through the membrane as shown in Figure 3 [5].

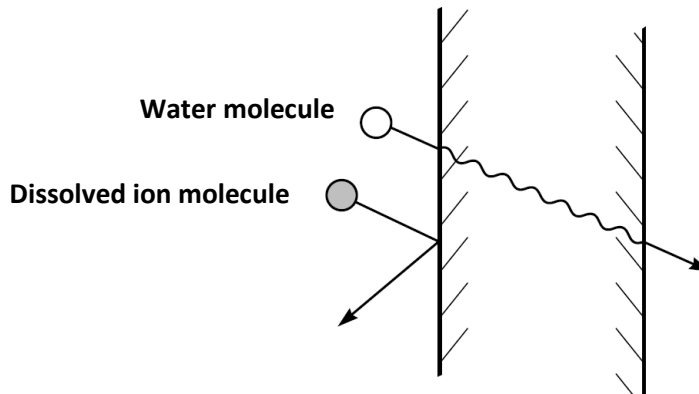


Figure 3 Molecular transports by solution-diffusion mechanism [5].

The quantity of water diffused through the membrane is indicated in the term of water permeance while the rejected percentage of dissolved ion molecules is referred in the term of salt rejection or salt retention described as follows.

Water permeance

Water permeance (A) or water permeability determines the rate of water permeated through the membrane which can be expressed by the following equation;

$$A = \frac{V}{A_m \Delta t (\Delta P - \Delta \pi)} = \frac{J_w}{(\Delta P - \Delta \pi)} \quad (1)$$

where A is water permeance ($\text{Lm}^{-2}\text{h}^{-1}\text{bar}^{-1}$), V is the volume of diffused water (L), A_m is the effective area of membrane (m^2), Δt is the permeation time (h), ΔP is the system pressure (bar) and $\Delta \pi$ is the osmotic pressure of feed, J_w is water flux ($\text{Lm}^{-2}\text{h}^{-1}$).

Salt rejection

The salt retention (R) or salt rejection of membranes operated implies how well the membrane can retain the dissolved salts and can be expressed as the following equation;

$$R = \left(1 - \frac{c_p}{c_f}\right) \times 100 \quad (2)$$

where C_f is the salt concentration of feed (ppm), C_p is the salt concentration of permeate (ppm) and R is the salt rejection (%).

2.1.2 NF and RO membranes

Membranes typically used in NF and RO are Loeb-Sourirajan anisotropic membranes (mostly cellulosic membranes) and thin film composite (TFC) membrane. The comparison of the two membrane types is summarized in Table 1.

Table 1 Comparison of cellulosic membrane and TFC membrane [3]

Feature	Cellulosic membrane	TFC
NaCl rejection (%)	95-99.9%	97-99.5%
Water permeability ($\text{m}^3/\text{m}^2 \cdot \text{day}$ at 840 psi)	0.03-0.05	0.13-1.0
Operating pH	4-6	2-12
Fouling resistance	High	Low
Chlorine tolerance (ppm)	1 ppm	<0.1 ppm

Cellulosic membrane is made of a polymer with a cellulose linkage structure with specific functional groups such as acetyl groups (see Figure 4) forming cellulose acetate membrane. These polymers are easy to produce, have mechanical stability and process good chlorine resistance. Cellulose acetate membrane once provided the highest performance for RO process but recently was surpassed by TFC membrane in both salt rejection and water permeability. However, cellulosic membrane still remains its share in the membrane market because of its high chlorine tolerance (up to 1 ppm) [5].

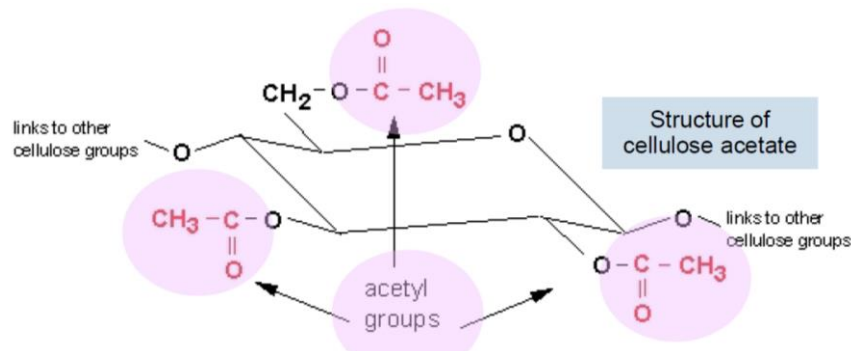


Figure 4 Cellulose acetate structures [6].

Thin film composite membrane (TFC) is composed of a selective thin film layer on top of a porous support with or without non-woven fabric layer as shown in Figure 5. TFC membranes have a better performance (nearly 20 times of water permeability with comparable salt rejection) compared to most cellulosic membranes. This is due to the very thin selective layer of TFC membranes that results in very low mass transfer resistance. Besides its outstanding separation performance, the formation of TFC allows a vast possibility to tailor the membrane properties in that both thin film and the support layer can be modified separately.

This work has paid an attention on the surface modification at the thin selective layer of TFC. Therefore, in the next section the background of membrane formation based only on the TFC is discussed in detail.

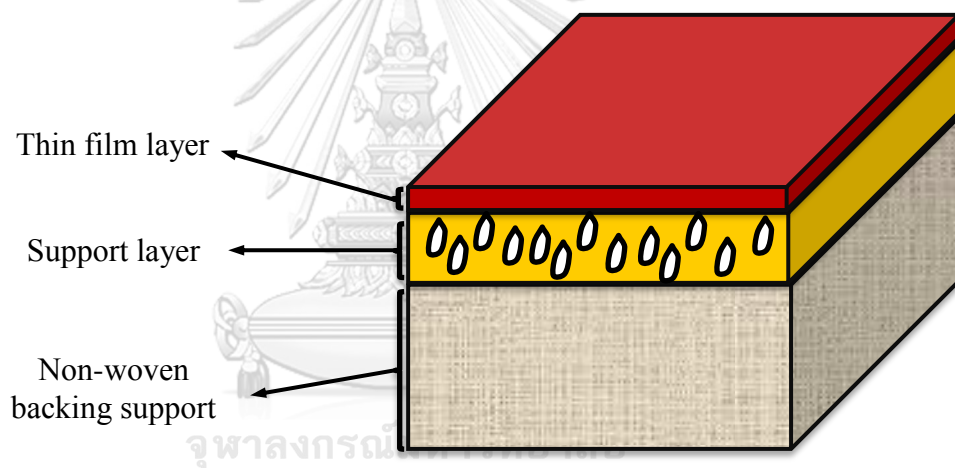


Figure 5 Thin film composite membrane structure.

2.1.3 Fabrication of TFC membrane

As mentioned previously, TFC membrane comprises of two main layers that can be fabricated separately. The support layer is normally prepared by a phase inversion technique while the thin film can be formed by various techniques such as interfacial polymerization, dip-coating, film coating, plasma polymerization and spin coating. This work will only discuss the fabrication of support via phase inversion briefly and focus on interfacial polymerization in more detail for the thin film formation. Other fabrication techniques can be found elsewhere [5].

Phase inversion

Phase inversion is a phase change of homogeneous polymer solution in a coagulation bath to form a solid structure under a controlled condition [7]. The cast homogeneous polymer solution is immersed into a non-solvent coagulation bath. The exchange between solvent and non-solvent causes a precipitation of polymer. In addition, the structure of phase inverted polymer depends on the solvent-non solvent exchange rate. For the fast exchange rate, an instantaneous demixing takes place in the phase inversion, consequently resulting in membrane with finger-like structure. On the other hand, the slow exchange rate called delayed demixing precipitating results in membrane with sponge-like pore structure as illustrated in Figure 6.

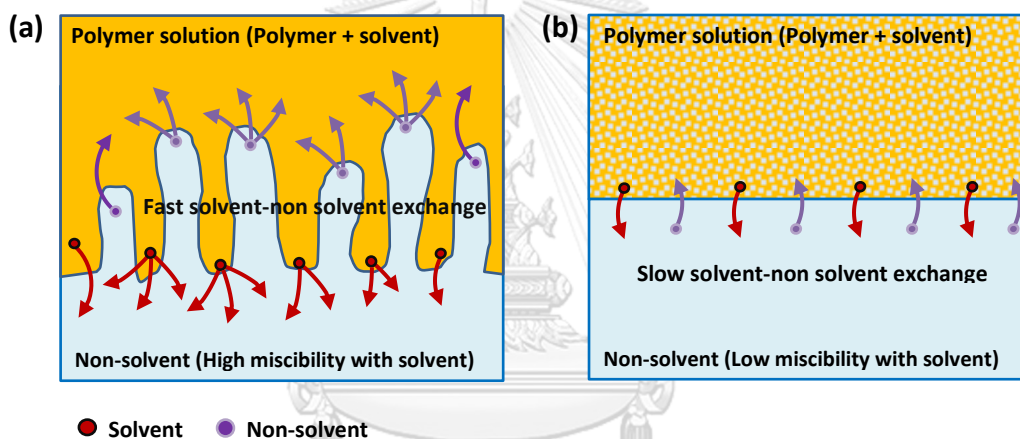


Figure 6 Porous support structure from phase inversion with different rate of demixing

(a) instantaneous demixing (b) delayed demixing.

Interfacial polymerization (IP)

Polyamide (PA) thin film layer can be synthesized on the support layer via an interfacial polymerization (IP) reaction of a monomer pair containing amine functional group in one monomer and acyl chloride in the other. The acyl chloride is dissolved in organic phase and the diamine is dissolved in an aqueous phase. These two reagent solutions are immiscible in each other; therefore, once they are brought in contact the reaction is taking place at the interface of the immiscible solutions forming a polyamide thin film on the support. Monomers frequently used for IP

reaction are m-phenylenediamine (MPD) (in water) and 1,3,5-Benzenetricarbonyl chloride (TMC) (in n-hexane). Their reaction is shown in Figure 7.

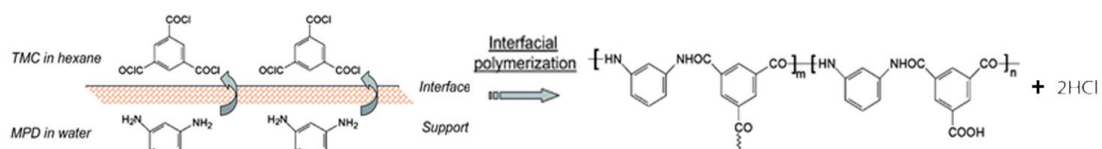


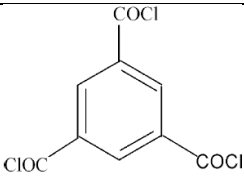
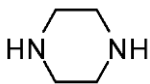
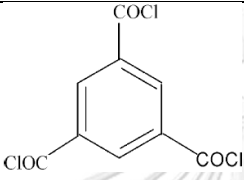
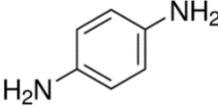
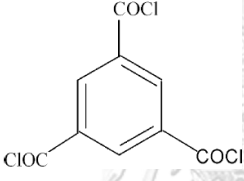
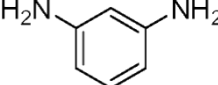
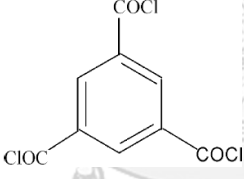
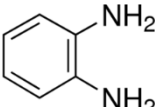
Figure 7 Interfacial polymerization reaction [8].

The fabrication of PA thin film to achieve a desired performance depends on fabrication conditions such as monomers pair, monomers concentrations, drying time, and reaction time of IP reaction.

(1) Monomer pairs

A various pairs of acyl chloride in organic phase and diamine in aqueous phase were used as reactants for IP reaction. To investigate the effects of chemical structures of the amine counterpart, various diamine monomers, including piperazine (PIP), p-phenylenediamine (PPD), m-phenylenediamine (MPD), and o-phenylenediamine (OPD) were paired with TMC. The ratio of TMC/diamine is controlled at 0.05/0.5 by mass [9]. The results revealed that amine chemical structures highly have an influence on the final membrane properties. TMC/MPD pair yielded the most outstanding performance with 99% of NaCl salt rejection and $22 \text{ Lm}^{-2}\text{hr}^{-1}$ of water flux while the other diamines owned lower salt rejection (see Table 2) [9]. Membranes prepared from aromatic amine monomers (PPD, MPD, and OPD) performed higher salt rejection compared to the alicyclic amine like PIP. The aromatic diamine could form a denser film by stacking the aromatic rings. Moreover, the different position of amine isomeric altered the PA film formation with different degree of cross-linking that results in different permeance and selectivity [10].

Table 2 the comparison of TMC monomer paired with amine monomers

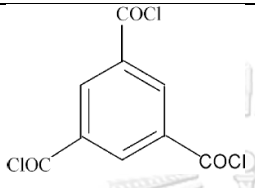
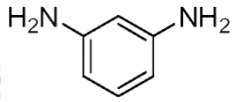
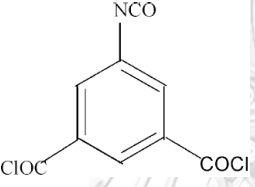
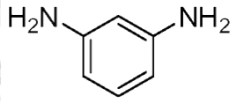
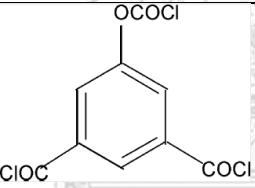
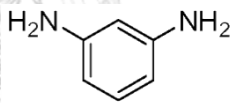
Monomer pair (Acyl chloride/Amine)	Acyl chloride Structure	Amine Structure	NaCl rejection	Water flux ($\text{Lm}^{-2}\text{hr}^{-1}$)
TMC/PIP			53%	50
TMC/PPD			90%	25
TMC/MPD			99%	22.5
TMC/OPD			63%	20

*Operating condition: Cross-flow with 15.5 bar pressure and 0.8 l/min of feed (2000 ppm of NaCl as feed)

Likewise, different types of acyl chloride, trimesoyl chloride (TMC), 5-isocyanatoisophthaloyl chloride (ICIC) and 5-chloroformyloxy-isophthaloyl chloride (CFIC) paired with MPD was investigated. It revealed that TMC/MPD was the most appropriate pair of monomer for IP reaction with high NaCl salt rejection (almost 99%), reasonable water flux and the highest chlorine tolerance. This was because of its tight chemical structure of the cross-linked PA film compared with that of other pairs [11]. Even though TFC membrane from ICIC-MPD pair gained the highest water permeance at comparable salt rejection, this membrane exhibited the least chlorine tolerance due to the existing of $-\text{NHCONH}-$ and $-\text{NHCOOH}$ groups that make it easy for N-chlorination [11]. In short, TMC/MPD pair was frequently chosen

for IP reaction due to its distinguished performances and chlorine tolerance compared to the other pairs.

Table 3 the comparison of MPD monomer paired with acyl chloride monomers

Monomer pair (Acyl chloride/Amine)	Acyl chloride Structure	Amine Structure	NaCl rejection	Water flux ($\text{Lm}^{-2}\text{hr}^{-1}$)
TMC/MPD			98.5%	55
ICIC/MPD			98.6%	63
CFIC/MPD			98.7%	45

*Operating condition: Cross-flow with 16 bar pressure and 1 l/min of feed (2000 ppm of NaCl as feed)

(2) Monomers concentration

Monomer concentration is one of important parameters determining cross-linking degree of PA and thus the separation performance of the final membranes. In general, MPD is provided in excess compared to TMC to enhance the diffusion of MPD crossing the diffusion resistance of nascent PA thin film to further react with TMC in the reaction zone. The influence of MPD monomers concentration was widely examined [12]. The results revealed that the suitable concentration range of MPD to obtain the sufficient cross-link degree of PA with reasonable salt retention and permeability is 1 to 2 wt%. Similarly, 0.1 to 0.2 wt% of TMC was the proper range to obtain 94 – 96 % of salt rejection. Moreover, the optimum molar ratio of MPD to TMC range for a good cross-link was 24 - 50 while the excessive ratio

(higher than 60) lowered the percentage of salt rejection due to the negative effect on PA formation [12].

(3) Reaction time

The duration of IP reaction is the one of the key factors, controlling the cross-linking degree of PA. Normally, the longer period of IP reaction allows the higher cross-linking degree of PA thin film. Insufficient reaction time can affect the insufficient degree of PA cross-link causing poor salt rejection performance while too long reaction time have no significant improvement of the performance due to the diffusion limitation of diamine monomers. Klaysom et al., indicated that after 20 second of the reaction time for TMC/MPD pair on polyacrylonitrile (PAN) support, the sufficient degree of dense PA thin film cross-link was formed with 94% of NaCl rejection and $0.88 \text{ Lm}^{-2}\text{h}^{-1}\text{bar}^{-1}$ of permeability [12]. At longer period of reaction, the salt rejection gradually increased while the permeance slightly reduced to $0.71 \text{ Lm}^{-2}\text{h}^{-1}\text{bar}^{-1}$ [12].

(4) Additives

Sodium dodecyl sulfate (SDS)

SDS is known as a wetting agent or anionic surfactant added into an aqueous solution for interfacial polymerization to achieve a proper wettability of substrate or support layer and improve a transportation of monomers from the organic phase to the inorganic phase [13]. A proper concentration of SDS in organic phase (0.1 - 0.2 wt%) led to an improved flux and salt rejection of the overall TFC performance [12, 13]. However, an excess amount of SDS could also lead to a defect in PA thin film due to the formation of SDS micelles. Whereas, a lower quantity of SDS (lower than 0.1% w/v) has insignificant effect for the TFC formation and performance of final membranes [14]. The concentration of 0.1%w/v SDS was recommended to achieve a proper salt rejection and water flux without defects or cracked surface [13].

Triethylamine (TEA)

During IP reaction, hydrochloric acid (HCl) is produced as a by-product, which can protonate the diamine monomers in organic phase and reduce the IP rate as

shown in Figure 8 [15]. TEA is a widely used as an acid acceptor to eliminate the acid by-product in the IP reaction to prevent the protonation of diamine monomers. Furthermore, TEA can keep the reactivity of diamines by controlling the proper basicity range, pH of 9.0 of the organic phase solution and promote a thicker formation of PA thin film [16, 17]. Typically, 0.5-2.0 wt% of TEA was recommended to be added in MPD solution [18].

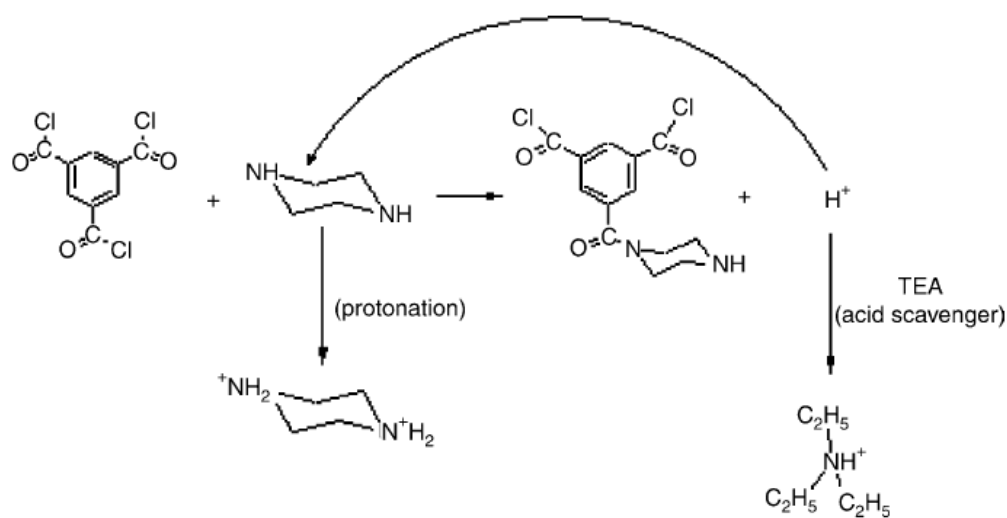


Figure 8 The acid scavenged by TEA (acid acceptor) in IP reaction [15].

Ethanol

The IP reaction between two monomers at the immiscible interface of water-organic solutions is mainly controlled by the amine monomers diffusion onto the organic side of the solutions interface. The utilization of alcohol can extend the miscibility zone of organic-water-ethanol [19]. Moreover, a presence of ethanol can act as a mild swelling agent for the PA nascent film, allowing easy diffusion of diamine molecules to the miscible zone [20]. As a result, the transport of amine monomer to react with acyl chloride in the organic phase was enhanced. It was believed that the amine monomer could thus fulfill a surface ridge-and-valley voids and resulted in smoother membrane surface [20]. In conclusion, the addition of alcohols can affect the thickness, properties and surface morphology of PA thin film by enhancing the solubility and diffusivity of diamine monomers through the interface [20]. Khorshidi et al., proved that the presence of 6 wt% ethanol could lower the surface contact angle of PA thin film from $62.5 \pm 3.7^\circ$ to $49.0 \pm 4.1^\circ$ and also lower

the root mean square surface roughness from 156 ± 12 nm to 131 ± 12 . Moreover, water flux was improved from $14.5 \text{ Lm}^{-2}\text{h}^{-1}$ to $30 \text{ Lm}^{-2}\text{h}^{-1}$ without a decline of salt rejection.

(5) Support layer properties

PA thin film is normally fabricated on a support layer to enhance the overall mechanical strength of the membrane. Thus, the properties of a support layer also play an important role for IP reaction. The hydrophilicity and pore size of the support greatly influence the morphology of the result PA film. Since, the amine aqueous phase must be impregnated by the support layer. The pore size and porosity of the support for aqueous phase to diffuse and fill in thus have a great influence on IP reaction and stability of resultant thin film. Commonly, 1 to 100 nanosize pores are difficult for aqueous phase to wet because of the Laplace pressure (pressure difference between inside and outside of the pores) but provide a stable interface during evaporation. While micro pore sized are easy for aqueous to fill in and wet but also too easy for removal and evaporation leading to an unstable interface [21]. Similarly, the hydrophilicity of the porous support also has a crucial influence for wetting step. The hydrophilic support is readily wetted and might stably formed a thin water layer on top of the support leading to an uniform IP reaction over the support surface better than the hydrophobic which tends to restrict the water inside the pore [22]. Hence, the hydrophilic with nanopore support layer is satisfied for amine aqueous wetting prior IP reaction.

2.1.4 Membrane Fouling

Fouling is the depositions of foulants accumulated on the membranes surface or inside the membrane pores resulting in drastically decline of permeate flux and loss of product quality. An example of permeance decay after a period of operation and permeance recovery after cleaning of nanofiltration membrane in fouling evaluation is shown in Figure 9.

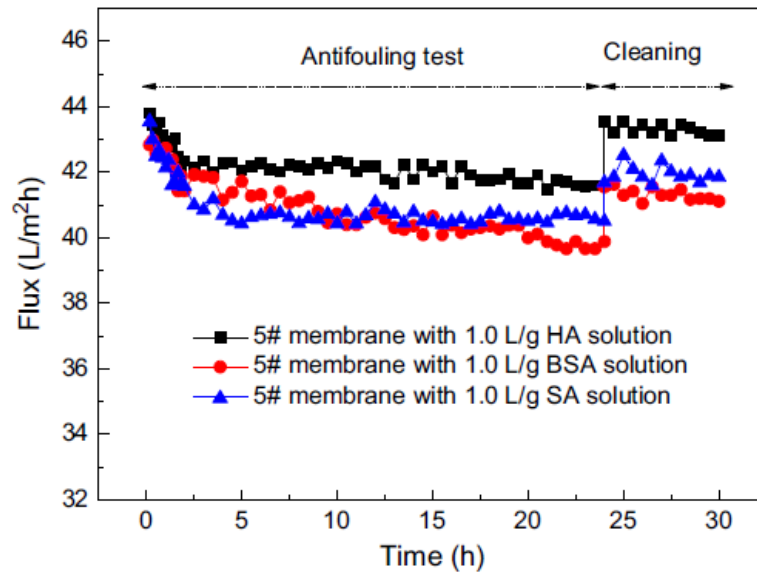


Figure 9 Time dependent fluxes of tannic acid and TMC composite nanofiltration membrane in antifouling evaluation [2].

The variables associated with membrane fouling evaluation are flux decay ratio and flux recovery ratio explained as follows.

Flux decay ratio is a ratio of the declined flux of the initial flux which can be calculated by the following equation.

$$DR = \left(\frac{J_{w0} - J_{wt}}{J_{w0}} \right) \times 100 \quad (3)$$

where DR is the flux decay ratio (%), J_{w0} is the initial water permeate flux ($\text{Lm}^{-2}\text{h}^{-1}$) and J_{wt} is water permeate flux at time t ($\text{Lm}^{-2}\text{h}^{-1}$).

The flux recovery ratio (FRR) compares the water permeate flux of after cleaning the used membranes and the water permeate flux of the fresh one. High percentage of FRR implies the good anti-fouling property of membrane. The FRR can be calculated by following equation;

$$FRR = \left(\frac{J_{wi}}{J_{w0}} \right) \times 100 \quad (4)$$

where FRR is the flux recovery ratio (%), J_{wi} is the water permeation flux after cleaning ($\text{Lm}^{-2}\text{h}^{-1}$).

The mechanisms of fouling depend on membrane category. For porous membranes as in MF and UF, foulants are absorbed and clogged into the pores and on the surfaces while for dense membranes as in NF and RO, foulants always deposit on the surfaces as illustrated in Figure 10. Therefore, RO and NF fouling are dominantly related to the foulants-surface interaction [23].

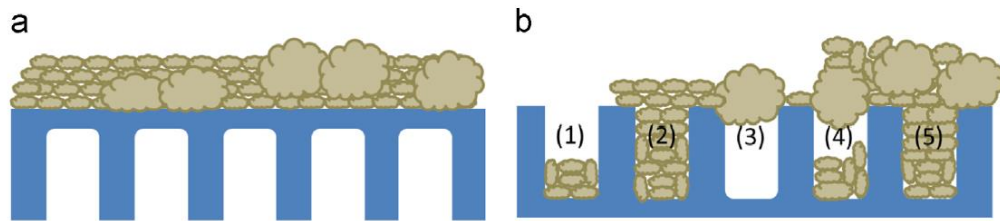


Figure 10 (a) surface fouling for dense membrane and (b) internal and surface fouling for porous membrane [24].

Great effort has been paid to investigate the causes and preventions of fouling on membranes surface. The deposition of foulants is a complex phenomenon involving physical and chemical properties of both foulants and membranes. Normally, the factors affecting fouling rate can be classified into; hydrodynamic condition, compositions and properties of feed, and membrane surface properties.

Factor affecting fouling rate

(1) Hydrodynamic conditions

Hydrodynamic conditions such as velocity of fluid flow, water flux and operating temperature have a great influence on the fouling rate. The acceleration of fluid velocity tends to reduce the fouling rate because, an increased shear force of fluid flow help dragging foulants away from the membrane surface. On the other hand, the process operation with a larger volume of water permeance and high temperature tends to promote fouling rate they induce the conversion of foulants to the membrane surface.

(2) Compositions and properties of feed

Feed water characteristics such as types, concentrations, physical properties, chemical properties and interactions of foulants also have a strong impact on the rate of fouling.

Generally, foulants can be classified into scale, slit, biofoulant and organic foulant. Three types of foulants commonly used in research studies include bovine serum albumin (BSA), humic acid (HA) and sodium alginate (SA) for representing protein, humic substance and polysaccharide respectively (properties shown in table 4). Thus, to prolong the membrane lifetime, membrane properties are needed to be modified in accordant to these foulants charge and properties.

Table 4 foulants properties [23, 25]

Foulant	Category	Charge (at pH 6-8)
BSA	Protein	Negative
HA	Humic substance	Negative
SA	Polysaccharide	Negative

The organic foulants, including biomacromolecules such as BSA and natural organic matter (NOM) such as HA and SA, were categorized as non-migratory foulants. Non-migratory foulants can deposit and form a fouling cake layer by foulant-membrane and foulant-foulant interactions in either specific or non-specific forms. For the specific interaction, covalent bonds can be formed between the specific functional groups of foulants such as metal-carboxyl and amino-carboxyl, while non-specific interactions are the foulants-membrane surface interactions forming hydrogen bonds, van der Waals interaction, adhesion and electrostatic attraction [26]. In waste water purification application, the feed solution containing proteins and NOM molecules is always in pH range of 6-8, which is over their iso-electric points so they are in a negatively charged [23, 25]. Thus, these foulant molecules are easily absorbed on a hydrophobic surface and tend to have more electrostatic interaction with positively charged surface.

(3) Membrane surface properties

Foulants can be deposited to the surface of membrane by hydrophobicity interaction, van der Waals interaction, hydrogen bonding and electrostatic force. Therefore membrane surface properties such as hydrophilicity, surface roughness and surface charge have a great impact on foulants deposition rate and tendency [27]. The membrane properties to repel foulants can be easily improved via the modification of membranes surface. Effects of each parameter are discussed in detail as follows

(i) Hydrophilicity

The hydrophilicity of membrane surface is one of major causes for fouling deposition. Generally, hydrophilic surface exhibit good fouling resistance to most foulants which are hydrophobic. A hydrophilic membrane surface with high surface tension induces a thin water layer boundary on their surface, forming hydrogen bonds with water molecules so that it is hard for hydrophobic molecules (foulants) to break such layer [28].

(ii) Surface roughness

It is well acknowledged that rough surface could promote an adhesion of two surfaces. Bowen and co-workers investigated the surface roughness on surface-colloidal particle adhesion. They found that the adhesion force between the surface and colloid (foulant) was reduced by the smoother membrane surface [29]. In addition, the film at thinner “valleys” regions (see Figure 11) locally has higher flux than the thicker “ridges” regions. Therefore, the valley regions may more likely to initiate the deposition of foulants [30].

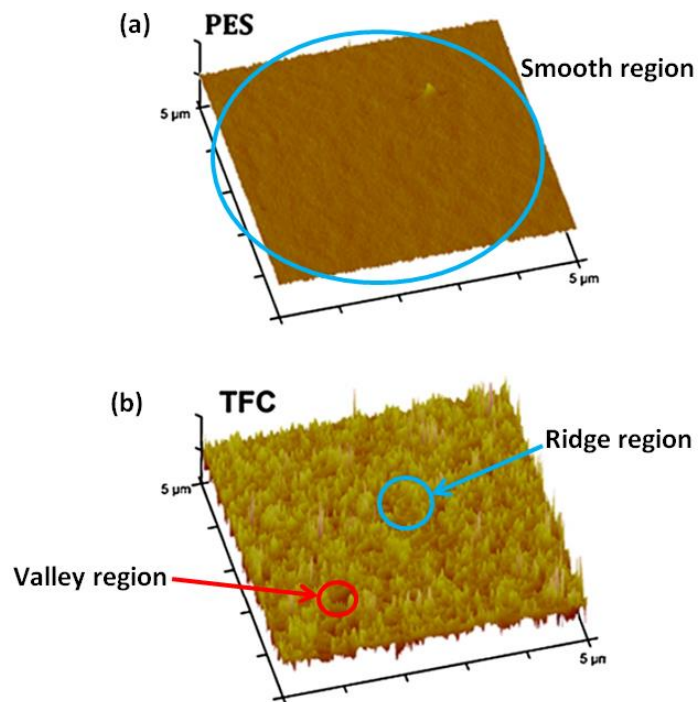


Figure 11 Surface morphology from an AFM of (a) smooth surface of polyethersulfone (PES) support layer (b) ridge and valley formation of TFC membrane surface from AFM technique [31].

(iii) Surface charge

The surface charge of UF, NF and RO membranes is often modified to be a negative charge for enhancing rejection of dissolved salts and foulants, which mostly have negative charges. The reduced foulant adsorption on the charged membrane surface is mainly due to the electrostatic repulsion of the similar charge between the surface and foulants [32].

2.2 Literature review

This section reviews the recent research developments on TFC membranes, focusing on the strategies applied to enhance anti-fouling properties of the membrane.

Recent development of fouling resistance membranes

In order to modify membranes performance, various types of additive have been applied to the selective layer of membranes to improve desired characteristics of the membrane surface such as hydrophilicity, smoothness, surface charge and functionality. Various types of nanoparticles with different characteristics and properties were applied to the PA thin film selective layer, forming thin film nanocomposite (TFN) to achieve the better membranes performances and extend their life-span as shown in Table 5.



Table 5 performance of modified thin film nanocomposite membranes.

Monomer pair	Filler		Contact angle (°)	Surface roughness (RMS,nm)	Testing conditions: solution (concentration) pressure	Performance		Anti-fouling test			Ref.			
	Type (phase it was dispersed in)	Content (wt%)				Rejection (%)	Pressue-normalized water flux (L/m ² .h.bar)	Feed	Flux Decay (%)	Flux Recovery (%)				
TMC/MPD	SiO ₂ non-porous (TMC)	0	57.1	135.5	NaCl (2000ppm) 20.68 bar	98.1	1.38	N/A	N/A	N/A	[33]			
		0.005	46.2	N/A		N/A								
		0.01	40.7	97.4		1.36								
		0.025	36.1	97.4		1.55								
		0.05	31.7	97.3		1.67								
	SiO ₂ porous, MCM-41 (TMC)	0.1	30.6	133.9	97.7	1.74	N/A	N/A	N/A	N/A				
		0.005	41.8	135.6	97.6	1.61								
		0.01	35.8	156.2	97.9	1.89								
		0.025	30.9	159.8	97.9	2.06								
		0.05	28.8	169.1	97.8	2.26								
TMC/MPD	SiO ₂ (MPD)	0.1	27.9	N/A	NaCl (11000ppm) 44 bar	97.8	2.25	NaCl (11000ppm)	31.0	10.0	16.0	13.0	15.0	0.0
		0	82.0			92.5	0.73							
		0.005	N/A			96.5	0.75							
		0.01	79.2			95.5	0.83							
		0.05	61.9			91.3	0.90							
		0.1	56.9			92.5	1.12							
		0.5	N/A			89.6	1.01							

Table 5 performance of modified thin film nanocomposite membranes (continue).

Monomer pair	Filler		Contact angle (°)	Surface roughness (RMS,nm)	Testing conditions: solution (concentration) pressure	Performance			Anti-fouling test			Ref.
	Type (phase it was dispersed in)	Content (wt%)				Rejection (%)	Pressure-normalized water flux (L/m ² .h.bar)	Feed	Flux Decay (%)	Flux Recovery (%)		
TMC/DA	CNTs (DA)	0	65.5	N/A	MgCl ₂ (2mol/L) 1 bar	N/A	5.8	HA (5mg/L)	53.0	55.6	[36]	
		0.01	67.5				N/A		N/A	N/A		
		0.05	65.1				8.9		29.4	79.8		
		0.1	67.3				N/A		N/A	N/A		
TMC/MPD	GO (MPD)	0	63.7	N/A	DI water 8 bar	N/A	2.35	Natural water	26.0	N/A	[38]	
		0.004	57.2				2.91		10.5			
		0.008	56.4				2.61		16.2			
		0.012	55.0				2.51		7.1			
TMC/MPD	TiO ₂ (TMC)	1	N/A	N/A	MgSO ₄ (2000ppm) 6 bar	88.9	1.92	N/A	N/A	[30]		
		3					93.8				1.63	
		5					96.4				1.45	
		7					38.6				11.55	
		9					26.6				12.85	
TMC/MPD	TiO ₂ (MPD)	0	79.0	95.0	NaCl (2000ppm) 7.58 bar	50.0	1.62	N/A	N/A	[39]		
		0.1	69.8				1.48					
		0.005	75.8				1.73					
		0.05	62.7				2.70					
		0.1	59.0	72.0		33.5	3.56					

*Remark: Dopamine hydrochloride (DA)

Table 5 performance of modified thin film nanocomposite membranes (continue).

Monomer pair	Filler		Contact angle (°)	Surface roughness (RMS, nm)	Performance		Anti-fouling test				Ref.
	Type (phase it was dispersed in)	Content (wt%)			Testing conditions: solution (concentration) pressure	Rejection (%)	Pressure-normalized water flux (L/m ² .h.bar)	Feed	Flux Decay (%)	Flux Recovery (%)	
TMC/MPD	TiO ₂ sol (MPD)	0	79.1	12.4	94.8	0.052	BSA (200ppm)		2.0	N/A	[40]
		1	78.1	N/A	93.4	0.155			2.5		
		3	N/A	N/A	94.1	0.219			N/A		
		5	N/A	N/A	95.6	0.361			N/A		
		10	N/A	N/A	95.0	0.613			N/A		
TMC/PIP	-	0	67.0	357	30.4	4.83	BSA (500ppm)		40.5	N/A	[41]
		0.005	54.7	134	33.0	5.47			22.8		
		0.005	50.4	107	35.6	5.10			26.1		
		0.002	54.3	164	35.6	5.80			19.5		
		0.005	52.9	37	36.6	6.06			8.7		
		0.01	51.3	80	34.5	6.14			10.1		
		0.02	47.2	112	35.3	6.11			14.3		

SiO₂ nanoparticles (NPs)

Silicon dioxide (SiO₂) nanoparticles (NPs) or nanosilica are known as a chemical-thermal-mechanical stable, low toxicity, hydrophilic and commercialized inorganic material [33]. Hence, SiO₂ NPs are widely used for various applications such as catalytic application, biomedical application, strengthening additive for composite materials and also as the filler for membrane modification.

SiO₂ (non-porous) and MCM-41 SiO₂ (porous) nanoparticles were applied to the PA layer on polysulfone (PS) support [34]. The presence of SiO₂ significantly lowered the contact angle from 57.1° to around 27.9° at 0.1 wt% loading [34] and flux decay ratio to 0% at 0.5 wt% loading [35] due to the ultra-high hydrophilicity characteristics. Besides, water permeability was enhanced with a slight reduction of salt rejection around 0.3 %. This was because of the lower degree of IP and microporous defect between NPs and polymer film (PA). However, the surface roughness of membranes was elevated due to the aggregation at the high loading SiO₂ (0.1 %). In addition, the MCM-41 SiO₂ resulted in higher hydrophilicity and water permeability compared to the non-porous one due to the shorter internal pathway for water molecules to diffuse through the pores of MCM-41 [34, 35].

Carbon nanotubes (CNTs)

Carbon nanotubes (CNTs), have also gained attention as the additive for composite membranes due to their high mechanical stability and anti-fouling property [36]. Furthermore, the unique tube structure of CNTs is considered to be flux enhancing paths to improve the water permeance without a salt rejection decline.

The incorporation of carbon nanotubes (CNTs) with PA thin film was examined through a FO process [37]. The performance results showed 55% of water flux and around 25% of flux decay and flux recovery were enhanced by the addition of 0.05 wt% CNTs, even though the hydrophilicity of the TFN membranes was reduced. The researchers claimed that the improved water flux might be attributed from the larger water uptake effect of the nanocorridors between the CNTs and polymer matrix [37].

Graphene oxide (GO)

One of the most popular nanoparticles in this decade is graphene oxide (GO). GO is a single layer of carbon nanosheet with covalent oxygen containing bonds [38]. GO has a great potential for membrane developments. In addition, GOs are flexible for chemical functionalization and high hydrophilic [39].

Graphene oxide (GO) was also cooperated to modify the PA thin film layer for natural organic matter removal in UF process [39]. The results revealed that the presence of GO could enhance membrane hydrophilicity (55° of contact angle at 0.012 wt%) and reduce flux decay ratio up to 20% (tested with natural water). The higher foulant repelling was attributed to the elevated hydrophilicity that enhanced water molecules bonding on membrane surface and prevents the foulant deposition. In addition, negative charges of GO repelled negatively charged foulants and thus reduced fouling tendency. Furthermore, the water flux of the modified membranes was enhanced about 10 – 30 % [39].

TiO₂ nanoparticles

Titanium dioxide (TiO₂) nanoparticles (NPs) are known as multifunctional nanoparticles due to its various advantages for many applications such as antibacterial, antiseptic, photo catalyst and hydrophilic additive. Furthermore, the TiO₂ NPs are commercial available. In membrane technologies, TiO₂ NPs are considered as an effective additive for improving hydrophilicity and anti-fouling property of TFC membranes [40].

TiO₂ and TiO₂-N-[3-(Trimethoxysilyl) propyl] ethylenediamine (AAPTS) nanoparticles cooperated in PA layer on a PES support were successfully fabricated [31, 40]. Commercial TiO₂ nanoparticles were dispersed in TMC solution before being contacted with aqueous MPD solution to perform IP reaction. The addition of TiO₂ improved the membrane hydrophilicity and also reduced the roughness of PA surface. It was found that 5 wt% of TiO₂ loading was the optimum ratio to accomplish the highest MgSO₄ salt rejection (96.42 %). To overcome the agglomeration of TiO₂ at the thin film, AAPTS silane coupling agent was grafted on the TiO₂ surface. The

modified TiO₂ (TiO₂-AAPTS) showed an improved dispersion compared to the unmodified TiO₂ which was confirmed by SEM image and EDX mapping analysis shown in Figure 12. The presence of silane functional group on TiO₂-AAPTS allowed amine molecules to diffuse onto their surface causing polydispersity of polymer chains that lead to more uniform distribution of TiO₂-AAPTS in PA layer. Furthermore, the higher loading of TiO₂-AAPTS changed the formation of PA surface from ridge-and-valley to leaf-like morphologies and smoothed the PA surface by fulfilling of TiO₂-AAPTS. At highest loading (0.1%) of TiO₂-AAPTS the surface roughness of PA thin film was reduced from 95 nm to 72 nm [31]. However the obtained TFN membrane with 0.005% loading of TiO₂ AAPTS showed only a slight improvement in NaCl salt rejection from 50% to 53.83% and water flux from 12.25 to 13.13 Lm⁻²h⁻¹.



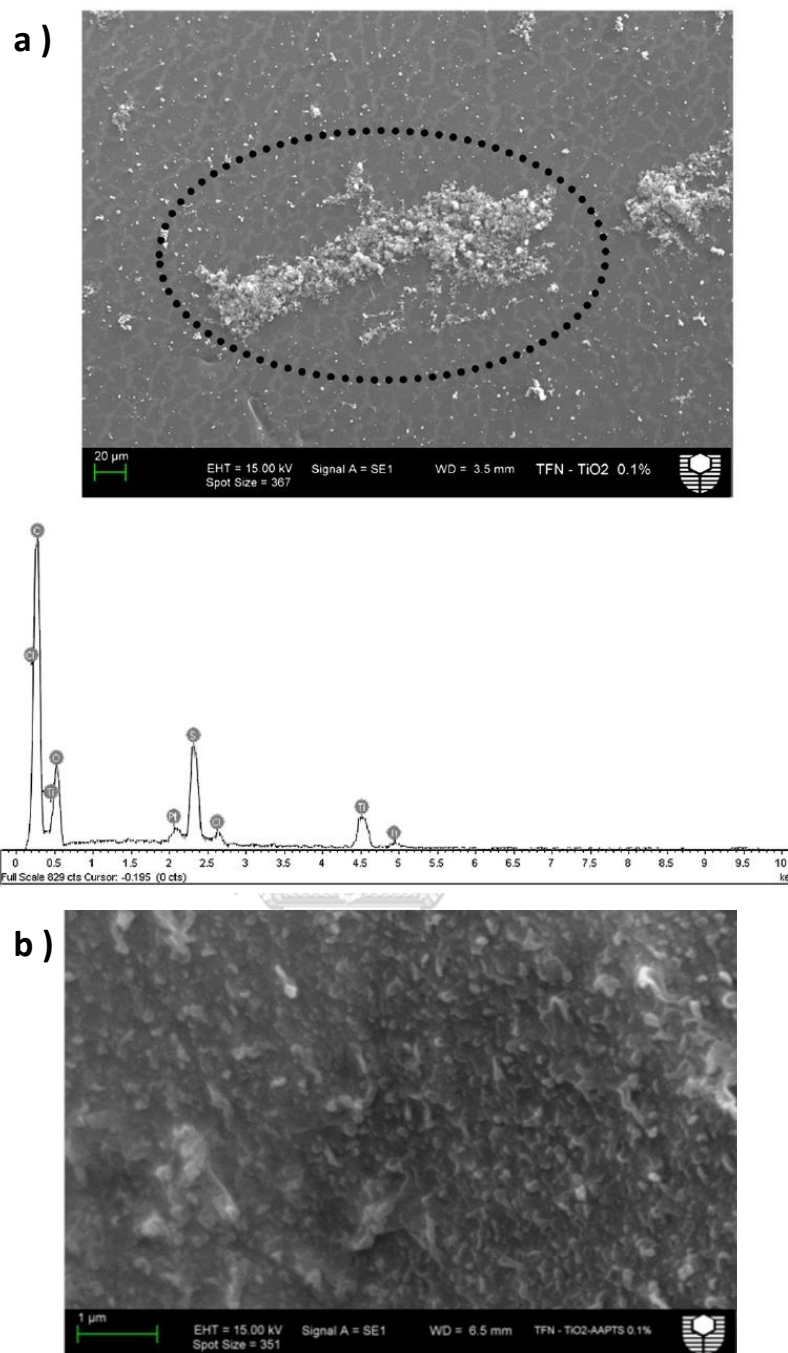


Figure 12 SEM images of a) 0.1 wt% loading of pure TiO₂ TFN with EDX analysis
b) 0.1 wt% loading of AAPT-TiO₂ TFN membrane[31].

TiO₂ sol was also used as an additive in an aqueous monomer solution forming TFN membranes. It was revealed that the addition of TiO₂ colloidal solution can also lower the contact angle about 1° at 1 wt% loading. In addition, water flux was increased about 1150% at 10 wt% loading without a sacrifice of the salt rejection. This was due

to the impregnation of TiO₂ colloidal solution enhanced the dispersion of the nanoparticles on the PA thin film without loosening the film structure. The investigation on fouling resistance of these TFN membranes revealed that the impregnation could mitigate the deposition of BSA on membrane surface [41].

Combinations of TiO₂ nanoparticles on reduced GO (rGO/TiO₂)

The combination of reduced GO and TiO₂ was investigated as the filler in TFN membranes. TiO₂ NPs have antifouling, high hydrophilic, high chemical stability, low toxicity and photocatalytic properties [40] while rGO provides high hydrophilic due to the presence of OH functional groups [42]. Thus, the dual characteristics of rGO and TiO₂ were merged and expected to bring out their both profits on improving water flux and anti-fouling properties of membrane.

The combination of TiO₂ and reduced GO (rGO/TiO₂) was embedded in PA thin film to develop fouling-resistance of NF membranes [42]. The optimum amount of rGO/TiO₂ that can provide the best performances was at 0.005 wt% loading. Furthermore, the water contact angle and water permeability were increased from 67° to 52.9° and from 48.3 to around 60 Lm⁻²h⁻¹, respectively. Ultra-high hydrophilicity characteristics of the modified membranes can also lead to anti-fouling property, which can reduce the deposition of fouling [42].

From the literature study, various NPs were cooperated into PA thin film to improve the performance and anti-fouling properties of membranes via enhancing the hydrophilicity and smoothening surface roughness. Among those NPs, TiO₂ showed a great potential in improving both performance and fouling resistant of the membranes. However, most of NPs were added into the monomer solution in form of powder causing the poor dispersion and agglomeration [31]. TiO₂ in form of solution was recommended to directly added into the monomer solution to enhance its dispersion and [41]. However, there was still a lack in systematic investigation on how the addition of different forms of TiO₂ affect the formation of thin film and separation performance of the resultant film. In addition, there are still plenty rooms to further improve membrane property and performance via the addition of TiO₂.

CHAPTER 3

SCOPE OF WORK

This work attempted to fabricate thin film nanocomposite membrane (TFN) by incorporating TiO_2 via an interfacial polymerization (IP). TiO_2 colloidal solution was added in an aqueous amine solution to react with an acyl chloride monomer. To establish a good correlation on how the additives affect the IP reaction and properties of resultant membranes, a systematic investigation was designed.

3.1 Objectives

- To develop fouling resistant membranes by introducing TiO_2 nanoparticle to the selective thin film on polyacrylonitrile (PAN) support forming TFN membranes.
- To investigate the effects of the addition of TiO_2 colloidal solution in an aqueous monomer solution for interfacial polymerization (IP) on characteristics of polyamide (PA) thin film and membrane performance.

3.2 Scope of work

TFN membranes were prepared via an interfacial polymerization. TiO_2 colloidal nanoparticles were chosen as an additive in MPD solution. Effects of the filler addition on membrane properties were investigated. The detail and scope of this research are described as follows;

3.2.1 Membrane preparation and characterization

The PAN support layer and thin film layer were fabricated from a phase inversion and interfacial polymerization, respectively. The studied parameters are listed as follows

PAN support layer (Fixed parameter)

Polymer	:	Polyacrylonitrile (PAN)
Solvent	:	Dimethylformamide (DMF)

Polymer concentration : 16 wt%
 Casting thickness : 0.25 mm

Thin film layer (via an interfacial polymerization)

MPD solution : 2 wt% of m-phenylenediamine (MPD) in
 DI water

TMC solution : 0.15 wt% of 1,3,5-Benzenetricarbonyl
 chloride (TMC) in n-hexane

The addition of TiO₂ colloidal solution : 0–60 vol% of MPD solution

Fix additives in aqueous MPD solution : 2.0 wt% of TEA
 0.1 wt% of SDS

Additives for individual study : 0 - 1.8 vol% of Ethanol in MPD solution
 0 – 4.7 wt/vol% of commercial TiO₂ in
 MPD solution
 0 – 4.7 wt/vol% of dried TiO₂ colloidal
 solution in MPD solution
 0 – 30 vol% of dilute nitric acid with pH
 1.5 in MPD solution

Drying time prior IP reaction : 80 second

Reaction time of IP : 80 second

Membrane characterization

Surface chemical and functional group : Attenuated Total Reflectance Fourier
 Transform Infrared (ATR-FTIR)

Hydrophilicity of membranes surface : Contact angle

Membrane morphologies : Scanning Electron Microscope (SEM)

Membrane surface roughness : Atomic Force Microscope (AFM)

Membrane performance

Feed solution : Pure DI water and 2000 ppm of NaCl solution

Fouling agent : 1000 ppm of Sodium alginate (SA) in DI water

CHAPTER 4

RESEARCH METHODOLOGY

4.1 Materials

Polyacrylonitrile (PAN, Mw 150,000 Da), humic acid (HA, technical), Sodium dodecyl sulfate (SDS, $\geq 99\%$), Triethylamine (TEA, $\geq 99.5\%$), titanium (IV) oxide 21 nm (TiO_2 , $\geq 99.5\%$) and Bovine Serum Albumin (BSA, $\geq 98\%$) were purchased from Sigma Aldrich. N,N-dimethylformamide (DMF, anhydrous, 99.8%), n-hexane, sodium alginate (SA, AR) and titanium (IV) isopropoxide (TTIP, $\geq 98\%$) were obtained from Acros Organics and 1,3,5-Benzenetricarbonyl chloride (TMC, AR) while m-phenylenediamine (MPD, AR) were supplied from Merck.

4.2 Synthesis of TiO_2 colloidal solution

35.7 vol% of TTIP in ethanol was continuously dropped into 1.5 pH DI (Deionized) water to produce 5 vol% of TTIP in the solution. pH of the solution was controlled to 1.5 by using a dilute nitric acid. The solution was continuously stirred at room temperature until a clear solution was obtained. Particle size and surface charge of the obtained TiO_2 were measured by Master Sizer (Malvern, MAL1099376).

4.3 Fabrication of membranes

4.3.1 Synthesis of porous support layer

16 wt% of PAN in DMF was stirred at 60 °C until a homogeneous solution was obtained. The polymer solution was then cooled at room temperature. The PAN solution was cast on a backing support (Novotexx 2470 from Freudenberg Germany) with a controlled thickness of 0.25 mm. The cast film was immediately immersed in a coagulation bath to conduct a phase inversion with deionized (DI) water. The prepared support layer was stored in DI water at room temperature until use.

4.3.2 Fabrication of polyamide thin film composite

The TiO₂ solution was diluted with DI water to a desired concentration (0 – 60 vol% of TiO₂ solution) for use as a stock solution. 2 wt% of MPD, 0.1 wt % of SDS and 2 wt% of TEA were added into the stock solution under a stirring condition at room temperature to obtain the aqueous MPD monomer. The support layer was immersed in the prepared aqueous solution for 30 min. After the immersion, an excess solution on the support surface was removed and left to dry partially under a fume hood at room temperature for 80 second. Then, 0.15 wt/vol% of TMC in n-hexane solution was poured onto surface of the support impregnated with MPD to initiate the interfacial polymerization reaction for 80 second and the reaction was terminated by rinsing the membrane surface with n-hexane. The polyamide thin film composite was kept in DI water at room temperature. The effects of the individual components in TiO₂ colloidal solution (ethanol, nitric acid, TiO₂ NPs) on thin film formation were also investigated. For instance, 0 - 2.7 vol% of ethanol was added in the MPD aqueous solution.

4.4 Membrane characterizations

The prepared membranes were chemical and physical characterized with various techniques described below.

Surface properties

All of the membrane surface chemistry was characterized via Attenuated Total Reflectance Fourier Transform Infrared (ATR-FTIR, Malvern, Nicolet6700) to identify chemical and functional groups on polyamide thin film surfaces.

The hydrophilicity of membrane surface was investigated by using contact angle goniometer (DataPhysics, DataPhysics, OCA-Series). Field emission scanning electron microscope (SEM, JEOL JSM-7610F) was used to identify membrane morphologies; top surface, cross-sectional and elemental analysis while the surface roughness of membranes was investigated by Atomic Force Microscope (AFM, Veeco Methodology group, Dimension 3100).

4.5 Membrane performance test

The membrane performances were evaluated through a dead-end membrane module connected with N₂ gas feed tank for pressurizing the system shown in Figure 13.

4.5.1 Salt Rejection

2000 ppm of NaCl in DI water was used as the feed solution with pressurization of 5 bar. Salt concentration in the feed and permeance were measured by using a conductivity meter (InLab731, METTLER TOLEDDO). The salt rejection was estimated by Eq. (2).

4.5.2 Permeation flux

The permeation flux from the salt solution and pure DI water as a feed was tested via the same dead-end module in 4.4.1 at various applied pressure from 1-5 bar. The quantity of permeated water was recorded for calculating permeation flux expressed in Eq (1).

4.5.3 Anti-fouling performance

1000 ppm of SA foulant solution was used for the investigation of anti-fouling property of the synthesized membranes compared to the commercial NF membrane (DOW FILMTEC™ NF270, DOW). The test was set in the same dead-end system at 5 bar. The experiment was conducted for 4 h to observe the flux decline of the synthesized membrane. The fouled membrane was then stirred to wash with 750 ml of water for 10 minutes and then drained for 6 cycles of cleaning. Then the water flux after surface cleaning was conduct with DI water to indicate the recovery flux.

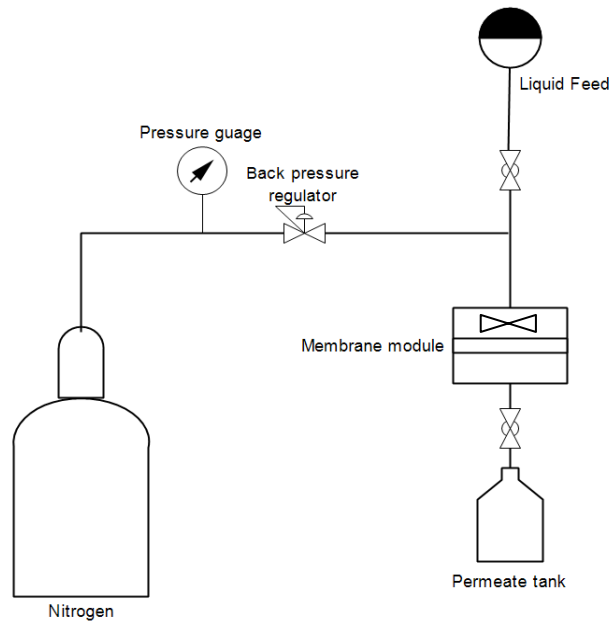
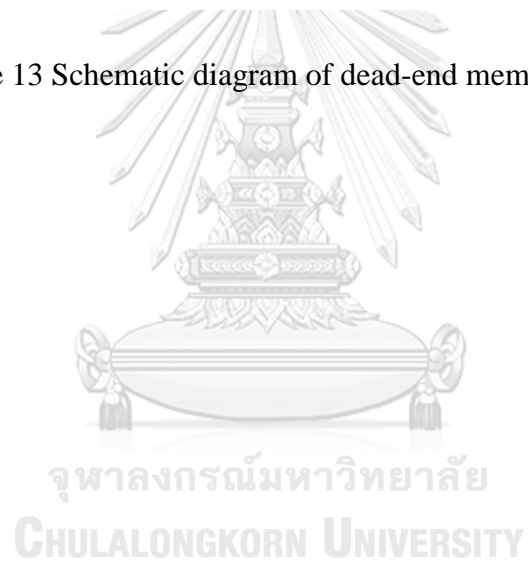


Figure 13 Schematic diagram of dead-end membrane module.



CHAPTER 5

RESULTS AND DISCUSSION

5.1 The influence of TiO_2 colloidal solution on the formation and performance of TFN membrane

TFN membranes were fabricated with different addition of TiO_2 colloidal solution, 0 - 60 % by volume. The effect of TiO_2 colloidal solution loading was studied through various characterizations, salt rejection and permeability.

Membrane morphology

The structure of bare PAN support on non-woven backing support is shown in Figure 14. The thickness of the support was measured to be around $130.8 \pm 4.3 \mu\text{m}$. The prepared PAN support layer is composed of a top dense skin layer ($2.8 \pm 0.6 \mu\text{m}$), an upper part layer with micro finger like pores ($12.8 \pm 3.3 \mu\text{m}$) and a lower part layer with macro finger like pores ($109.8 \pm 8 \mu\text{m}$). Figure 14 (b) illustrates the smooth top surface of the PAN support.

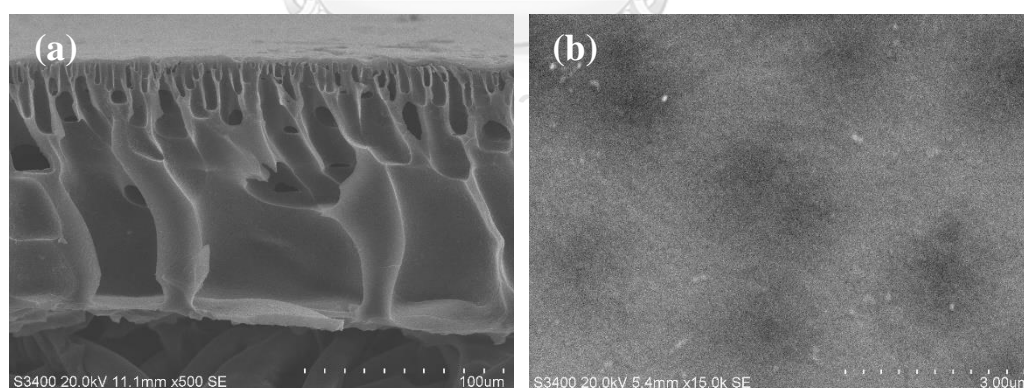


Figure 14 SEM images of PAN support structure (a) cross-sectional (b) top surface.

Figure 15 and Figure 16 demonstrate the SEM and AFM 3-dimensions images of surface morphology of TiO_2 - polyamide TFN membranes at 0%, 10%, 20%, 30% and 40% loading of TiO_2 colloidal solution, respectively. The bare polyamide thin film shows a rough surface formation called “ridge-and-valley” which has high degree of surface roughness. When TiO_2 solution was added up to 10 % loading, the

formation of thin film seems to form larger and rougher ridge-and-valley than the bare one. The observed change of formation mainly dominant by the relatively low amount of ethanol (lower than 1 wt%) that could cause multiple voids within the film [20]. Whilst at higher loading, the thin film morphology became smoother. The smoothed membrane surface might be caused by the co-effect of the multi components in aqueous MPD solution, consisting of TiO_2 NPS, ethanol and pH. The influence of each component as individual and combined was further clarified in the next sections.

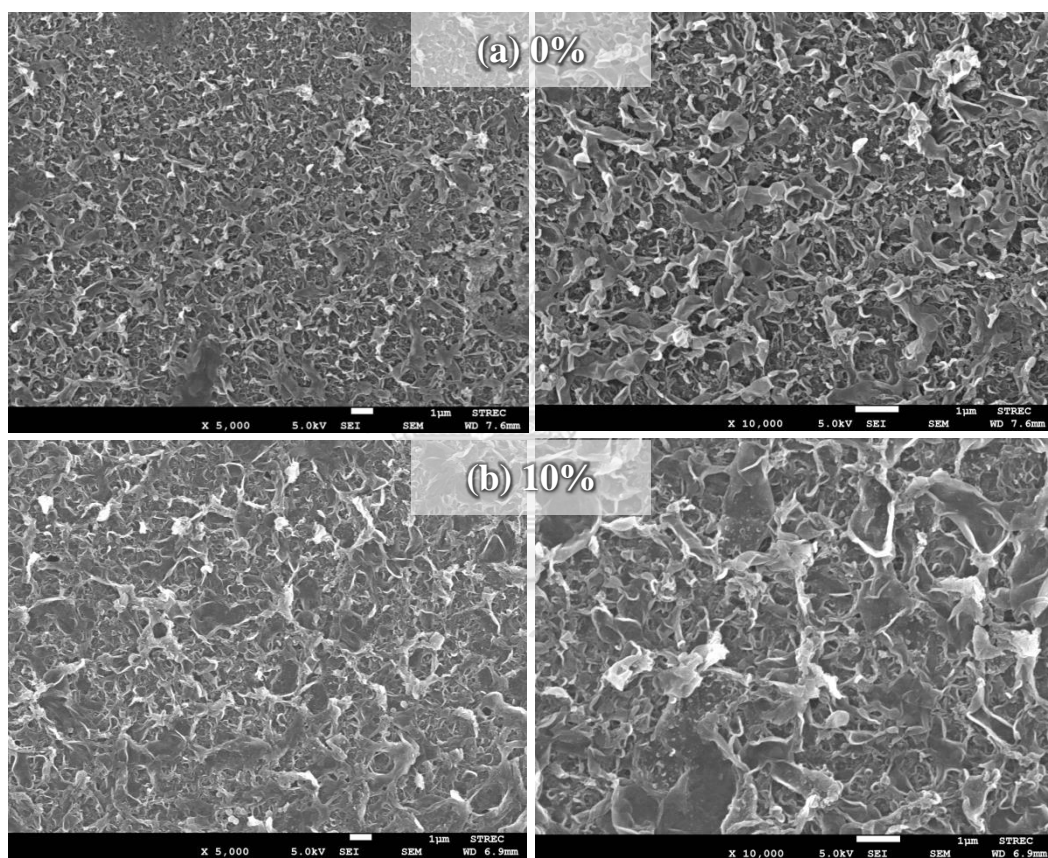


Figure 15 SEM images of top surface of TFN membranes at (a) 0 vol %, (b) 10 vol %, (c) 20 vol %, (d) 30 vol % and (e) 40 vol% loading of TiO_2 colloidal solution. The images in the left and right column were taken at 5,000 and 10,000 magnification, respectively.

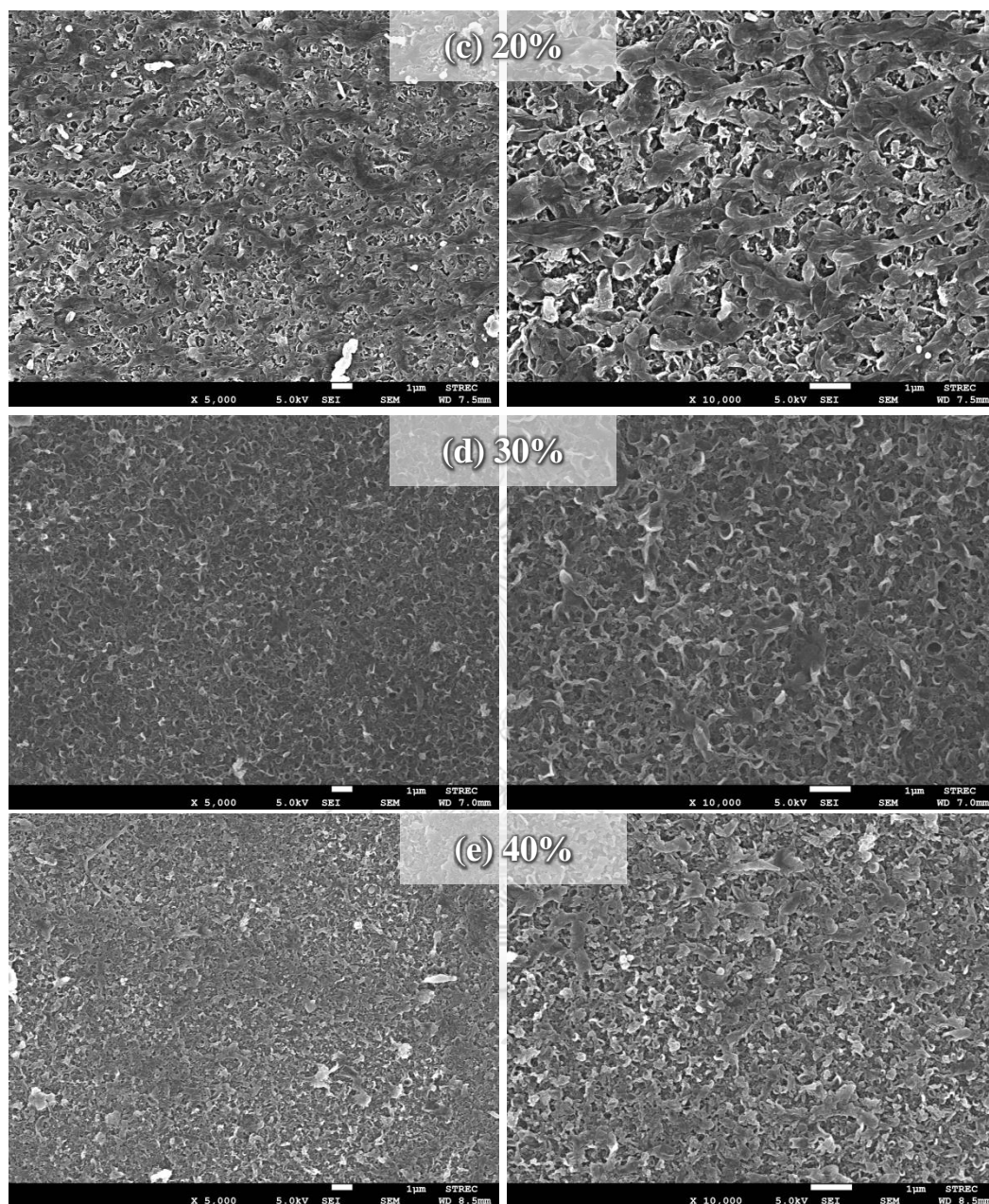


Figure 15 SEM images of top surface of TFN membranes at (a) 0 vol %, (b) 10 vol %, (c) 20 vol %, (d) 30 vol % and (e) 40 vol% loading of TiO₂ colloidal solution. The images in the left and right column were taken at 5,000 and 10,000 magnification, respectively (continued).

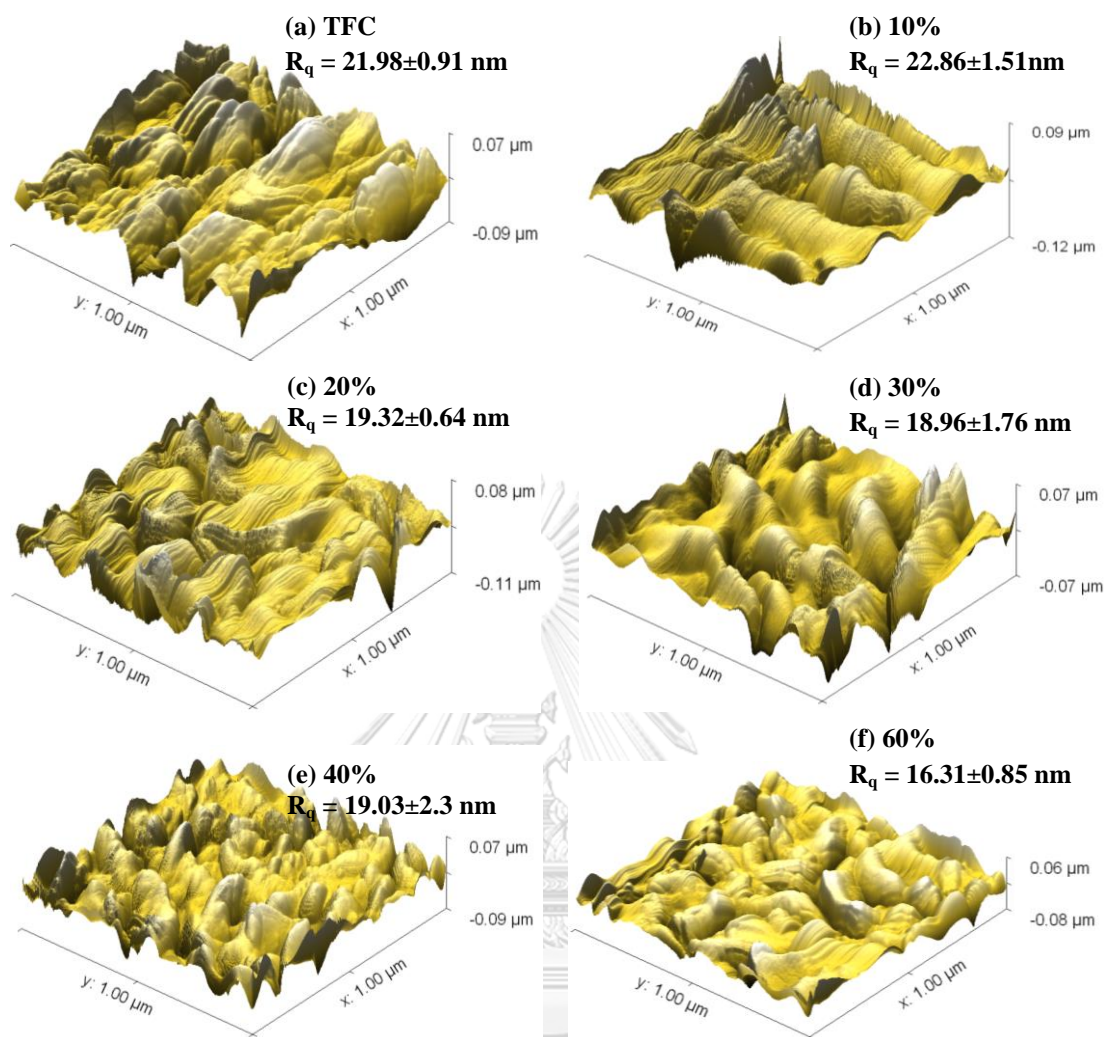


Figure 16 3-dimensions AFM images of TFN membranes at (a) 0 vol %, (b) 10 vol %, (c) 20 vol %, (d) 30 vol % and (e) 40 vol% loading of TiO_2 colloidal solution

Surface chemistry of the membranes

Figure 17 shows the ATR-FTIR spectra of TFN membranes at various ratio of TiO_2 solution loading. The spectrum indicates the surface chemistry of the fabricated membranes. The PAN support spectrum showed the characteristic peaks at 2938 cm^{-1} , 2243 cm^{-1} and 1452 cm^{-1} representing C-H stretching, $\text{C}\equiv\text{N}$ stretching and C-H bending, respectively. For TFN membranes, the peaks 1543 cm^{-1} , 1610 cm^{-1} and 1658 cm^{-1} were C-N stretching, aromatic ring breathing and C=O bonding of an amide group, respectively while a wide peak at 3320 cm^{-1} is -COOH function of carboxylic group on PA layer. The FTIR spectrum confirmed that the polyamide thin film was

successfully fabricated onto the PAN support and the different loading of TiO₂ has no effect to the surface chemistry of PA layer.

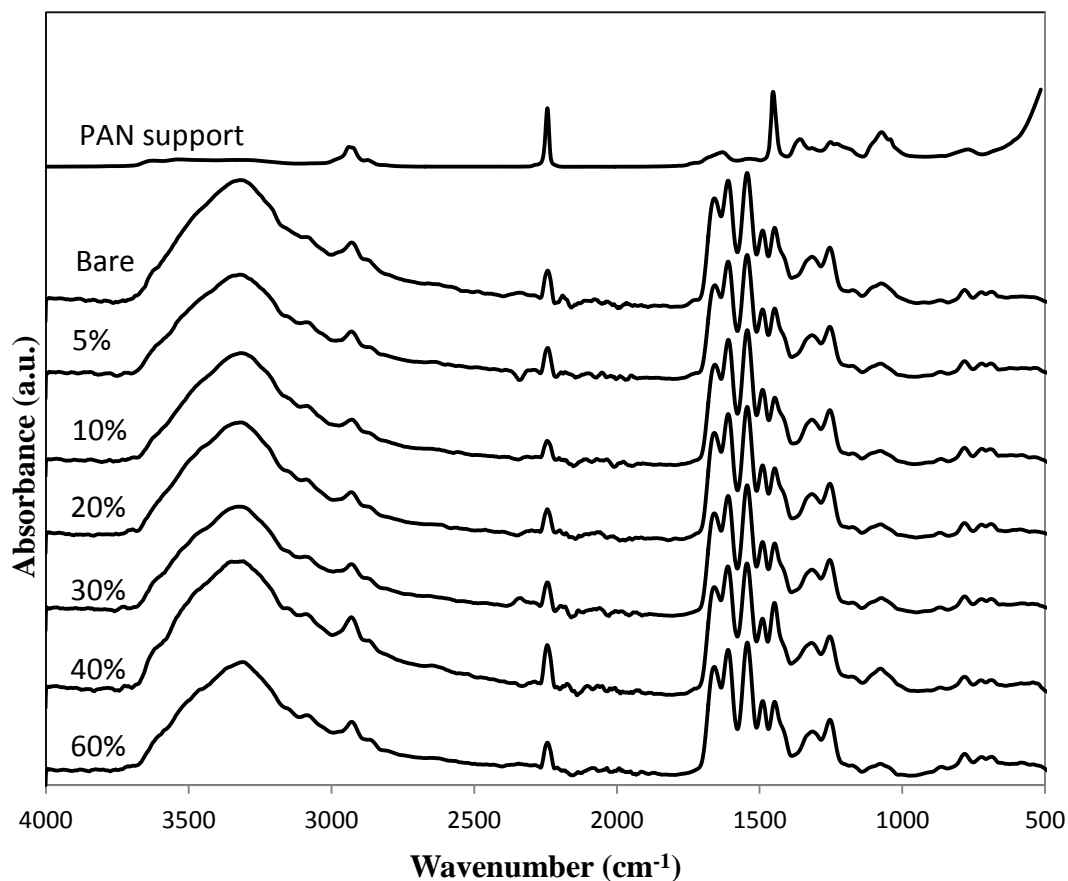


Figure 17 ATR-FTIR spectra of the TFN membranes loaded with different ratio of TiO₂ solution.

Hydrophilicity of membranes

The contact angle was operated to evaluate the surface hydrophilicity of the fabricated membranes. To indicate the hydrophilicity, 1 μ L of water was dropped onto the surface of membrane samples and the angle of water contacted on the membranes was then measured. A high angle between membrane and droplet interprets low hydrophilicity or high hydrophobicity of membrane surface while lower contact angle interprets higher hydrophilicity or hydrophilic of membrane surface.

Figure 18 presents the contact angle of TFN membranes with different loading of TiO₂ solution. The results show that the contact angles of droplet on the membrane surface reduced with the increased TiO₂ loading from $76.05 \pm 1.99^\circ$ to $51.83 \pm 6.91^\circ$

at 60%. In short, the hydrophilicity of bare PA layer is significantly improved by the addition of TiO_2 solution. The increased hydrophilicity of the modified membranes is due to the higher amount of embedded ultra-hydrophilic TiO_2 nanoparticles in the PA layer and the greater amount of oxygen derivative functional group left over on the PA surface from the nucleophile neutralization of TMC molecules in polymerization reaction. This result was in a good agreement with previous work concluded by Kin et al[41].

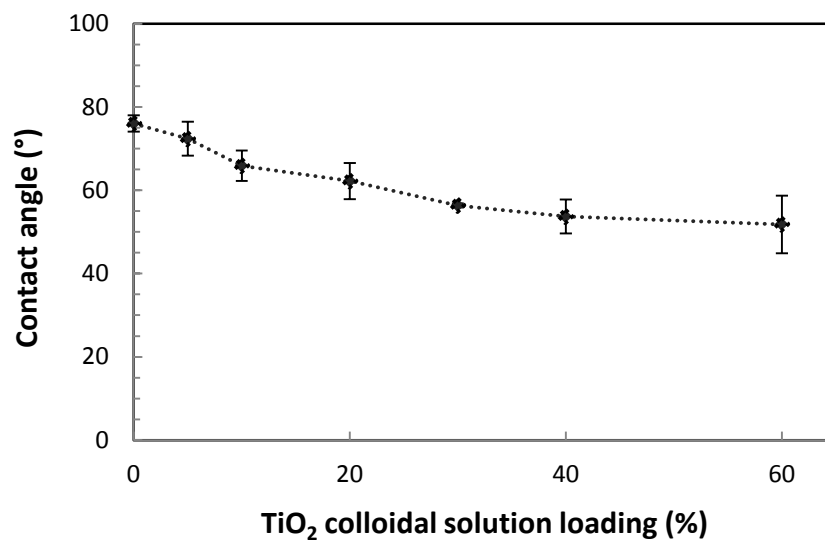


Figure 18 Contact angle of the TiO_2 solution loaded TFN membranes.

Performances of TFN membranes

The performance of fabricated membranes was tested by a dead end module at room temperature. Salt rejection and permeance of membranes was tested with 2000 ppm NaCl solution at 5 bar of feed pressure, whilst water permeability of membrane was measured with pure DI water at various feed pressures.

Figure 19 and 20 show NaCl rejection (R) and permeability (A) performances of TiO_2 loaded TFN membranes. The amount of TiO_2 colloidal solution added in MPD solution plays an important role in separation performance. As the loading was increased, the R of the fabricated membranes was gradually increased from 79.22% to the highest rejection (94.20%) at 20% loading. In contrast, too high loading of the

solution (more than 20%) could lead to the negative effect of drastically decline in R to 37.62% at 60% loading of TiO_2 as shown in Figure 19. The A of TFN membranes declined from 2.63 to 2.19 $\text{Lm}^{-2}\text{h}^{-1}\text{bar}^{-1}$ at 5% addition and then elevated to 2.94 $\text{Lm}^{-2}\text{h}^{-1}\text{bar}^{-1}$ at 20% loading before it gradually dropped as illustrated in Figure 20. The elevated R might be related to the co-influence of dropped pH from 12.35 to around 9.3 (see Figure 21) and also related to the higher quantity of ethanol that enhanced MPD monomer transport and polymerization. In fact, the NaCl rejection and permeability are normally traded-off to each other. However, in this work, both R and A seem to have similar trends. The results might be attributed from the combined-effect of ethanol, pH (nitric acid) and TiO_2 NPs containing in the colloidal solution. Therefore, by the individual effects of each component in TiO_2 colloidal solution was systematically examined.

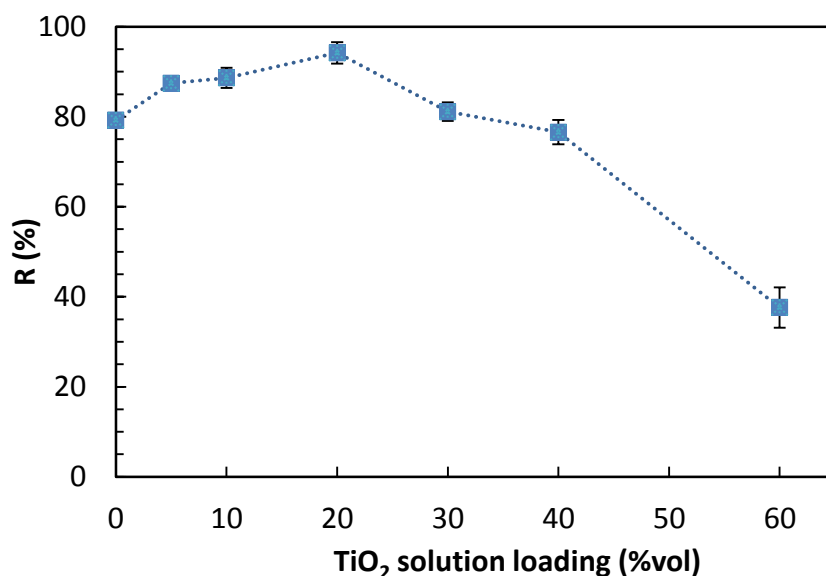


Figure 19 Salt rejection of TiO_2 solution loaded TFN membranes.

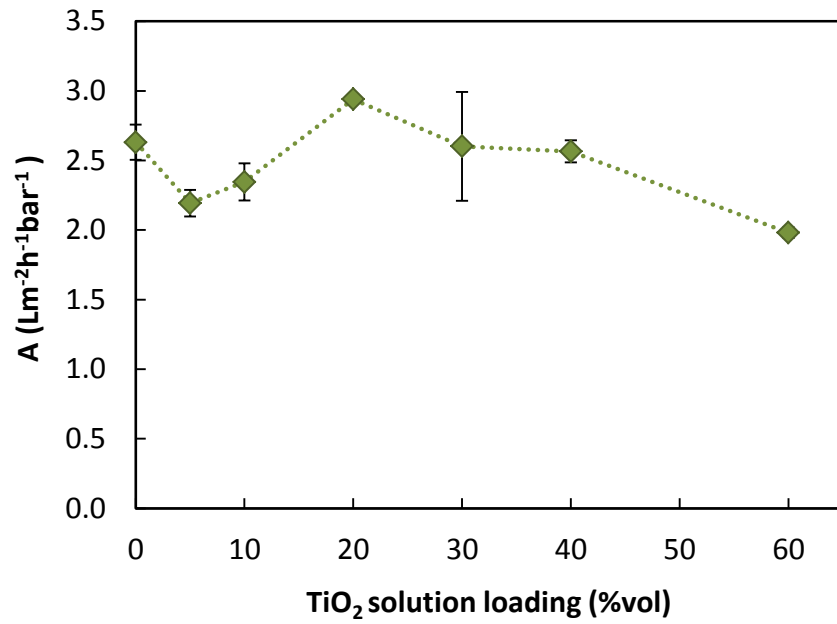


Figure 20 Permeability of TiO₂ solution loaded TFN membranes.

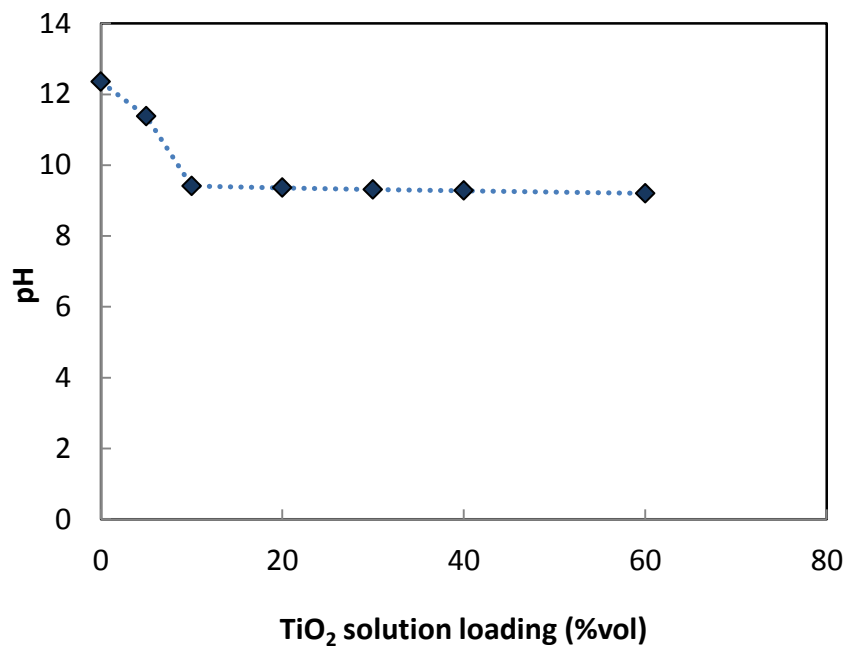


Figure 21 pH of MPD solution loaded with different TiO₂ solution ratio.

5.2 Effects of the individual component in TiO₂ colloidal solution

Since, the TiO₂ solution consisted of TiO₂ NPs, ethanol and dilute nitric acid, the observed thin film characteristics and performance could not be clearly explained that the change dominated from which factors. Thus, the study of individual components is of crucial. To observe the individual effect of each component in TiO₂ colloidal solution on membrane properties and performances, the concentrations of the studied components were duplicated from TiO₂ colloidal solution in aqueous MPD solution. The duplicated amount of each component presented in 0-30 vol% of added TiO₂ colloidal solution was summarized in Table 6. Moreover, the commercial TiO₂ were also studied to compare it effects on TFN membrane formation with the synthesized TiO₂.

Table 6 Summary of component composition in colloidal solution.

Vol % of TiO ₂ colloidal solution inn MPD aqueous solution	Composition		
	Ethanol (vol%)	pH (adjusted by nitric acid)	TiO ₂ (wt%)
0	0	12.35	0
5	0.45	11.39	0.79
10	0.9	9.41	1.57
20	1.8	9.36	3.14
30	2.7	9.31	4.71

5.2.1 Effect of ethanol

Membranes morphology and characteristics

The addition of ethanol is known as a chemical utilizer to promote the water-organic solubility and MPD monomer diffusion through the interface expected to improve the polymerization reaction and consequently change the polyamide surface formation and properties. Figure 22 and Figure 23 compares surface morphology and roughness of the bare TFC membrane and TFC membrane from MPD solution with 1.8 vol% loading of ethanol. When ethanol was added, the surface morphology of thin

film tended to be smoother. The observed change of PA surface can be explained by the extended miscibility zone water-n-hexane with the presence of ethanol that facilitated the diffusion of MPD monomer from water phase to polymerize with TMC over the interface as illustrated in Figure 24. In addition, the PA layer can be swelled by an ethanol allowing easier diffusion of MPD monomer through the nascent polymerized PA layer. As a result of the ethanol addition, the MPD transport is enhanced to react with TMC monomer over the polymerized thin film contributing to fulfill ridge-and-valley voids resulting in the smoother formation. The enhanced interfacial polymerization was confirmed by ratio of (-COOH)/(C-N) ratio estimated from characteristic peak of -COOH (from hydrolysis of -COCl) and (C-N) from amide group of cross-linked monomer (see Figure 25, Figure 26 and Table 7).

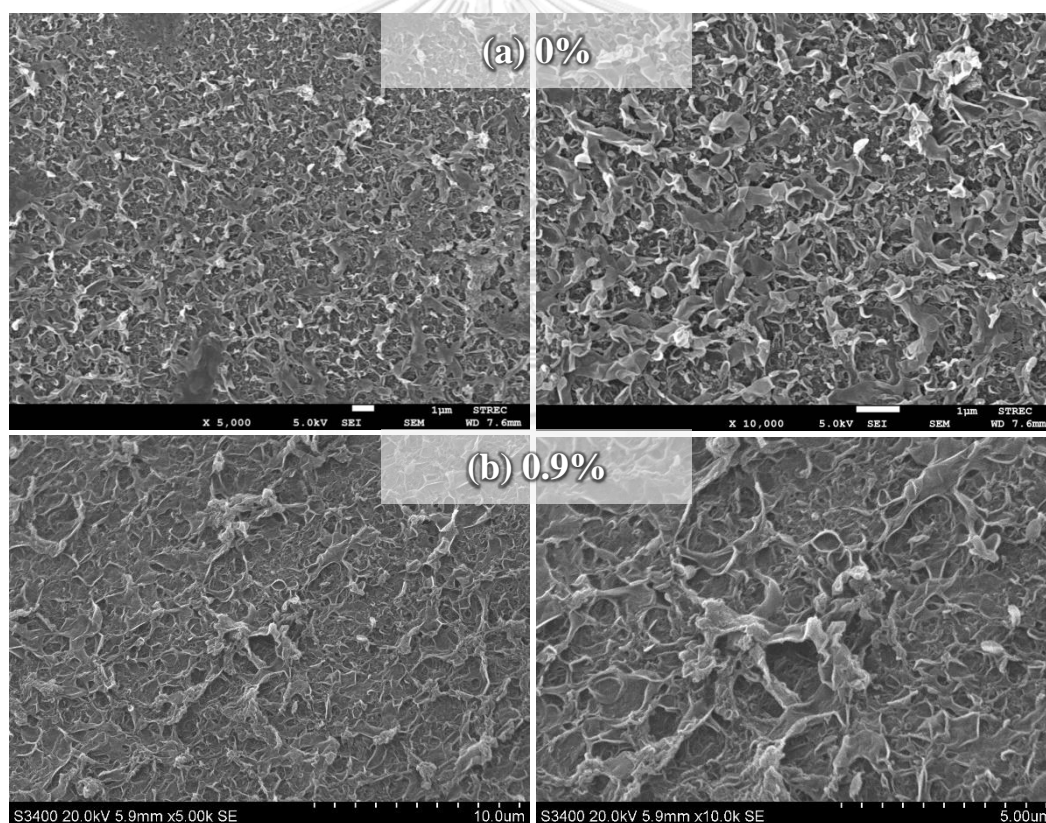


Figure 22 SEM images of TFC membranes top surface at (a) 0 vol% (b) 0.9 vol% (c) 1.8 vol% and (d) 2.7 vol% of ethanol in MPD solution. The images in the left and right column were taken at 5,000 and 10,000 magnification, respectively.

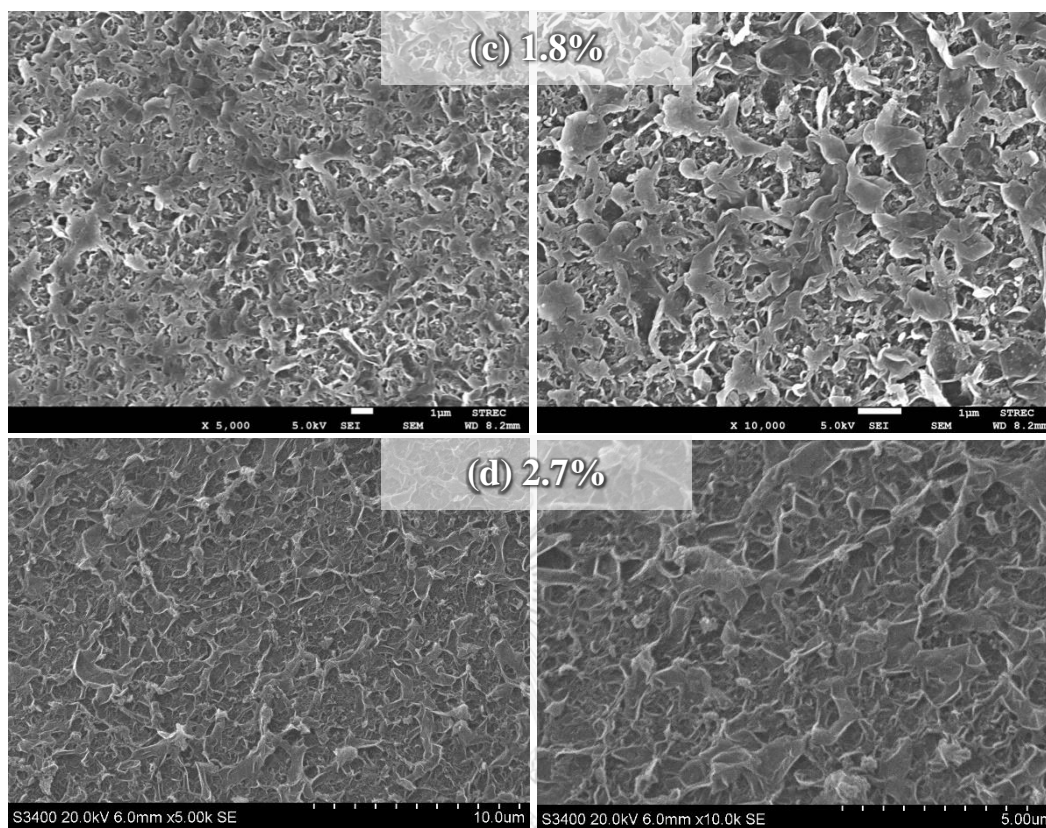


Figure 22 SEM images of TFC membranes top surface at (a) 0 vol% (b) 0.9 vol% (c) 1.8 vol% and (d) 2.7 vol% of ethanol in MPD solution. The images in the left and right column were taken at 5,000 and 10,000 magnification, respectively (continue).

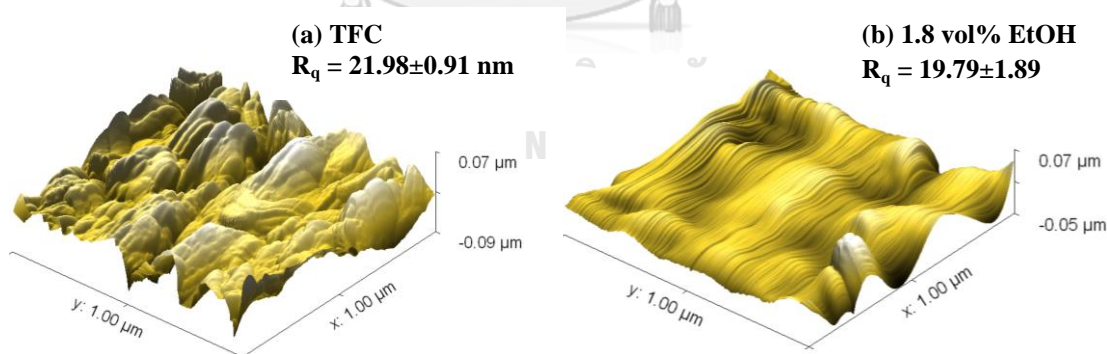


Figure 23 3-dimensions AFM images of TFN membranes top surface at (a) 0 vol% and (b) 1.8 vol% of ethanol in MPD solution.

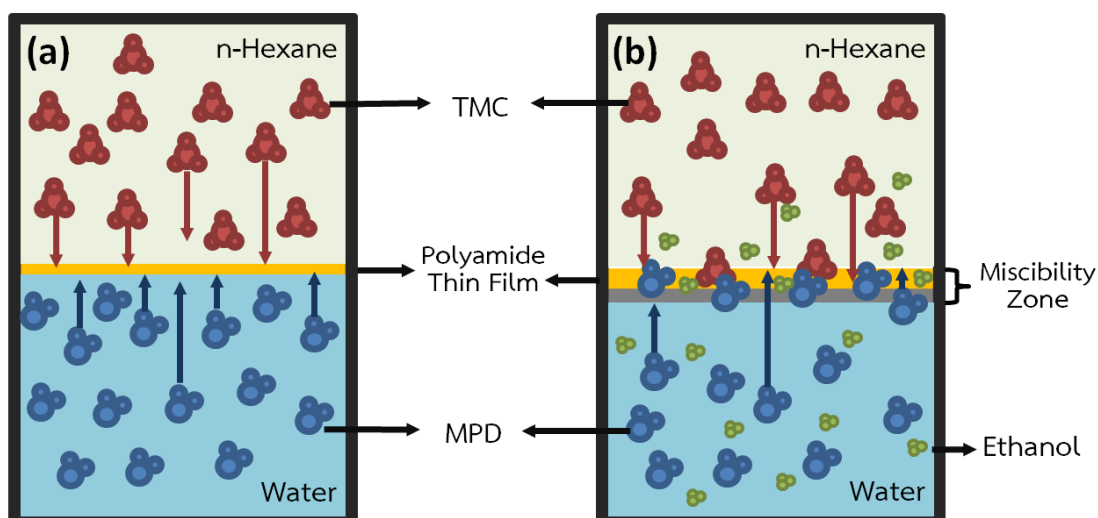


Figure 24 The schematic of monomers diffusion for interfacial polymerization reaction (a) without ethanol (b) with ethanol.

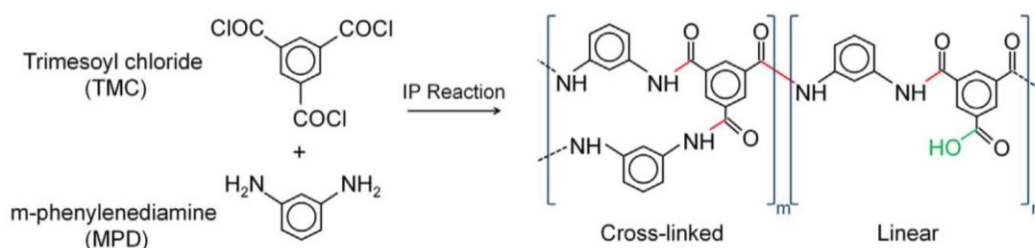


Figure 25 Chemical structure of cross-linked (contained more C-N) and linear (contained more -COOH) polyamide thin film synthesized by MPD and TMC monomer [20].

Figure 26 shows the ATR-FTIR spectra of TFC membranes at various ratios of ethanol loading. The characteristic peaks of the modified membranes were the same as the bare one but resulted in different intensity ratios of the -COOH to the C-N. Table 7 shows the rough estimation of the -COOH / C-N ratio of the membranes from different ethanol addition. It can simply imply that the addition of ethanol increased the number of C-O bond of PA network due to the TMC molecules neutralized zone by the nucleophile molecule (water and ethanol) in the extend miscibility.

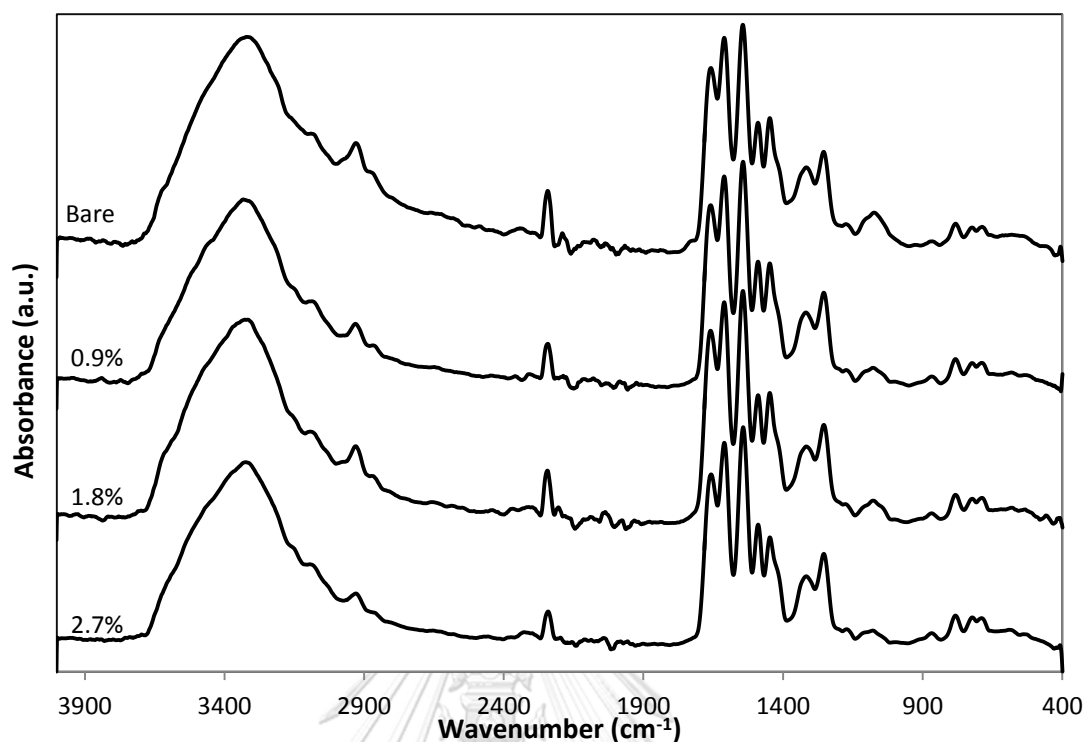


Figure 26 ATR-FTIR spectra of the TFC membranes loaded with different ratio of ethanol in aqueous solution.

Table 7 The roughly estimated ratio of (-COOH)/(C-N) functional groups of TFC membrane prepared from different ethanol addition

Ethanol loading (vol%)	$I_{(-COOH)}/I_{(C-N)}$
0	0.80
0.9	0.85
1.8	0.89
2.7	0.86

The water wettability of TFC membranes was also improved by increasing addition of ethanol as shown in Figure 27. The contact angle of membranes gradually decreases from $76.05^{\circ} \pm 1.99$ to $67.3^{\circ} \pm 1.84$ at 2.7 vol% loading of ethanol. The improved hydrophilicity is due to the higher amount of the hydrophilic oxygen functional group (from TMC neutralization by -OH group) in PA linkage derived from Table 7.

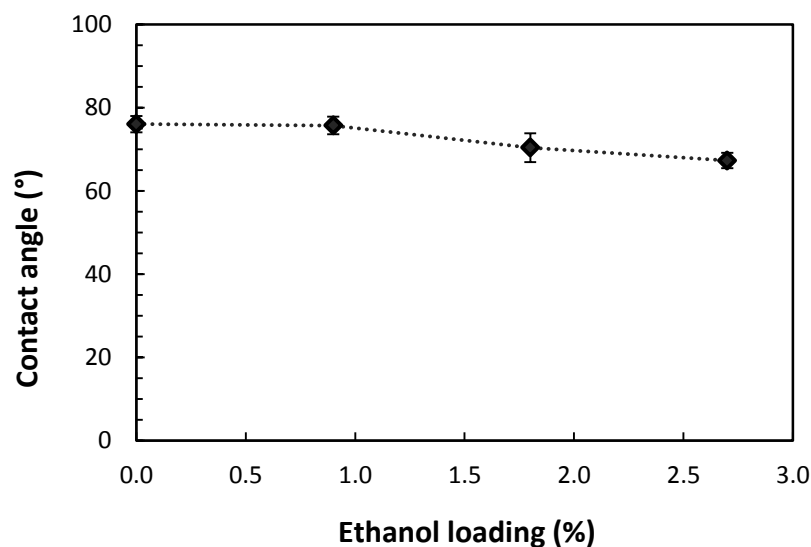


Figure 27 Contact angle of the TFC membranes modified with different loading of ethanol.

Performances of TFC membranes

Figure 28 shows NaCl salt retention and water flux related to ethanol effect. The results showed that the addition of ethanol to MPD solution moderately increased salt rejection from 79.22% to 84.37%. Moreover, the prepared membranes also gradually gained water flux from 8.45 LMH to 9.6 Lm⁻²h⁻¹ (LMH) with the increased ethanol addition. It can imply that the presence of ethanol in MPD solution significantly improves the both permeability and selectivity of TFC membranes. The improved water flux and salt retention were directly related to the PA structure and hydrophilicity. In the case of water flux, the addition of ethanol contributed two impacts on PA layer. Firstly, hydroxyl group of ethanol plays an important role of TMC neutralization by extending the miscibility zone which makes the oxygen nucleophile molecules from water and ethanol easy to eliminate the chlorine atom from TMC monomer during the polymerization reaction. Thus, the cross-link degree of PA thin film is lowered by the presence of ethanol allowing water molecules easier to diffuse through the PA layer. Moreover, the oxygen nucleophile molecules, substituting the chlorine molecule, supplied more wettability property and also enhanced the water flux for the thin film. The less cross-linked degree and higher

oxygen substitution can be roughly derived from the increasing of intensity ratio of C-N stretching and -COOH peaks from ATR-FTIR spectra representing cross-link bonds and substituted hydroxyl groups respectively as shown in Table 7 previously discussed. Secondly, the extend miscibility zone by ethanol favors the polymerization reaction increasing the film thickness [20] compensating the loosen and less cross-linking of PA leading to increase both water flux and rejection.

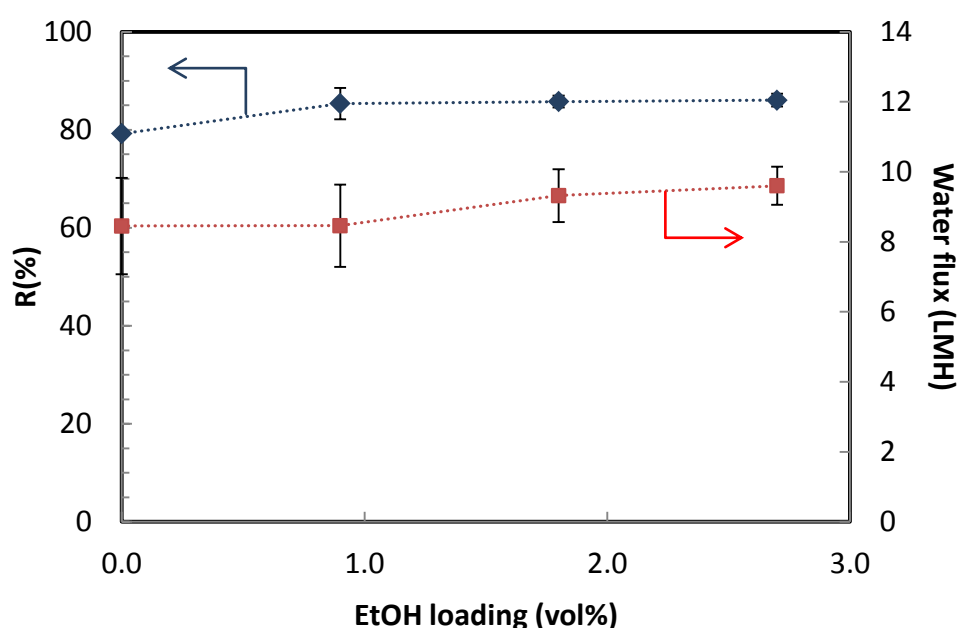


Figure 28 Salt rejection and permeability of ethanol added TFC membranes.

5.2.2 Effect of Nitric acid (pH)

Membranes morphology and characteristics

pH of aqueous monomer solution has been well investigated by previous work [16]. It was reported to affect the interfacial polymerization reaction and thus the properties of the resultant membranes [16].

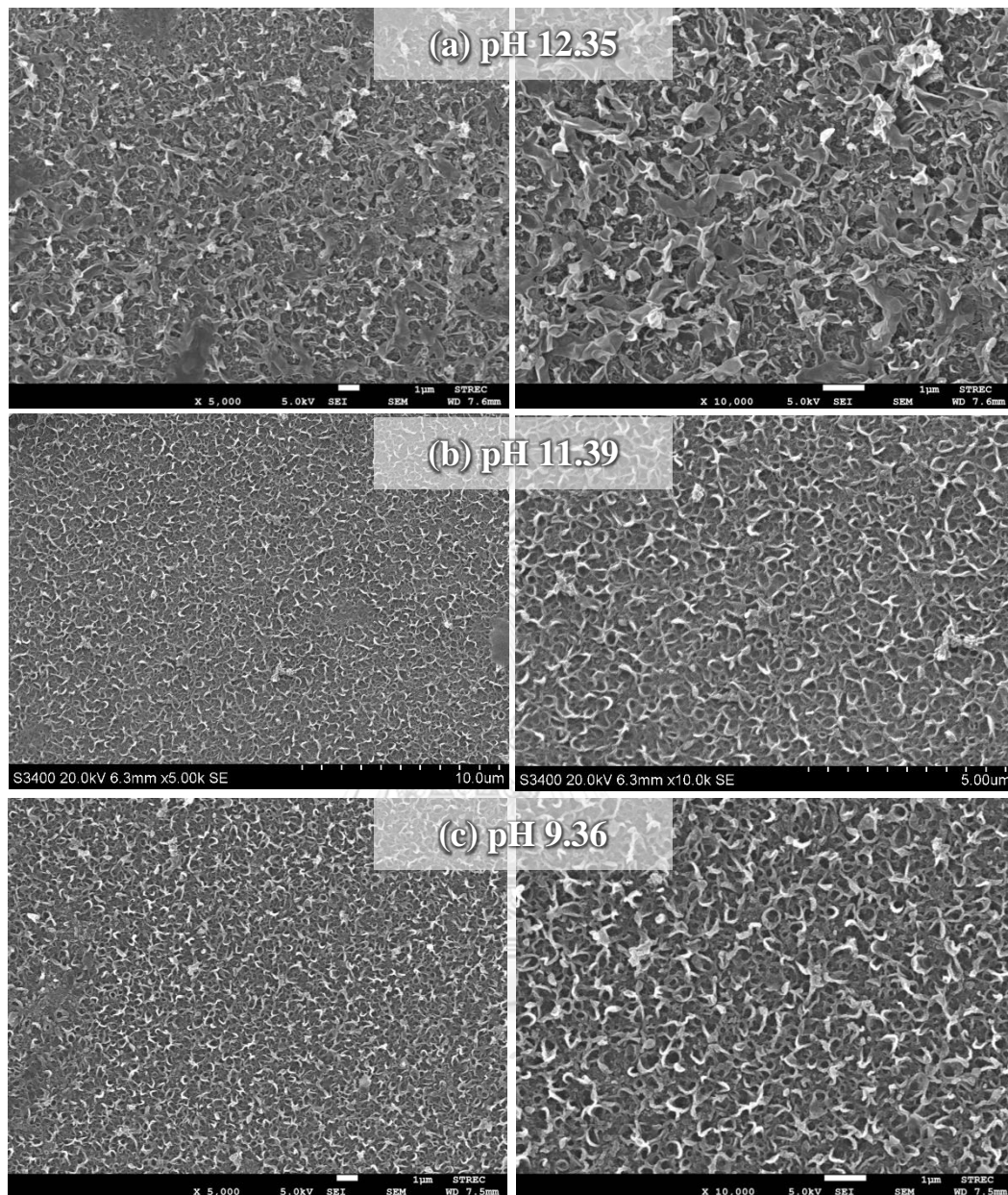


Figure 29 SEM images of TFC membranes top surface with (a) pH 12.35, (b) pH 11.39 and (c) pH 9.36 of MPD solution. The images in the left and right column were taken at 5,000 and 10,000 magnification, respectively.

Figure 29 and Figure 30 exhibits top surface SEM images and surface roughness of PA active layer fabricated at different pH level of MPD solution adjusted by dilute nitric acid. The PA thin film surface morphology prepared from high basic MPD solution (pH 12.35) formed a ridge and valley formation while at lower basicity MPD solution (pH 9.36) the PA film formed a smoother morphology. This morphology

change might be because of two phenomena. First, at lower pH of MPD solution delivered a higher quantity of initial proton decreasing the polymerization rate refer (see Figure 7) [15]. Second, the more acidic condition of MPD solution lowered the initial formed PA skin porosity (became denser) applying more MPD diffusion barrier for to react with TMC for further growth of PA layer [15].

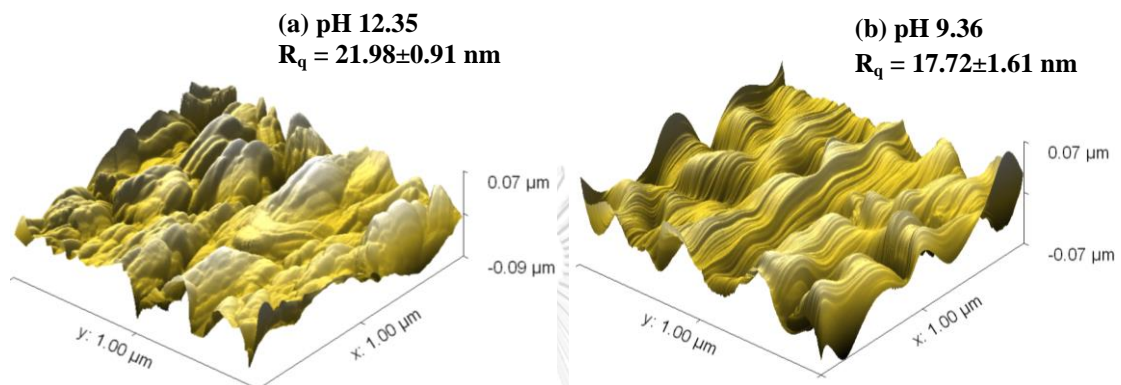


Figure 30 3-dimensions AFM images of TFN membranes top surface with pH 12.35 and pH 9.36 of MPD solution.

The ATR-FTIR spectra of TFC membranes with different pH of aqueous monomer solution are illustrated in Figure 31. The results showed that the pH change of aqueous solution has no effects to the FTIR spectra. It can imply that the surface chemistry of the membranes is not changed by pH of aqueous solution.

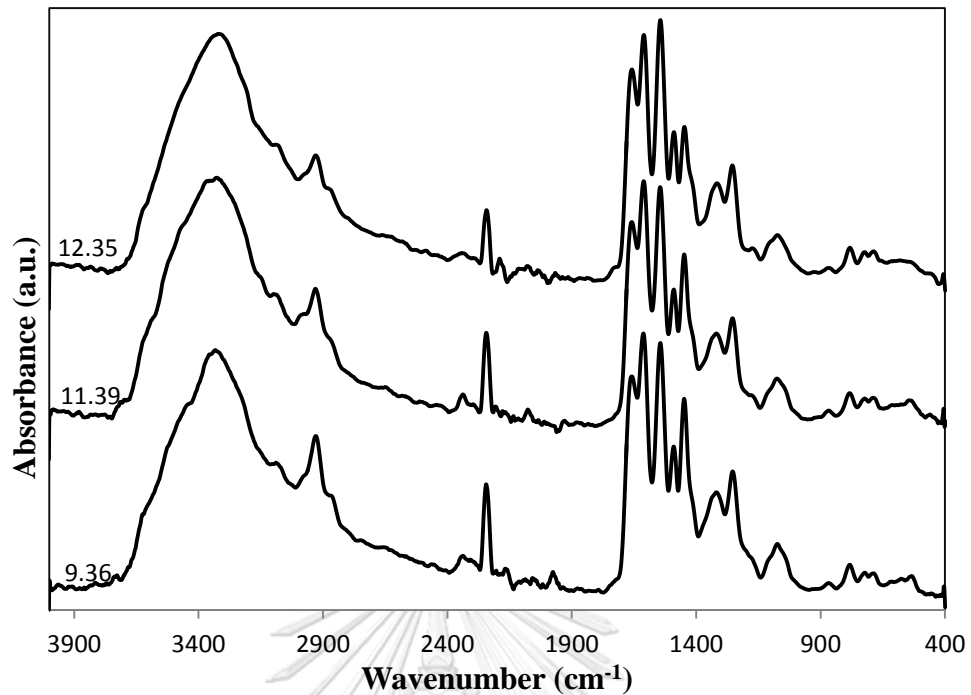


Figure 31 ATR-FTIR spectra of the TFC membranes prepared with different pH of aqueous solution.

As demonstrated in Figure 32, the elevated contact angle from $76.05 \pm 1.99^\circ$ at pH 12.35 to $99.47 \pm 0.57^\circ$ at pH 9.36 was distributed from the lower in surface roughness of PA film observed from Figure 30. The surface roughness relates to the hydrophilicity; a hydrophilic surface of PA film express more hydrophilic when the roughness is increased while express less hydrophilic when the roughness is decreased following the young's equation and Cassie-Wenzel model [43].

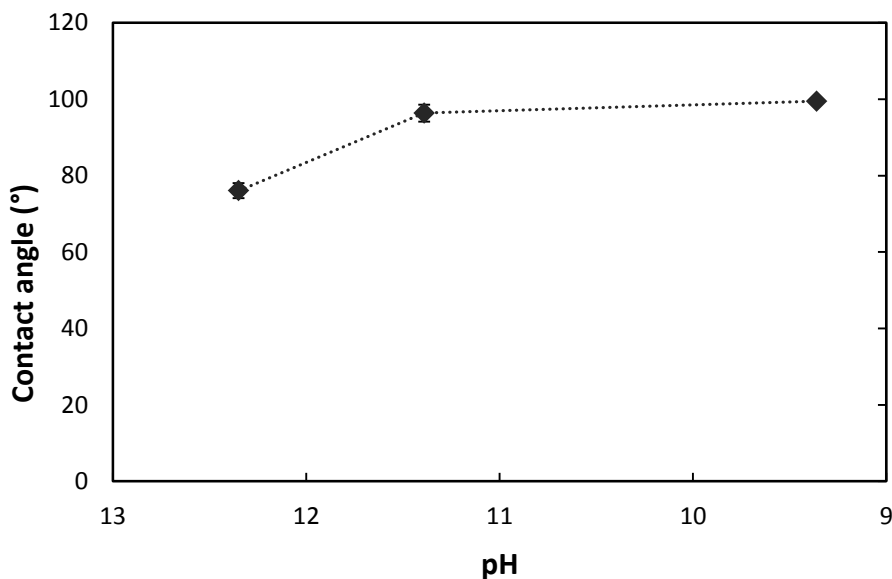


Figure 32 Contact angle of the TFC membranes with different pH of aqueous solution.

Performances of TFC membranes

The fabricated TFC membranes with different pH adjusted aqueous solution performances are illustrated in Figure 33. The results showed that the R was increased about 8% while the water flux was lowered almost 50% with the dropped pH from 12.35 to 9.36. It can be explained that under more acidic condition, the diamine molecular structure become closer and when polymerized, the PA layer also become denser than the basic condition. Ahmad et al., reported a similar result and proposed the structure shrink of PA as shown in Figure 34 [15].

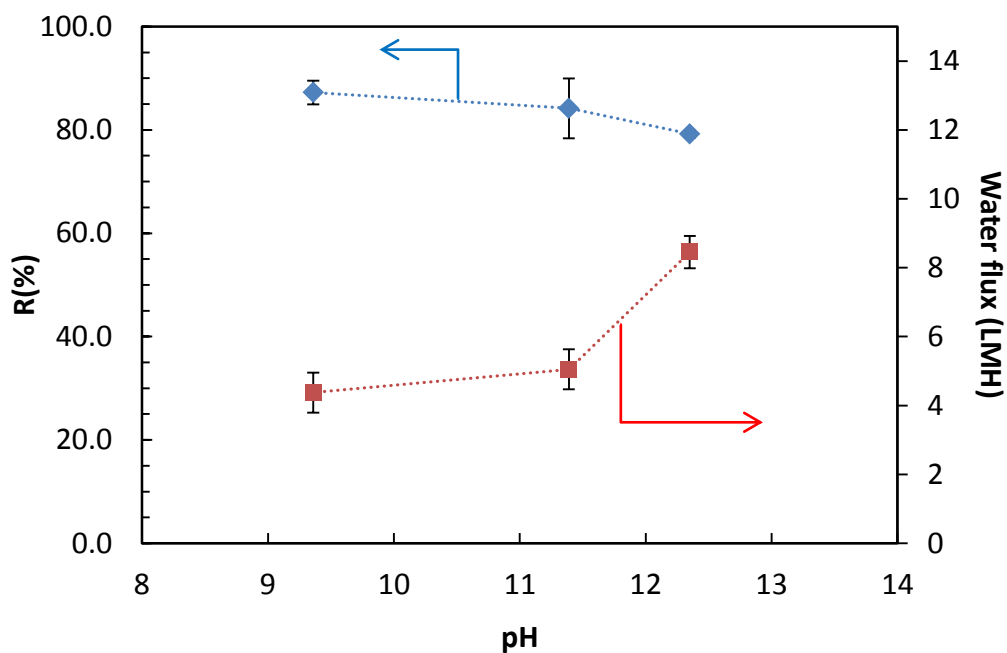


Figure 33 Salt rejection and permeability of different pH of MPD solution TFC membranes.

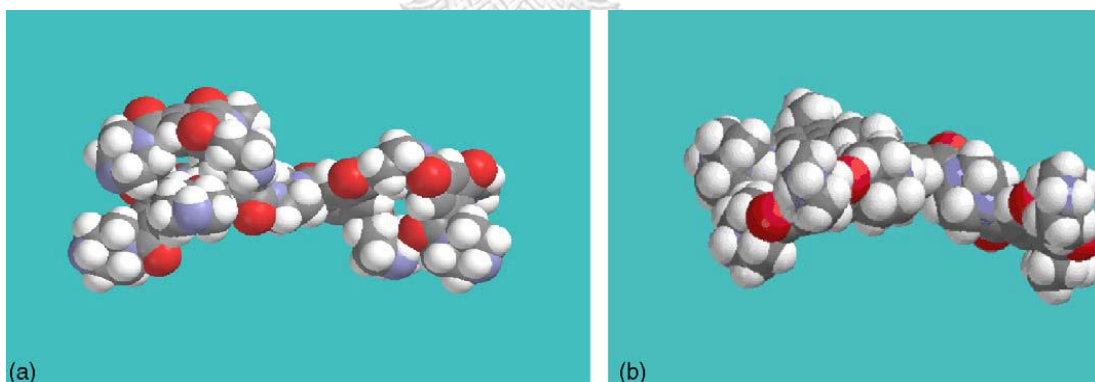


Figure 34 Simulated PA molar structures under (a) basic condition and (b) acidic condition[15].

5.2.3 Effect of Titanium dioxide (TiO_2)

To investigate the effect of TiO_2 loading and eliminate other component, the TiO_2 colloidal solution was dried and then the obtained TiO_2 powder was added and dispersed in MPD solution. Commercial TiO_2 powder was also used to compare the influence of filler properties prepared from different methods.

The TiO₂ colloidal solution, synthesized TiO₂ NPs from TiO₂ solution and commercial TiO₂ NPs were characterized by the Master sizer instrument to investigate the size and surface charge property of the TiO₂ particle. The average size of TiO₂ NPs in solution indicates a slightly smaller size than the commercial TiO₂ reported to be around 21 nm in diameter.

Figure 35 shows the electro static properties of particles related to pH of solution. The results showed that the dried synthesized NPs possessed the highest positive and lowest negative charge for acidity and basicity range respectively with 6.78 pH of isoelectric point. The TiO₂ colloidal solution showed its isoelectric point at pH of 6.34. This indicates that the surface of the synthesized TiO₂ particles in both colloidal and powder form remained their negative charge during IP reaction (pH around 9 - 12). The electro static charge on the NPs surface resulted in good dispersion which can be observed from the physical appearance from Figure 36. In contrast, the commercial TiO₂ remains the neutral zeta potential for entire range of pH which could lead to the poor dispersion and agglomeration (shown Figure 36).

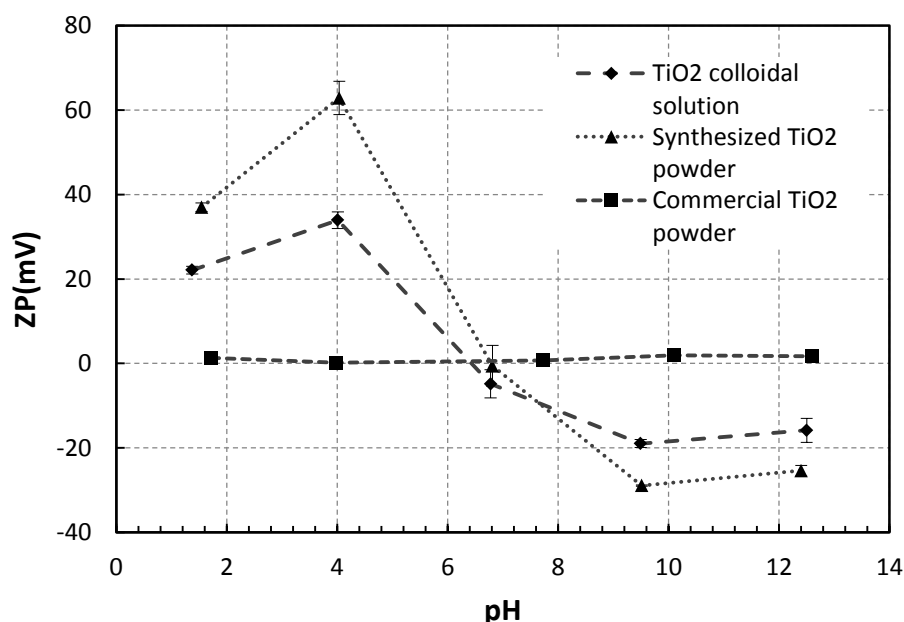
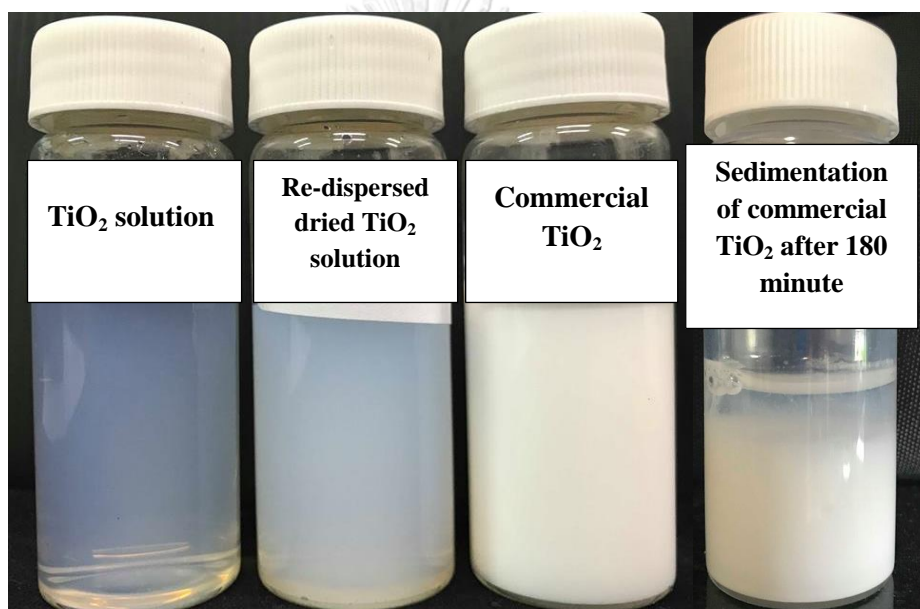


Figure 35 Zeta potential of different TiO₂ type at various pH.

The properties of TiO₂ NPs used as the additive in MPD solution for forming TFN membranes were summarized in Table 8.

Table 8 Summary of properties of TiO₂ NPs.

Type	Size (nm)	Isoelectric point	Surface charge
TiO ₂ colloidal solution	19.8±2.6	6.43	Strong
Synthesized TiO ₂ powder	19.8±2.6	6.78	Strongest
Commercial TiO ₂ powder	~ 21	N/A	none

Figure 36 The physical appearance of TiO₂ added MPD solution.

Membranes morphology and characteristics

Figure 37 and Figure 38 show top surface morphology and roughness of the 3.14 wt% of (a) commercial and (b) synthesized TiO₂ NPs impregnated PA thin film surface images. TFN membrane with commercial TiO₂ NPs has no obvious difference morphology and roughness from the bare membrane which might be because low residue amount of TiO₂ left over after the removing of excess MPD solution due to the agglomeration of TiO₂ which is hard to absorb on the support and easy to be wiped out. On the other hand, it can be obviously noticed that surface of TFN with dried synthesized TiO₂ smoother than that with commercial TiO₂ NPs and the bare one. It might be because the small size of the synthesized TiO₂ dispersed uniformly over the

support surface prior the polymerization obstructing the diffusion pathway for MPD to react with TMC monomer.

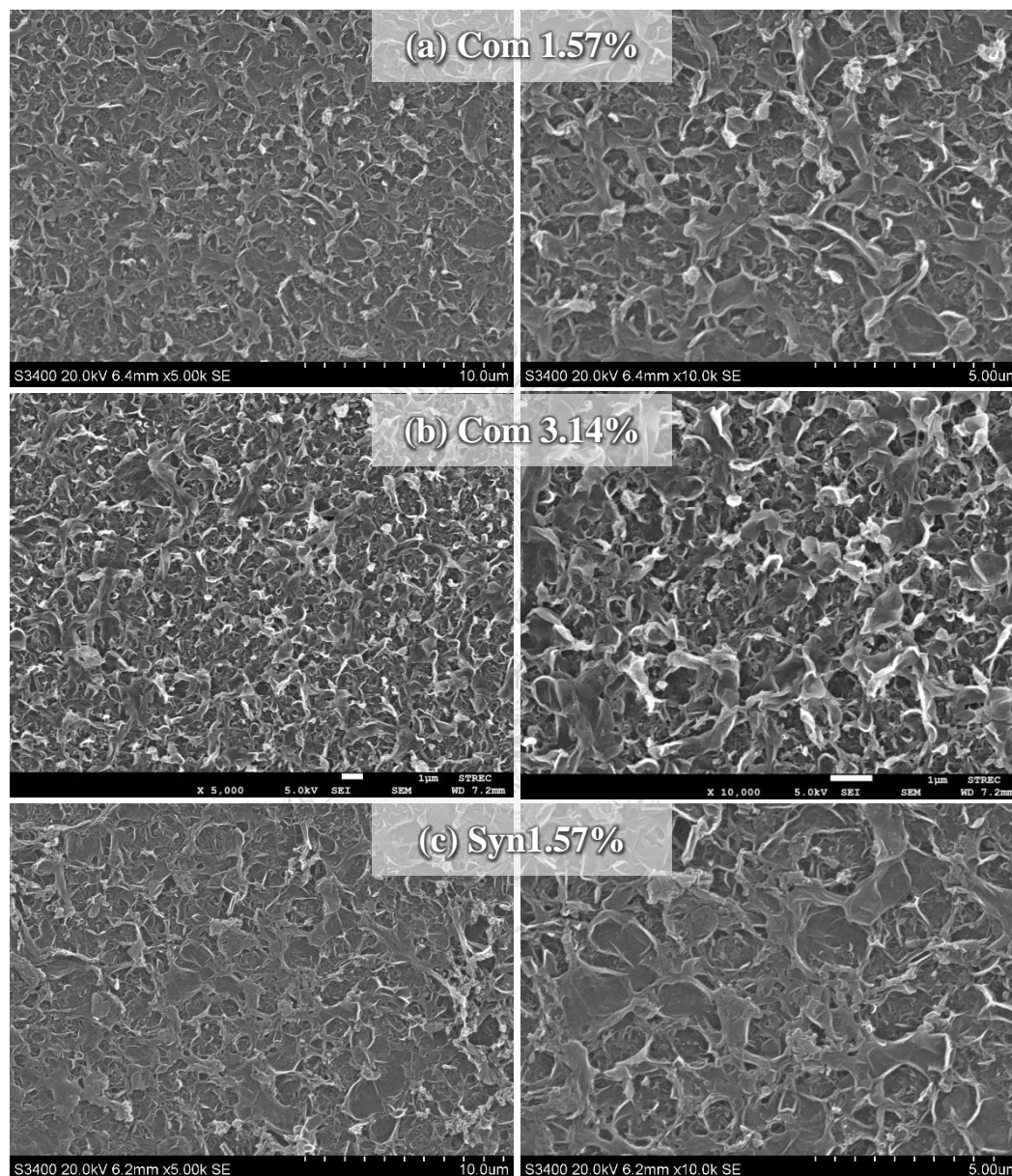


Figure 37 SEM images of TFN membranes top surface with (a) 1.57 wt% loading of commercial, (b) 3.14 wt% loading of commercial TiO₂, (c) 1.57 wt% synthesized TiO₂ and (d) 3.14 wt% synthesized TiO₂ in MPD solution.

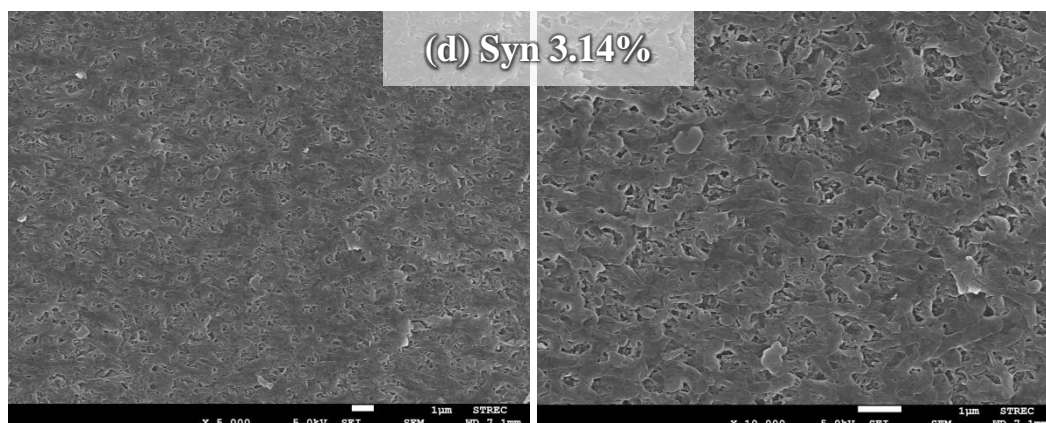


Figure 37 SEM images of TFN membranes top surface with (a) 1.57 wt% loading of commercial, (b) 3.14 wt% loading of commercial TiO_2 , (c) 1.57 wt% synthesized TiO_2 and (d) 3.14 wt% synthesized TiO_2 in MPD solution (continue).

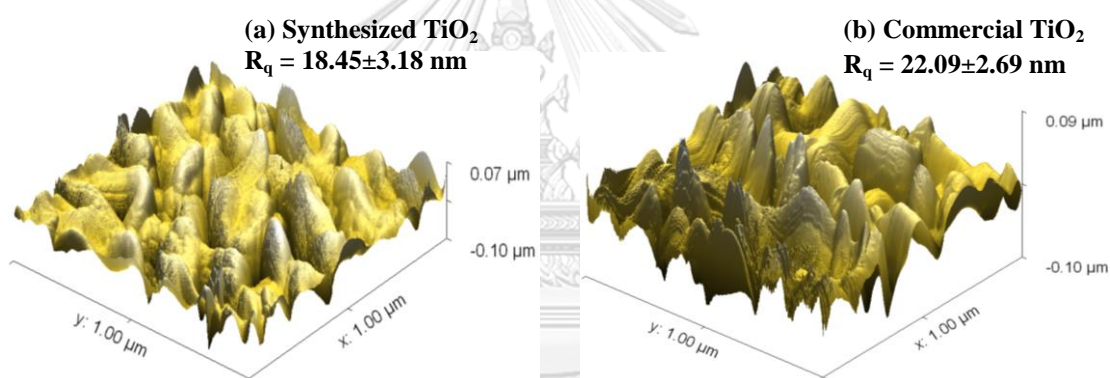


Figure 38 3-dimensions AFM images of TFN membranes top surface with 3.14 wt% loading of (a) commercial TiO_2 and (b) dried TiO_2 solution in MPD solution.

The ATR-FTIR spectra of TFN membranes with different type of TiO_2 NPs are illustrated in Figure 39. The addition of TiO_2 had no effect on chemical structure on surface TFN membranes.

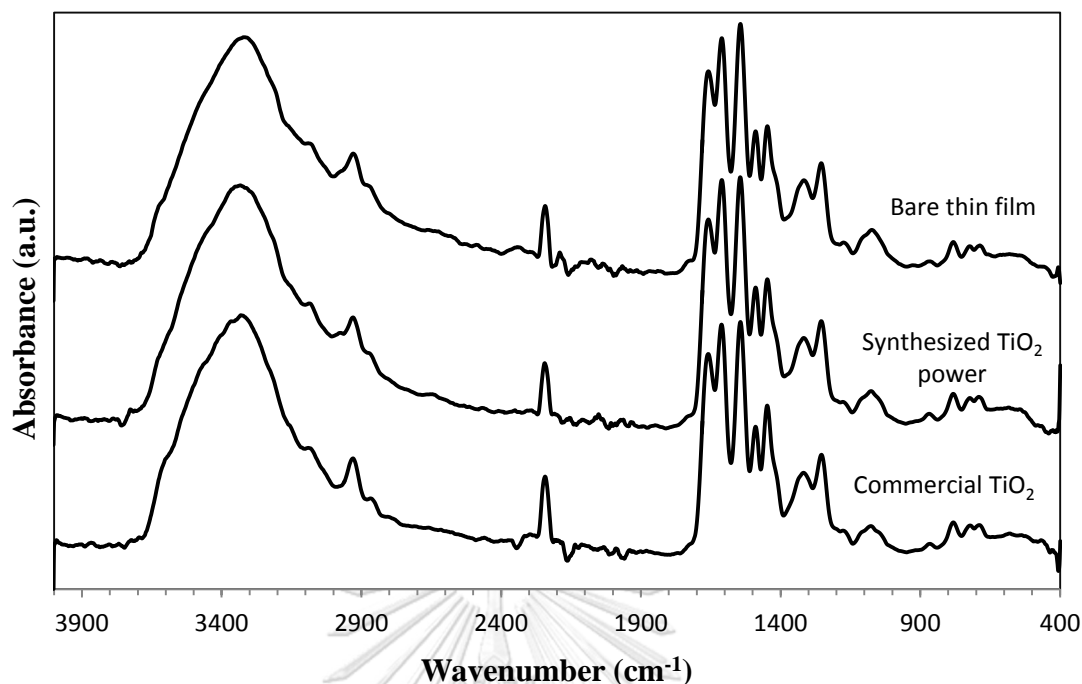


Figure 39 ATR-FTIR spectra of the TFN membranes with 3.14 wt% loading of dried synthesized and commercial TiO_2 .

The TiO_2 solution incorporated TFN membranes were analyzed via SEM-EDS to confirm the presence of TiO_2 inside the PA layer. Figure 40 shows the SEM-EDS elemental analysis and elemental mapping of TFN membranes. The existence of TiO_2 in the TFN membranes can be confirmed via the Ti element spectrum composition, sum spectrum and elemental mapping. The SEM-EDS element spectrum results of TFN membranes show higher Ti element composition from 0.84 wt% to 1.03 wt% with 20 vol% and 30 vol% addition of TiO_2 solution respectively (Figure 40 (a) and (b)). This can be used to confirm that higher ratio of TiO_2 solution in aqueous solution increased the embedded TiO_2 in the PA layer. In addition, the SEM-EDS elemental mapping illustrates a uniform distribution of Ti element (red dots) in the PA thin film.

The TFN membranes incorporated with 3.14 wt% of dried synthesized and commercial TiO_2 NPs were also elemental analyzed via EDS as shown in Figure 40 (c) and (d). The elemental spectrum of dried synthesized TiO_2 NPs loaded membrane contains 0.62 wt% of Ti element with well dispersion but the Ti element from membrane with the addition of commercial TiO_2 could not be detected. This can imply that the embedded amount of commercial TiO_2 NPs is too low for the

instrument to be detected. During immersion of support layer in TiO_2 dispersed MPD solution, the commercial TiO_2 powder might sediment and did not get properly impregnated by the support. It might also get wiping out with an excess MPD solution. In addition, the impregnated TiO_2 might not diffuse to the reaction zone to embed with the formed PA film.

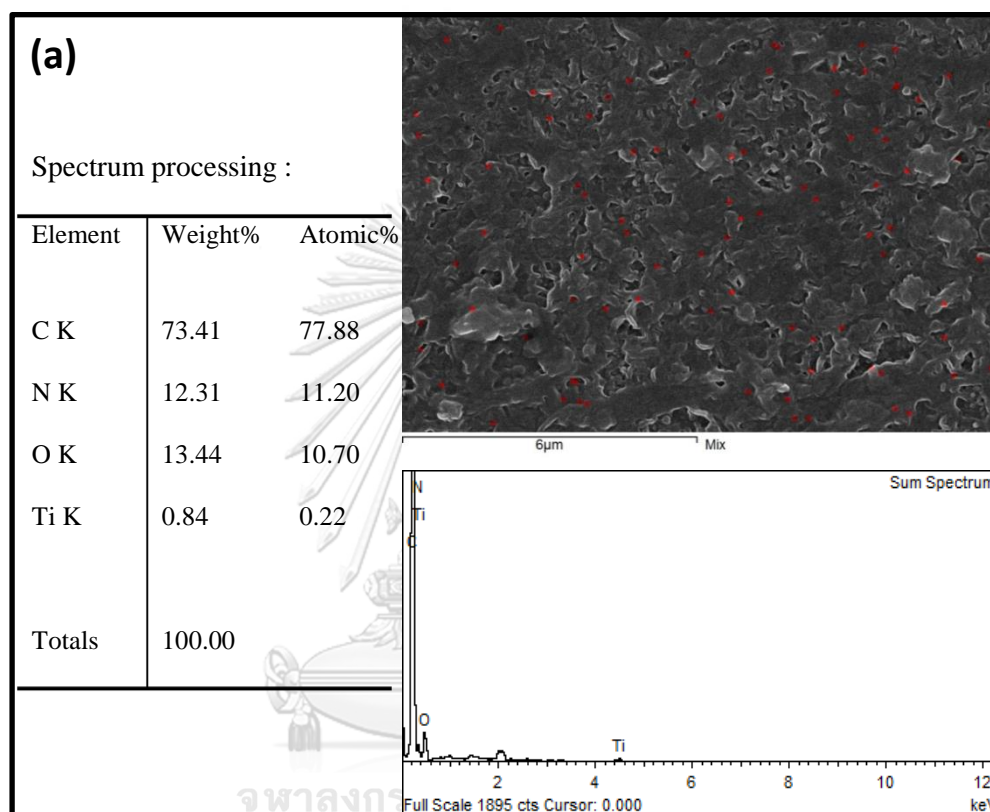
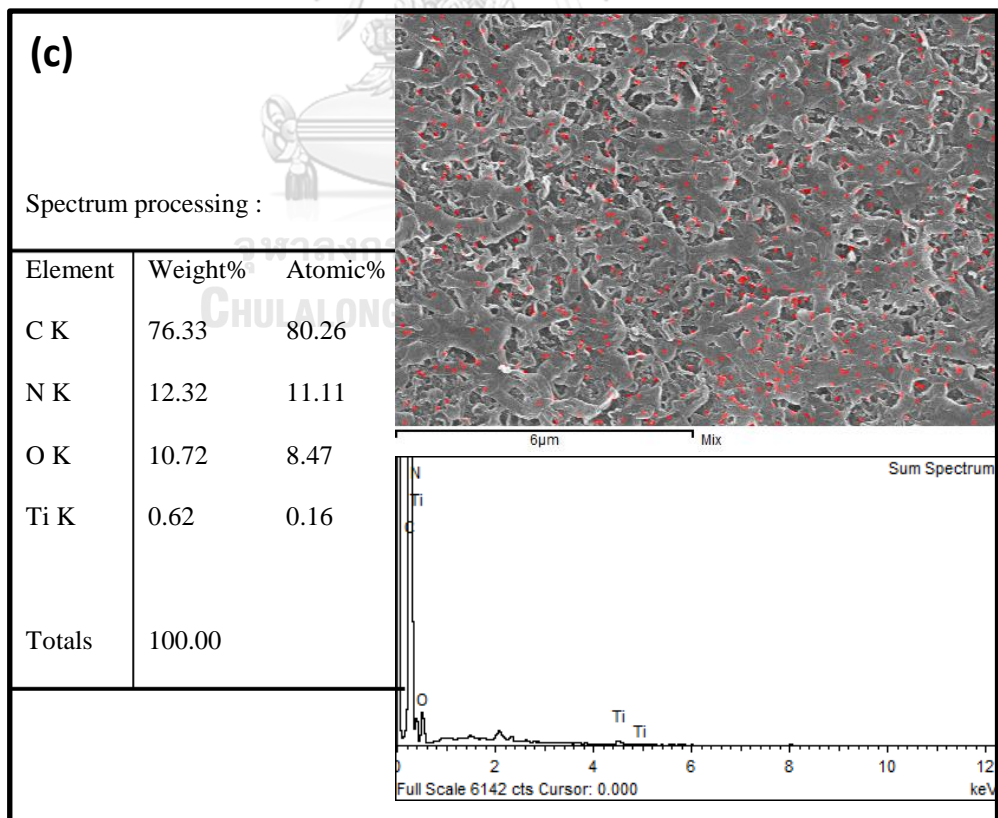
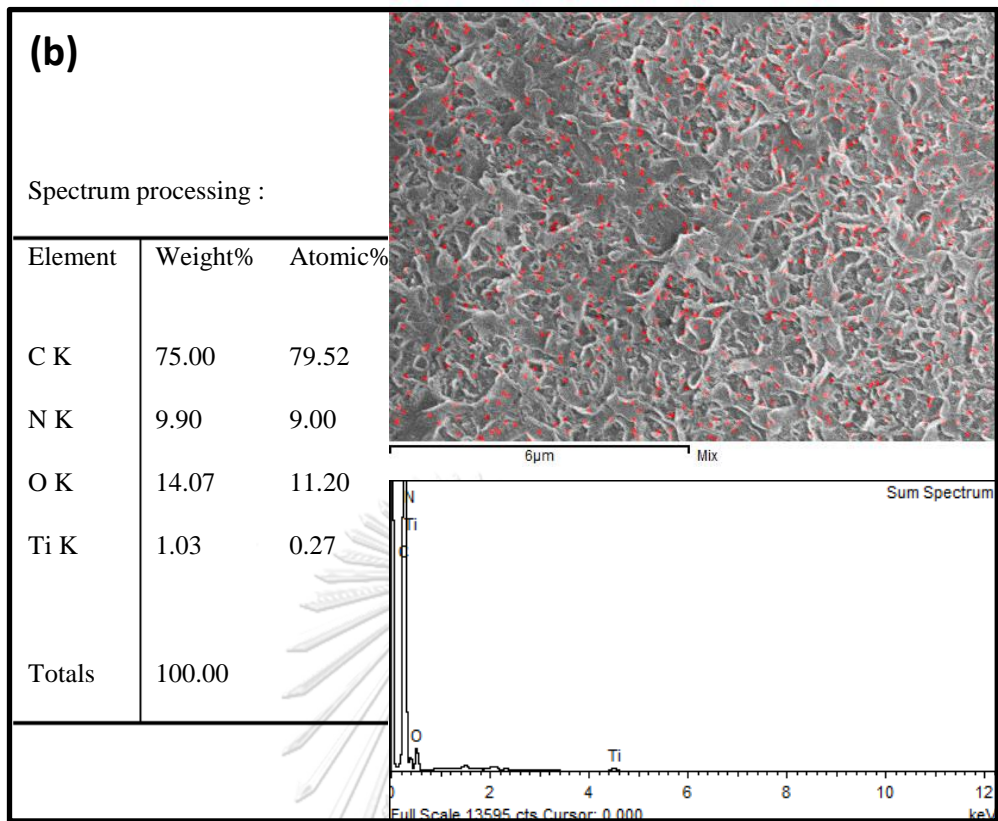


Figure 40 SEM-EDS data of top TFN membranes surface with (a) 3.14 wt% loading of TiO_2 in solution, (b) 4.71 wt% loading of TiO_2 in solution, (c) 3.14 wt% of dried synthesized TiO_2 NPs and (d) 3.14 wt% of commercial TiO_2 NPs.



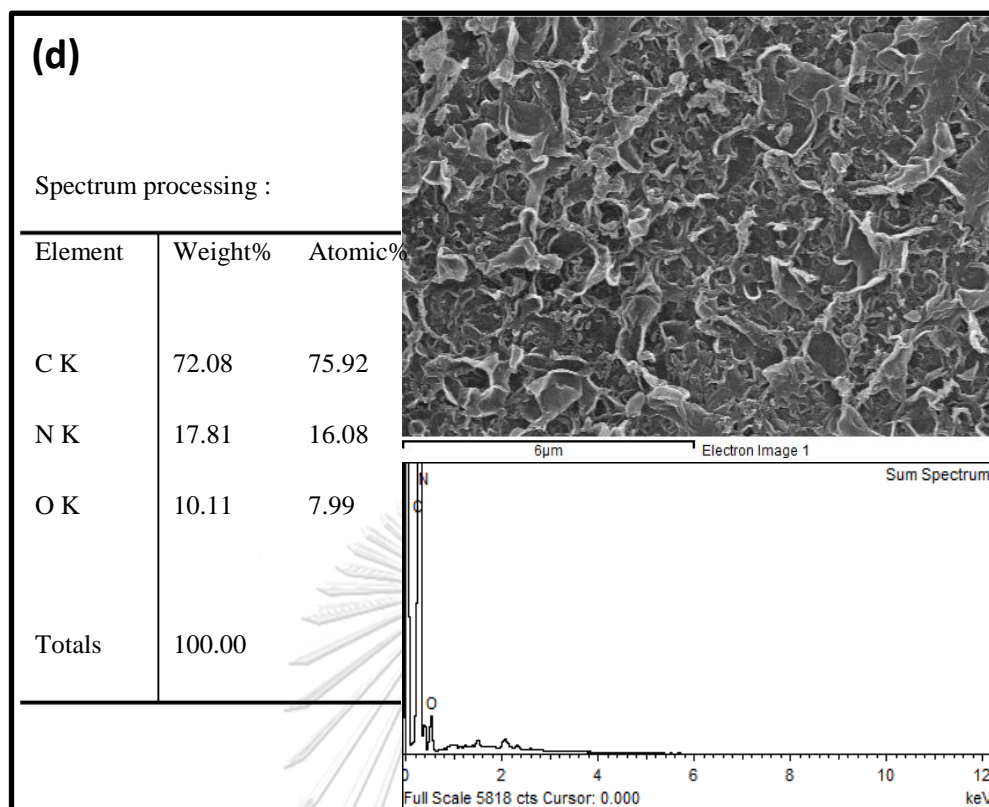


Figure 40 SEM-EDS data of top TFN membranes surface with (a) 3.14 wt% loading of TiO_2 in solution, (b) 4.71 wt% loading of TiO_2 in solution, (c) 3.14 wt% of dried synthesized TiO_2 NPs and (d) 3.14 wt% of commercial TiO_2 NPs (continue).

Figure 41 indicates the hydrophilicity of TFN membranes with different type and loading of TiO_2 NPs. The results show that the commercial NPs added TFN membranes exhibit the highest contact angle (lowest 69° at 4.71 wt% loading) due to less embedding amount of NPs while dried synthesized NPs and TiO_2 moderately lower and drastically drop the angle respectively. The decrease in contact angle of TFN membranes from the addition of synthesized TiO_2 and TiO_2 colloidal solution are mainly due to the greater amount of embedded ultra-hydrophilic TiO_2 NPs in PA layer confirmed from elemental analysis (Figure 40). But the extra hydrophilicity of the TFN membranes from TiO_2 solution which is higher than that from the dried synthesized TFN membranes was supplied from the higher number of oxygenate functional group supplemented by the presence of ethanol. The different number of oxygen derivative functional groups can be pointed out from elemental spectrum

Figure 40 (a) and (c); 13.44 wt% and 10.72 wt% for TiO_2 solution and dried synthesized TiO_2 NPs respectively.

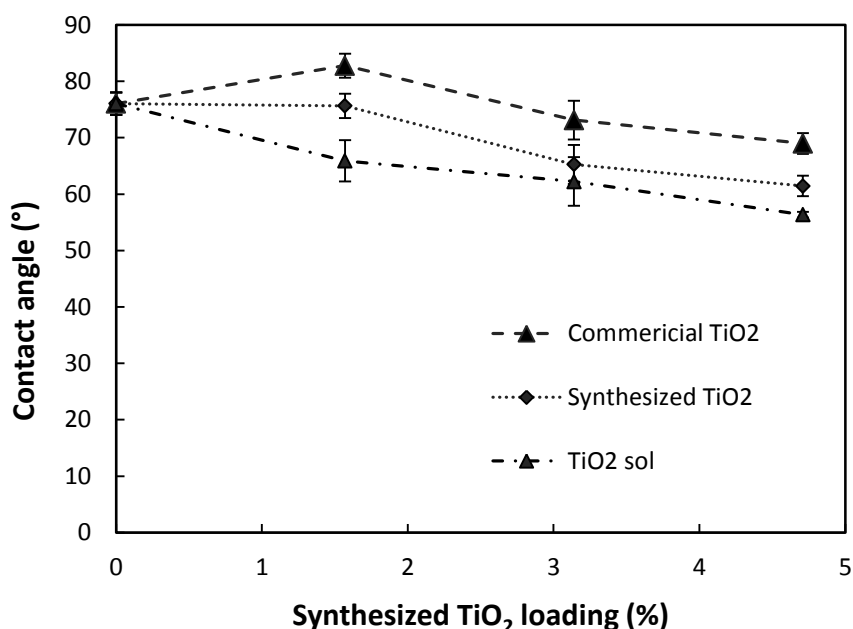


Figure 41 Contact angle of TFN membranes with different loading of TiO_2 NPs in solution, commercial and synthesized TiO_2 NPs.

Performances of TFN membranes

The commercial and synthesized TiO_2 NPs TFN membranes were fabricated to observe and compare the effect to the membranes performances. Figure 42 shows the TFN membrane performances with various loading of commercial TiO_2 NPs and synthesized TiO_2 . It was found that the addition of commercial TiO_2 has no influence on both NaCl rejection and water flux at higher loading. In fact, at higher loading of the ultra-hydrophilic NPs, the water flux should be increased because of the higher wettability of modified PA layer but in this case, the water flux still remain even at higher loading of commercial TiO_2 . The result was in a good agreement with other observed characteristics discussed earlier. The commercial TiO_2 might not successfully attach to PA film or it might be present in a very low amount. Therefore, no significant changes were observed.

Figure 43 shows the TFN membranes loaded with synthesized TiO_2 NPs. The performances indicated that the water flux was enhanced from 8.45 LMH to 10.26 LMH at 3.14 wt% loading of the NPs before decreasing to 8.95 LMH at 4.71 wt% loading while the retentions were still remained at around 80% for all loading. It can be implied that the addition of synthesized TiO_2 NPs improves the wettability of PA layer without water path blockage. This was mainly due to the electro repulsive force from the surface charge of NPs protects the agglomerate of NPs as shown in Figure 36.

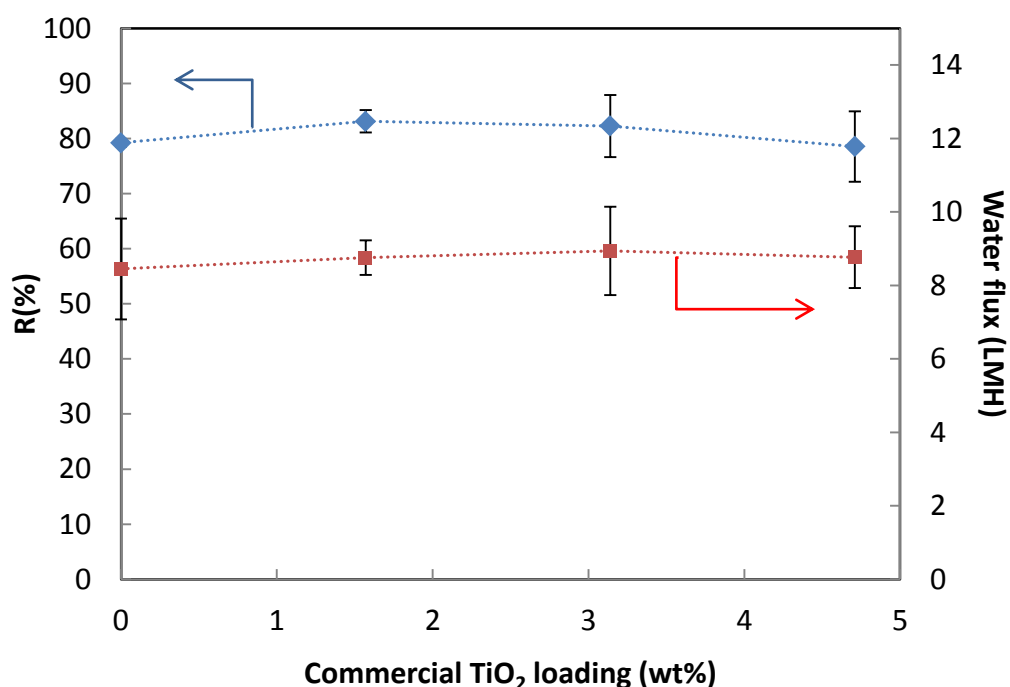


Figure 42 Salt rejection and permeability of commercial TiO_2 loaded TFN membranes

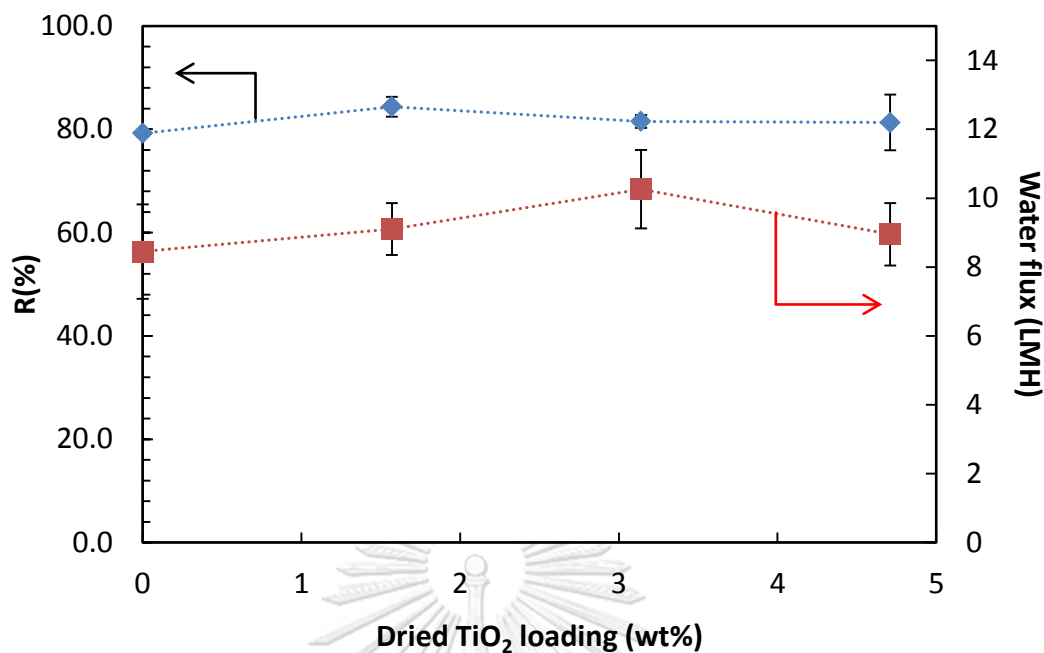


Figure 43 Salt rejection and permeability of synthesized TiO₂ loaded TFN membranes

To compare the effects of the added TiO₂ type Figure 44 and 45 are plotted to indicate the difference of NaCl retention and water flux respectively. The NaCl rejection results show that the TFN membranes modified with TiO₂ in solution own the outstanding 94.2% of rejection at 3.14 wt% loading while other remained at around 80%. It can be explained by the co-influence of ethanol existence and lowered pH of the aqueous solution. For the water flux performance, the synthesized TiO₂ NPs loaded TFN membranes show the biggest improvement compared to the others. The dropped flux of the solution loaded membrane at 1.57 wt% can be explained via the denser and thicker PA layer from the co-influence of ethanol and lowered pH which can also reasonably observe by the higher rejection. In contrast, at 3.14 wt% loading of TiO₂ in solution, water flux is jumped to 9.53 LMH without sacrifice of rejection which can be expressed by the higher wettability and loosen but thicker of PA layer affected by the influence of ethanol and NPs.

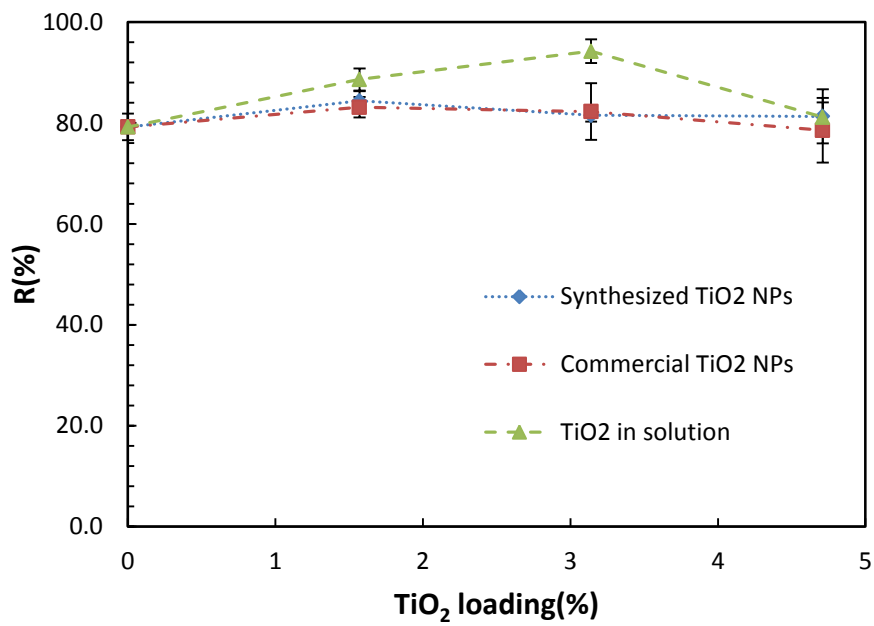


Figure 44 Salt rejection comparison of different TiO₂ type loaded membranes

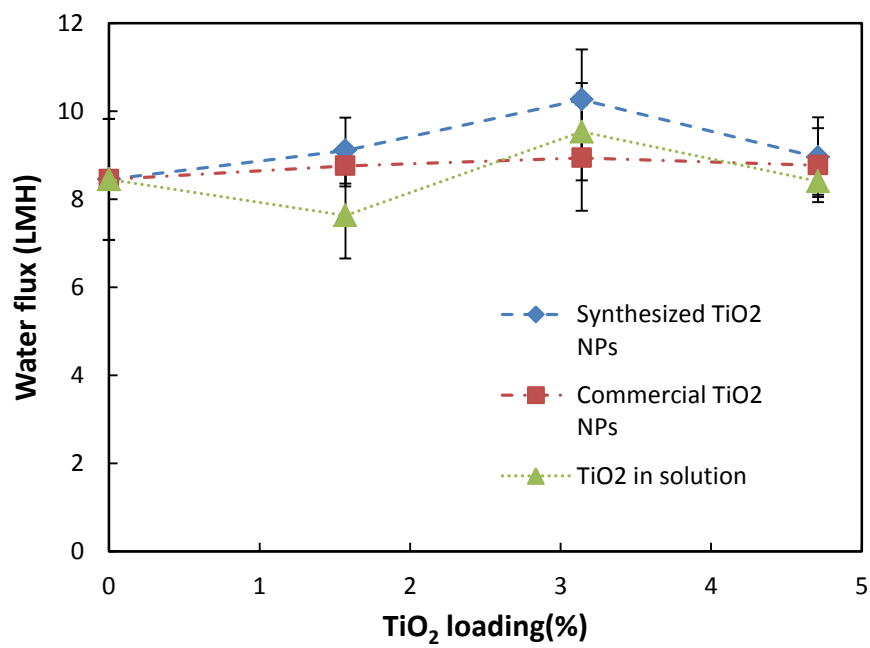


Figure 45 Water flux comparison of different TiO₂ type loaded membranes

5.3 Fouling evaluation

Fouling evaluation was conducted to indicate the fouling resistance property of the fabricated TFC and TFN membranes comparing to the commercial TFC membrane. The membranes were tested with 1000 ppm of SA foulant in DI water via dead-end module for 4 hr. Figure 46 shows the normalized flux decline dependent on time for TFC membrane, TFN membrane with 20 vol% loading of TiO₂ colloidal solution and NF270 commercial membrane. It can be noticed that the commercial membrane flux sharply declined to 30% of normalized flux within first 100 minutes while about 50% and 55% for the TFN and TFC membrane, respectively. In addition, the total declined flux (flux decay ratio) of the membranes at the end of this evaluation and flux recovery of the membrane after cleaning are shown in Figure 47. The result showed that the TFN membrane effectively prohibited the flux decay (decay only 58.64%) and achieved the best recovery flux ratio (up to 93.94%) while the commercial one performed the worst for both flux decay and recovery. This high fouling resistance capability was resulted on their high hydrophilicity (62.22° of contact angle), low roughness (19.32 nm of RMS roughness) and negative charge over TiO₂ surface.

To clarify, the factors decreasing the TFN membrane fouling are divided to be independently explained. First, the hydrophilicity improvement of TFN membrane conducts water film over the membrane surface protecting foulants to adsorb on the surface [28]. Second, the lowered surface roughness decreases initiation of foulants anchoring onto the membrane surface [29, 30]. Third, the negative supplied from the TiO₂ colloidal solution repelled the negative charged foulants to be adsorbed onto the surface [32].

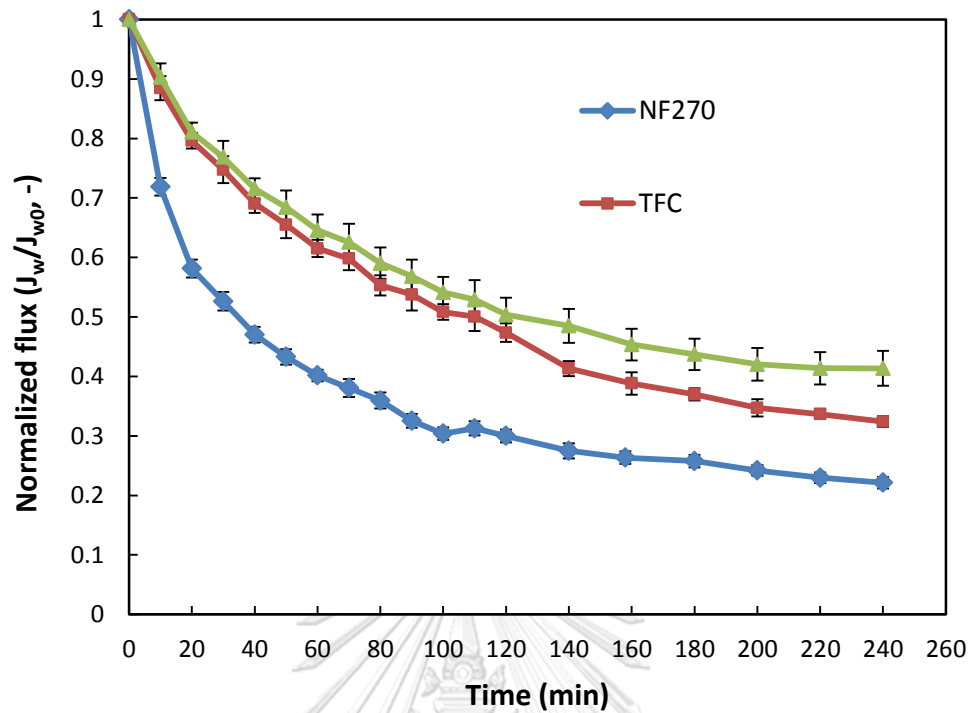


Figure 46 Normalized flux depending on time in SA fouling evaluation of bare TFC membrane, TFN membrane with 20% TiO₂ solution loading and Dow NF270 commercial membrane.

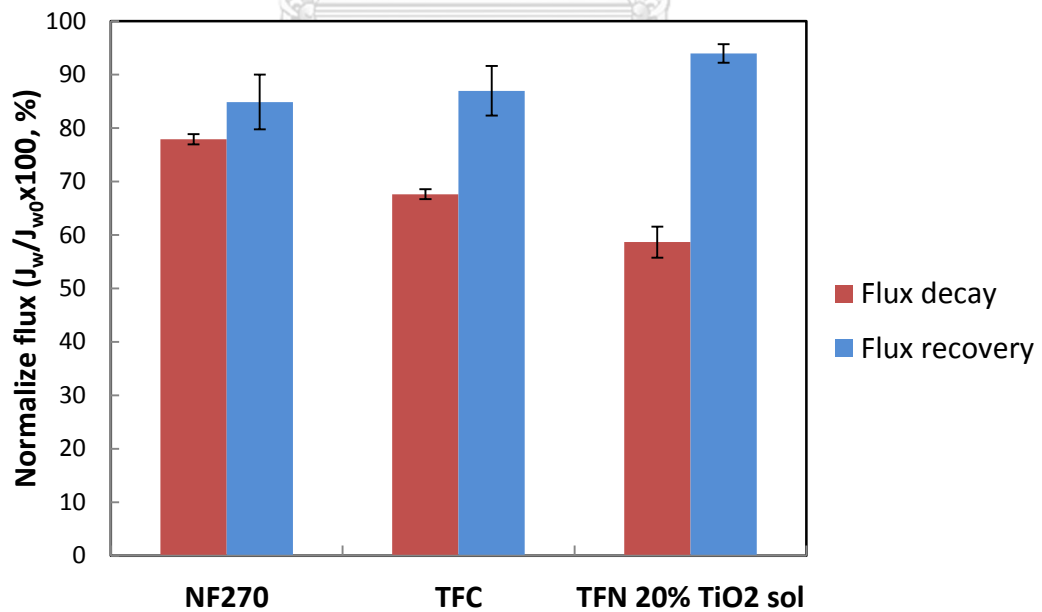


Figure 47 Percentage of membranes flux decay after a cycle of fouling evaluation and flux recovery of the fouled membranes after cleaning.

5.4 TiO₂ embedded TFN membranes performance comparison

Table 9 compares the TiO₂-TFN membranes prepared from this work and ones from an open literature. Obviously, the recently developed membrane from this work possessed the highest monovalent salt (NaCl) rejection with outstanding water permeability compared to the previous developed TFN membranes. Furthermore, our membrane shows lower contact angle (highly hydrophilic) and smoother surface than that of other membranes. These could benefit the reduced tendency for fouling. In addition, the recently fabricated membrane with TiO₂ colloidal solution showed promising results in separation and anti-fouling performances.



Table 9 Comparison of TiO₂ -TFN membranes performance.

Monomer pair	Filler		Contact angle (°)	Surface roughness (RMS, nm)	Testing conditions: solution (concentration) pressure	Performance		Anti-fouling test			Ref.
	Type (phase it was dispersed in)	Content				Rejection (%)	Pressue-normalized water flux (L/m ² .h.bar)	Feed	Flux Decay (%)	Flux Recovery (%)	
TMC/MPD	TiO ₂ sol (MPD)	20 (vol%)	62.2	19.3	NaCl (2000ppm) 5 bar	94.2	2.94	SA (1000ppm)	58.6	93.9	This work
TMC/MPD	TiO ₂ (TMC)	5 (wt%)	N/A	N/A	MgSO ₄ (2000ppm) 6 bar	96.4	1.45	N/A	N/A	N/A	[30]
TMC/MPD	TiO ₂ (MPD)	0.1 (wt%)	69.8	82.3	NaCl (2000ppm) 7.58 bar	53.9	1.48	N/A	N/A	N/A	[39]
TMC/MPD	TiO ₂ sol (MPD)	1 (wt%)	78.1	N/A	NaCl (2000ppm) 15.5 bar	93.4	0.155	BSA (200ppm)	2.5	N/A	[40]
TMC/PIP	TiO ₂ (MPD)	0.005 (wt%)	50.4	107	NaCl (2000ppm) 10 bar	35.6	5.1	BSA (500ppm)	26.1	N/A	[41]

CHAPTER 6

CONCLUSIONS AND RECOMMENDATIONS

6.1 Conclusions

The fouling resistant thin film nanocomposite membranes were successfully developed via an interfacial polymerization reaction by introducing TiO₂ NPs to the selective thin film. The membrane NaCl salt rejection and water permeability were controlled by the ratio of added TiO₂ colloidal solution. The optimal loading, 20 vol% of TiO₂ colloidal solution in the aqueous solution, possessed the highest NaCl salt rejection of 94.20% and water permeability of 2.94 Lm²h⁻¹bar⁻¹. Furthermore, the anti-fouling performance in terms of flux decay and flux recovery ratio was also enhanced. The improvement of rejection, water permeability and anti-fouling performance were influenced by multi components in the added TiO₂ colloidal solution during the interfacial polymerization reaction. The higher rejection was enhanced by the individual influence of ethanol extending the miscibility zone of aqueous-organic phase and nitric acid controlling pH of aqueous solution. Both components controlled the TMC neutralization and monomer transport resulting in thick, low cross-linked and dense PA layer with good salt partition capability. While the embedding of TiO₂ NPs and left over hydroxyl group formed by ethanol neutralization brought more water to contact with the membrane surface conducting higher water permeability due to its both hydrophilic characteristic.

The addition effect of TiO₂ colloidal solution in an aqueous monomer solution on membranes characteristics was revealed by various characterizations. The FTIR spectra and SEM images confirmed that the PA layer with well dispersed TiO₂ NPs was effectively fabricated onto PAN support. In addition, the results showed that the membrane hydrophilicity was improved upon higher loading of TiO₂ colloidal solution, while the surface roughness was decreased. Ultra-hydrophilicity of TiO₂ NPs and hydroxyl group from ethanol neutralization supplied more hydrophilicity of PA layer. Also, the surface was smoothed via surface voids fulfilling, NPs diffusion

obstructing and initial denser PA layer barrier caused by extend miscibility zone from ethanol, addition of TiO₂ NPs and lowered pH, respectively. In addition, PA layer was supplied more negative charge by the addition of TiO₂ colloidal solution. From all of those characteristics, the anti-fouling properties were favored and can repel foulants from anchoring on the membrane surface.

6.2 Recommendations

- Direct characterization of membrane surface charge is needed to be further clarified the electro static repulsive phenomenon.
- Wider composition range of individual component should be further investigated.
- Fouling evaluation with other foulants and real waste water are recommended.
- Fouling evaluation with cross flow system is suggested to simulate the real continuous process and to observe the membranes stability.
- Further characterization of the used membranes is recommended to elucidate the stability of embedded TiO₂ NPs in the thin film.

REFERENCES

- [1] Kay, P. Membrane Technologies Market in South East Asia Research Associate Environment & Building Technologies 2012.
- [2] Zhang, Y., et al. Composite nanofiltration membranes prepared by interfacial polymerization with natural material tannic acid and trimesoyl chloride. Journal of Membrane Science 429 (2013): 235-242.
- [3] Jhaveri, J.H. and Murthy, Z.V.P. A comprehensive review on anti-fouling nanocomposite membranes for pressure driven membrane separation processes. Desalination 379 (2016): 137-154.
- [4] Madsen, H.T. Membrane Filtration in Water Treatment – Removal of Micropollutants. (2014): 199-248.
- [5] Baker, R.W. Membrane Technology and Applications. Wiley, 2012.
- [6] Acetate Available from: <http://www.nfsa.gov.au/preservation/glossary/acetate>
- [7] Jiraratananon, R. Synthetic membrane separation process. Thaiseng, 2000.
- [8] Li, D. and Wang, H. Recent developments in reverse osmosis desalination membranes. Journal of Materials Chemistry 20(22) (2010): 4551.
- [9] Choi, W., et al. Thin film composite reverse osmosis membranes prepared via layered interfacial polymerization. Journal of Membrane Science 527 (2017): 121-128.
- [10] Wansuk Choi, J.-E.G., Sang-Hee Park, Seyong Kim, Joona Bang, Kyung-Youl Baek, and Byoungnam Park, J.S.L., Edwin P. Chan, and Jung-Hyun Lee. Tailor-Made Polyamide Membranes for Water Desalination. ACS Nano 9(1) (2015): 11.
- [11] Liu, M., Wu, D., Yu, S., and Gao, C. Influence of the polyacyl chloride structure on the reverse osmosis performance, surface properties and chlorine stability of the thin-film composite polyamide membranes. Journal of Membrane Science 326(1) (2009): 205-214.
- [12] Klaysom, C., Hermans, S., Gahlaut, A., Van Craenenbroeck, S., and Vankelecom, I.F.J. Polyamide/Polyacrylonitrile (PA/PAN) thin film

- composite osmosis membranes: Film optimization, characterization and performance evaluation. Journal of Membrane Science 445 (2013): 25-33.
- [13] Mansourpanah, Y., Madaeni, S.S., and Rahimpour, A. Fabrication and development of interfacial polymerized thin-film composite nanofiltration membrane using different surfactants in organic phase; study of morphology and performance. Journal of Membrane Science 343(1-2) (2009): 219-228.
- [14] Mansourpanah, Y., Alizadeh, K., Madaeni, S.S., Rahimpour, A., and Soltani Afarani, H. Using different surfactants for changing the properties of poly(piperazineamide) TFC nanofiltration membranes. Desalination 271(1-3) (2011): 169-177.
- [15] Ahmad, A.L. and Ooi, B.S. Optimization of composite nanofiltration membrane through pH control: Application in CuSO₄ removal. Separation and Purification Technology 47(3) (2006): 162-172.
- [16] Liu, M., Yu, S., Tao, J., and Gao, C. Preparation, structure characteristics and separation properties of thin-film composite polyamide-urethane seawater reverse osmosis membrane. Journal of Membrane Science 325(2) (2008): 947-956.
- [17] Gohil, J.M. and Ray, P. A review on semi-aromatic polyamide TFC membranes prepared by interfacial polymerization: Potential for water treatment and desalination. Separation and Purification Technology 181 (2017): 159-182.
- [18] Khorshidi, B., Thundat, T., Pernitsky, D., and Sadrzadeh, M. A parametric study on the synergistic impacts of chemical additives on permeation properties of thin film composite polyamide membrane. Journal of Membrane Science 535 (2017): 248-257.
- [19] Kong, C., Kanezashi, M., Yamamoto, T., Shintani, T., and Tsuru, T. Controlled synthesis of high performance polyamide membrane with thin dense layer for water desalination. Journal of Membrane Science 362(1-2) (2010): 76-80.
- [20] Khorshidi, B., Soltannia, B., Thundat, T., and Sadrzadeh, M. Synthesis of thin film composite polyamide membranes: Effect of monohydric and polyhydric

- alcohol additives in aqueous solution. Journal of Membrane Science 523 (2017): 336-345.
- [21] de Gennes, P.G., Brochard-Wyart, F., and Quere, D. Capillarity and Wetting Phenomena: Drops, Bubbles, Pearls, Waves. Springer New York, 2013.
- [22] Raaijmakers, M.J.T. and Benes, N.E. Current trends in interfacial polymerization chemistry. Progress in Polymer Science 63 (2016): 86-142.
- [23] Jiang, S., Li, Y., and Ladewig, B.P. A review of reverse osmosis membrane fouling and control strategies. Sci Total Environ 595 (2017): 567-583.
- [24] She, Q., Wang, R., Fane, A.G., and Tang, C.Y. Membrane fouling in osmotically driven membrane processes: A review. Journal of Membrane Science 499 (2016): 201-233.
- [25] Wang, Q., Wang, Z., Zhu, C., Mei, X., and Wu, Z. Assessment of SMP fouling by foulant-membrane interaction energy analysis. Journal of Membrane Science 446 (2013): 154-163.
- [26] Zhang, R., et al. Antifouling membranes for sustainable water purification: strategies and mechanisms. Chem Soc Rev 45(21) (2016): 5888-5924.
- [27] Asadollahi, M., Bastani, D., and Musavi, S.A. Enhancement of surface properties and performance of reverse osmosis membranes after surface modification: A review. Desalination 420 (2017): 330-383.
- [28] Lalia, B.S., Kochkodan, V., Hashaikeh, R., and Hilal, N. A review on membrane fabrication: Structure, properties and performance relationship. Desalination 326 (2013): 77-95.
- [29] Richard Bowen, W. and Doneva, T.A. Atomic Force Microscopy Studies of Membranes: Effect of Surface Roughness on Double-Layer Interactions and Particle Adhesion. J Colloid Interface Sci 229(2) (2000): 544-549.
- [30] Al-Jeshi, S. and Neville, A. An investigation into the relationship between flux and roughness on RO membranes using scanning probe microscopy. Desalination 189(1-3) (2006): 221-228.
- [31] Rajaeian, B., Rahimpour, A., Tade, M.O., and Liu, S. Fabrication and characterization of polyamide thin film nanocomposite (TFN) nanofiltration membrane impregnated with TiO₂ nanoparticles. Desalination 313 (2013): 176-188.

- [32] Van der Bruggen, B., Mänttari, M., and Nyström, M. Drawbacks of applying nanofiltration and how to avoid them: A review. Separation and Purification Technology 63(2) (2008): 251-263.
- [33] Jadav, G.L. and Singh, P.S. Synthesis of novel silica-polyamide nanocomposite membrane with enhanced properties. Journal of Membrane Science 328(1-2) (2009): 257-267.
- [34] Yin, J., Kim, E.-S., Yang, J., and Deng, B. Fabrication of a novel thin-film nanocomposite (TFN) membrane containing MCM-41 silica nanoparticles (NPs) for water purification. Journal of Membrane Science 423-424 (2012): 238-246.
- [35] Peyki, A., Rahimpour, A., and Jahanshahi, M. Preparation and characterization of thin film composite reverse osmosis membranes incorporated with hydrophilic SiO₂ nanoparticles. Desalination 368 (2015): 152-158.
- [36] Jia, Y.-x., Li, H.-l., Wang, M., Wu, L.-y., and Hu, Y.-d. Carbon nanotube: Possible candidate for forward osmosis. Separation and Purification Technology 75(1) (2010): 55-60.
- [37] Song, X., Wang, L., Tang, C.Y., Wang, Z., and Gao, C. Fabrication of carbon nanotubes incorporated double-skinned thin film nanocomposite membranes for enhanced separation performance and antifouling capability in forward osmosis process. Desalination 369 (2015): 1-9.
- [38] Li, N., Tang, S., Dai, Y., and Meng, X. The synthesis of graphene oxide nanostructures for supercapacitors: a simple route. Journal of Materials Science 49(7) (2014): 2802-2809.
- [39] Xia, S., Yao, L., Zhao, Y., Li, N., and Zheng, Y. Preparation of graphene oxide modified polyamide thin film composite membranes with improved hydrophilicity for natural organic matter removal. Chemical Engineering Journal 280 (2015): 720-727.
- [40] Lee, H.S., Im, S.J., Kim, J.H., Kim, H.J., Kim, J.P., and Min, B.R. Polyamide thin-film nanofiltration membranes containing TiO₂ nanoparticles. Desalination 219(1-3) (2008): 48-56.

- [41] Kim, S.-J., Lee, P.-S., Bano, S., Park, Y.-I., Nam, S.-E., and Lee, K.-H. Effective incorporation of TiO₂nanoparticles into polyamide thin-film composite membranes. Journal of Applied Polymer Science 133(18) (2016): n/a-n/a.
- [42] Safarpour, M., Vatanpour, V., Khataee, A., and Esmaeili, M. Development of a novel high flux and fouling-resistant thin film composite nanofiltration membrane by embedding reduced graphene oxide/TiO₂. Separation and Purification Technology 154 (2015): 96-107.
- [43] Moreira, A.S.H.M.a.A.L.N. Influence of Surface Properties on the Dynamic Behavior of Impacting Droplets. in International Conference on Liquid Atomization and Spray Systems, 2003.



APPENDIX

Appendix A: Sample calculation of membrane performances

Salt rejection

To indicate the concentration of salt filtered permeate solution, the conductivity meter was used to measure the conductivity of permeate for converting to the NaCl concentration in ppm using the conducted calibration curve. The calibration curve was conducted by measuring the certain concentrations of NaCl solution as shown in table A-1.

Table A-1 Conductivity data of various certain concentration of NaCl.

NaCl concentration (ppm)	Conductivity ($\mu\text{S}/\text{cm}$)
4000	7680
3000	5170
2000	3890
1000	1960
750	1343
500	1017
250	543
125	260
62.5	130
31.25	65.3
15.625	34.4
0	0.3

The conductivity data and the NaCl concentration were fitted to obtain the linear equation $\text{NaCl concentration} = 0.5248(\text{conductivity})$ as shown in Figure A-1.

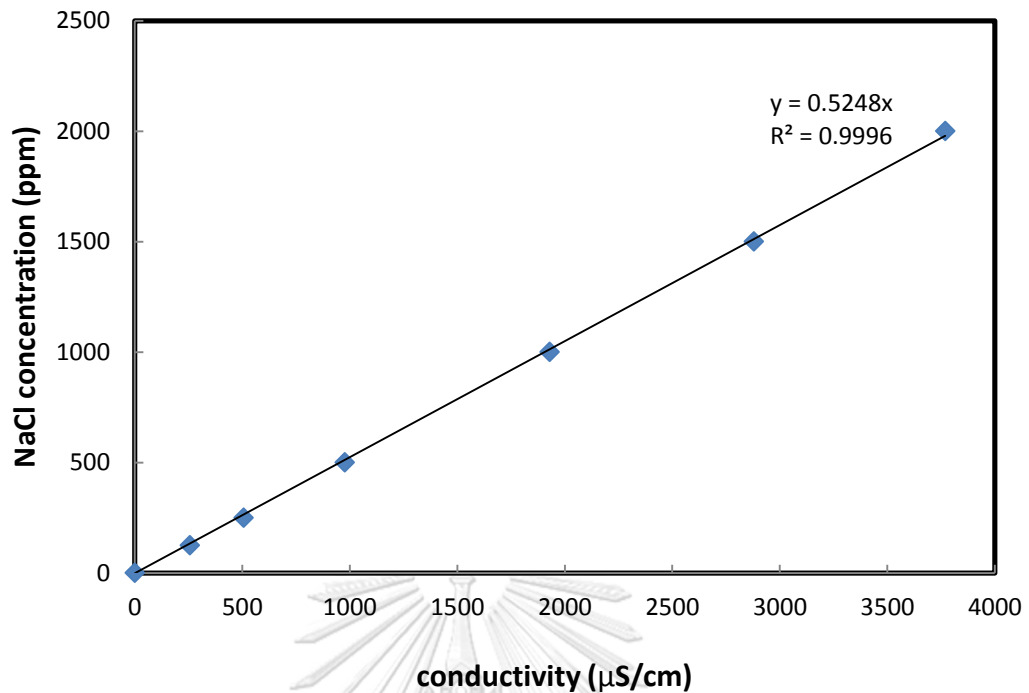


Figure A-1 Calibration curve of NaCl concentration.

After a period of permeance collection, the filtered solution weight was measured for flux calculation and then measured the conductivity to be converted to concentration for further calculation by salt rejection equation as follows

$$R = \left(1 - \frac{C_p}{C_f}\right) \times 100$$

where C_f is the salt concentration of feed (ppm), C_p is the salt concentration of permeate (ppm) and R is the salt rejection (%).

Sample calculation

First, the conductivity of feed is 3720 µS/cm. So the concentration of feed is calculated as follows.

$$\text{Feed concentration} = 0.5248(\text{conductivity})$$

$$\text{Feed concentration} = 0.5248(3720)$$

$$\text{Feed concentration} = 1952.26 \text{ ppm}$$

The conductivity of measured permeate solution is 247 $\mu\text{S}/\text{cm}$. So the concentration of permeate is calculated as follows.

$$\text{Permeate concentration} = 0.5248(\text{conductivity})$$

$$\text{Permeate concentration} = 0.5248(247)$$

$$\text{Permeate concentration} = 129.63 \text{ ppm}$$

Then, the salt rejection can be calculated by following.

$$R = \left(1 - \frac{C_p}{C_f}\right) \times 100$$

$$R = \left(1 - \frac{129.63}{1952.26}\right) \times 100$$

$$R = \left(1 - \frac{C_p}{C_f}\right) \times 100$$

$$R = 93.36\%$$

Hence, salt rejection of the membrane is 93.36%

Water permeability and water flux

From the water permeability equation

$$A = \frac{V}{A_m \Delta t (\Delta P - \Delta \pi)} = \frac{J_w}{(\Delta P - \Delta \pi)}$$

$$J_w = \frac{V}{A_m \Delta t}$$

where A is water permeance ($\text{Lm}^{-2}\text{h}^{-1}\text{bar}^{-1}$), V is the volume of diffused water (L), A_m is the effective area of membrane (m^2), Δt is the permeation time (h), ΔP is the system pressure (bar) and $\Delta \pi$ is the osmotic pressure of feed, J_w is water flux ($\text{Lm}^{-2}\text{h}^{-1}$).

Sample calculation

First, water flux at the various desired pressure was calculated for water permeability calculation

Period per collection of sample (Δt) = 10 minute = 0.167 h

Membrane effective area (A_m) = $4.393 \times 10^{-4} \text{ m}^2$

Obtained permeance solution = 0.3459 g

(Density of dilute salt solution $\approx 1 \text{ g/cm}$ at room temperature)

Then, obtained permeance solution = $0.3459 \text{ g} = 0.3459 \text{ cm}^3 = 3.459 \times 10^{-4} \text{ L}$

Thus,

$$J_w = \frac{3.459 \times 10^{-4}}{(4.393 \times 10^{-4})(0.167)} = 4.715 \frac{\text{L}}{\text{m}^2\text{h}}$$

From the water permeability equation

$$A = \frac{V}{A_m \Delta t (\Delta P - \Delta \pi)} = \frac{J_w}{(\Delta P - \Delta \pi)}$$

ΔP is the system pressure (bar) and $\Delta \pi$ is the osmotic pressure of feed. If the tested solution is DI water, thus the osmotic pressure is set to zero. Then the equation is changed to $A = \frac{J_w}{\Delta P}$ which means the permeability is the slope of water flux and system pressure.

Sample calculation

The water flux collected from 1, 3 and 5 bar of pressure are 3.49, 10.32 and 18.26 $\text{Lm}^{-2}\text{h}^{-1}$ are plotted as a linear graph as shown in Figure A-2. Then, the permeability of this membrane obtained from the slope of the linear line is $3.593 \text{ Lm}^{-2}\text{h}^{-1}\text{bar}^{-1}$.

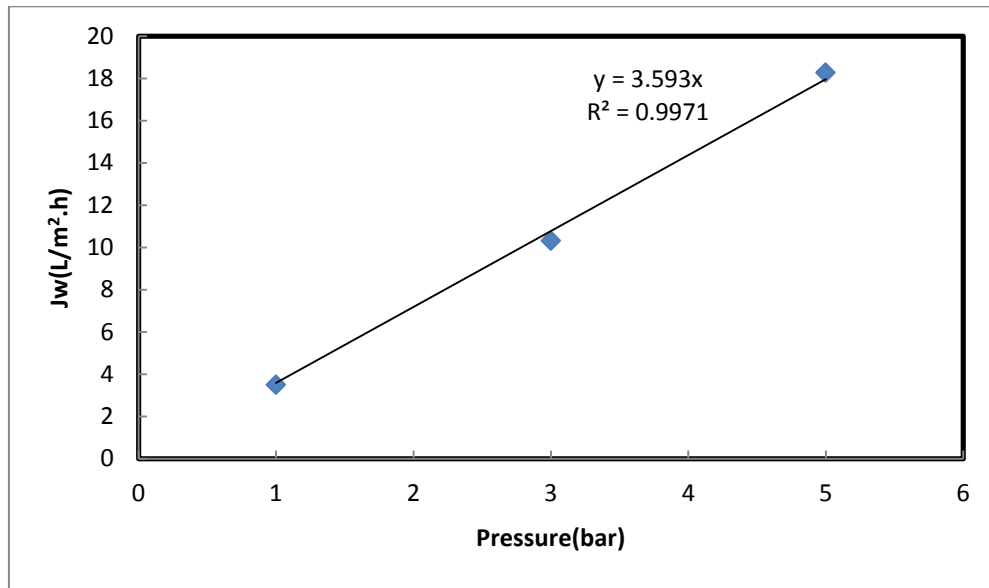
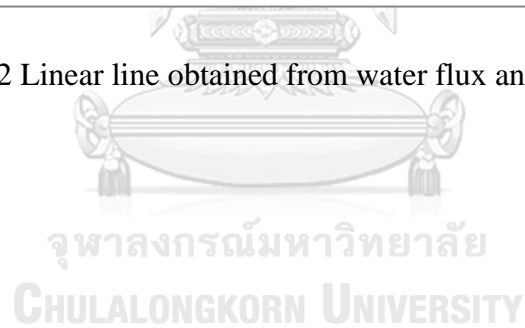


Figure A-2 Linear line obtained from water flux and pressure plotted.



Appendix B: characterization of TiO₂ colloidal solution

Size distribution of synthesized TiO₂ NPs in solution form

Figure B-1 shows the size distribution by intensity of TiO₂ solution. The result shows that the particle size distributes as a normal curve with an average of particle diameter at 19.8 ± 2.6 nm.

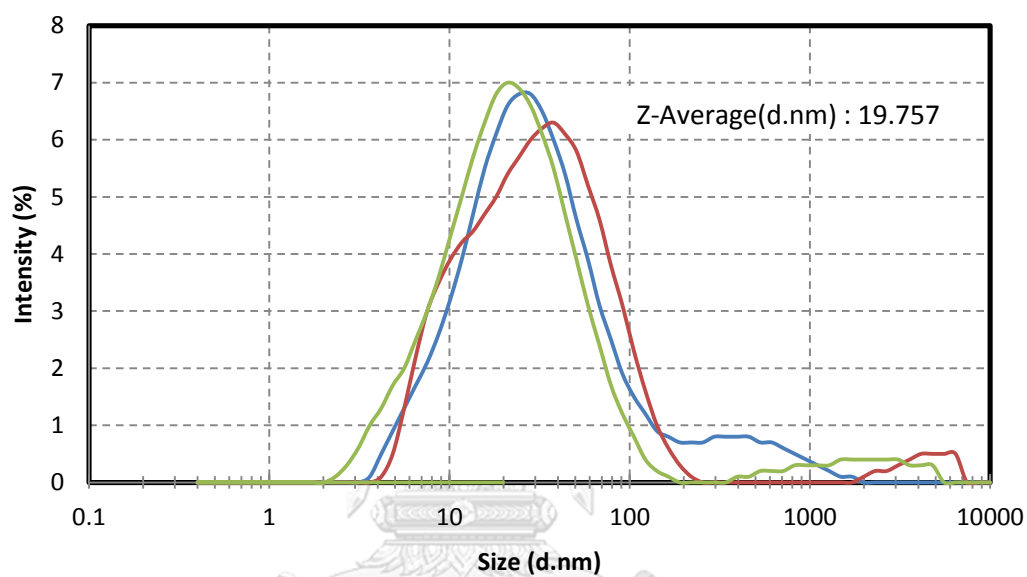


Figure B-1 Size distribution of synthesized TiO₂ NPs

Appendix C: Surface roughness of fabricated membranes

Table C-1 Surface roughness data of fabricated membranes from AFM instrument.

Additive in MPD solution	R _q (RMS roughness, nm)	R _a (Mean roughness, nm)
-	21.98±0.91	17.19±0.77
10 vol% of TiO ₂ solution	22.86±1.51	17.48±1.45
20 vol% of TiO ₂ solution	19.32±0.64	15.12±1.20
30 vol% of TiO ₂ solution	18.96±1.76	14.33±1.73
40 vol% of TiO ₂ solution	19.03±2.30	14.97±1.77
60 vol% of TiO ₂ solution	16.31±0.85	12.72±0.64
3.14 wt% of synthesized TiO ₂ powder	18.45±3.18	14.06±2.72
3.14 wt% of commercial TiO ₂ powder	22.09±2.69	17.05±2.22
1.8 vol% of Ethanol	19.79±1.89	15.03±0.91
Nitric acid (MPD solution pH 9.36)	17.72±1.61	13.67±1.29

VITA

Palach Kedchaikulratwas born on 12th August 1993 in Bangkok, Thailand. He graduated a Bachelor degree in field of Chemical Engineering from Chulalongkorn University, Bangkok, Thailand in 2016. Then, he aimed to achieve a Master degree in Chemical Engineering from Chulalongkorn University, Bangkok, Thailand in 2018.





จุฬาลงกรณ์มหาวิทยาลัย
CHULALONGKORN UNIVERSITY